Ontario

We are committed to providing accessible customer service.
If you need accessible formats or communications supports, please contact us.

Nous tenons à améliorer l’accessibilité des services à la clientèle.
Si vous avez besoin de formats accessibles ou d’aide à la communication, veuillez nous contacter.

N.T.S. 41P14

Petrographic and Electron Microprobe Examination of Listwanite Samples from the Laroma Prospect, Midlothian Lake Property, Larder Lake Mining Division, Midlothian Township, Ontario

By: Dr. Jim Renaud of Renaud Geological Consulting Ltd.,

London, Ontario

January 30 2022

Index

Petrographic and Electron Microprobe Examination of Listwanite Samples from the Laroma Prospect, Midlothian Property

Summary

This report details the petrographic work completed on 4 rocks submitted for petrographic and electron- microprobe investigation by Mr. Robert Dillman and Mr. Jim Renaud. The main purpose of the study was to examine the rocks and provide details of textures and mineral compositions, alteration, assemblages and associated mineralization and to find occurrences of gold-bearing phases. The samples were collected from the Laroma Prospect on the Midlothian property during a site visit on September 18 2020. The samples investigated were ML-47, ML-49, ML-50, and ML-51. The samples were collected as part of a traverse by property owners: Dr. Jim Renaud and author, Robert Dillman. The samples were collected between Midlothian Lake and Mitre Lake, on claim:

549439, cell 41P15E081

The traverse was initiated to prospect for fuchsite (green mica) and quartz-carbonate alteration noted in historic reports. The samples were submitted for assay and the best assay was 14.5 ppm Au (Sample ML-50) taken in a large pit at the Laroma Prospect.

Location and Access

The Midlothian Lake Property is situated in Midlothian Township in the Larder Lake Mining Division of Ontario. The property is located approximately 23 kilometres southwest of the town of Matachewan (Figure 1). The property is accessible by truck and ATV. From the town of Matachewan, the property can be reached by travelling 2.9 km southwest on Highway 566 to the Asbestos Mine Road. Go west on the mine road for 23 km at which point the road is washed out and the rest of the journey must be made on ATV along a narrow forest trail.

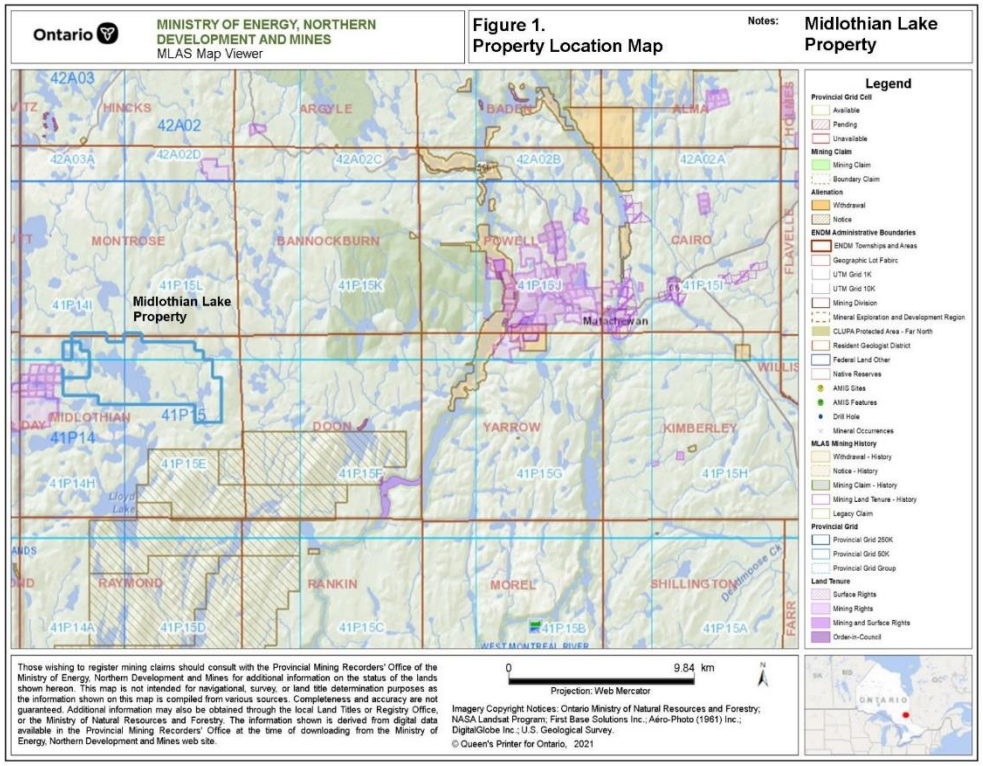

Claim Logistics and Location of Work

The Midlothian Lake Property consists of 113 mining claim cells. The property covers an approximate area of 2450 hectares (Figure 2). All claims comprising the Midlothian Lake Property are held by Robert Dillman of Mount Brydges, Ontario and author, Jim Renaud of London, Ontario.

Land Status and Topography

The Midlothian Lake Property is situated entirely on Crown Land. The property is uninhabited. There are no buildings or habitats. An electrical powerline follows the Asbestos Mine Road which crosses the southeast section of the property. A system of non-maintained logging roads provide access to most areas of the property. Sections of the property have been logged within the last 3 decades. Some of these areas are partially reforested with spruce trees. Uncut forest consisting of large spruce, balsam and poplar trees can be found bordering bodies of water and growing in higher elevations. Cedar trees and alders grow in lower areas.

The property is at a mean elevation ranging between 360 to 400 metres above sea level. Most of the property has gentle relief with rounded hills averaging 20 metres in height. Rugged terrain exists east of Elizabeth Lake where steep hills rise over 40 metres above the lake and close to Midlothian Lake where ridges and knobby outcrops range between 5 to 40 metres in height and follow the outline of the lake. The northeast section of the property where the traverse was done is situated at the base of a large, steep hill rising over 540 metres above sea level. There are several lakes on the property. The largest is Midlothian Lake which covers an approximate area of 366 hectares.

Outcrop exposure in many sections of the property is good. Outcrops are abundant in higher elevations and variable exposures occur in lower elevations. Overburden is generally shallow and consists of glacial till deposited by a glacier initially moving from the northeast to the southwest and shifting northwest to southeast in its final advance.

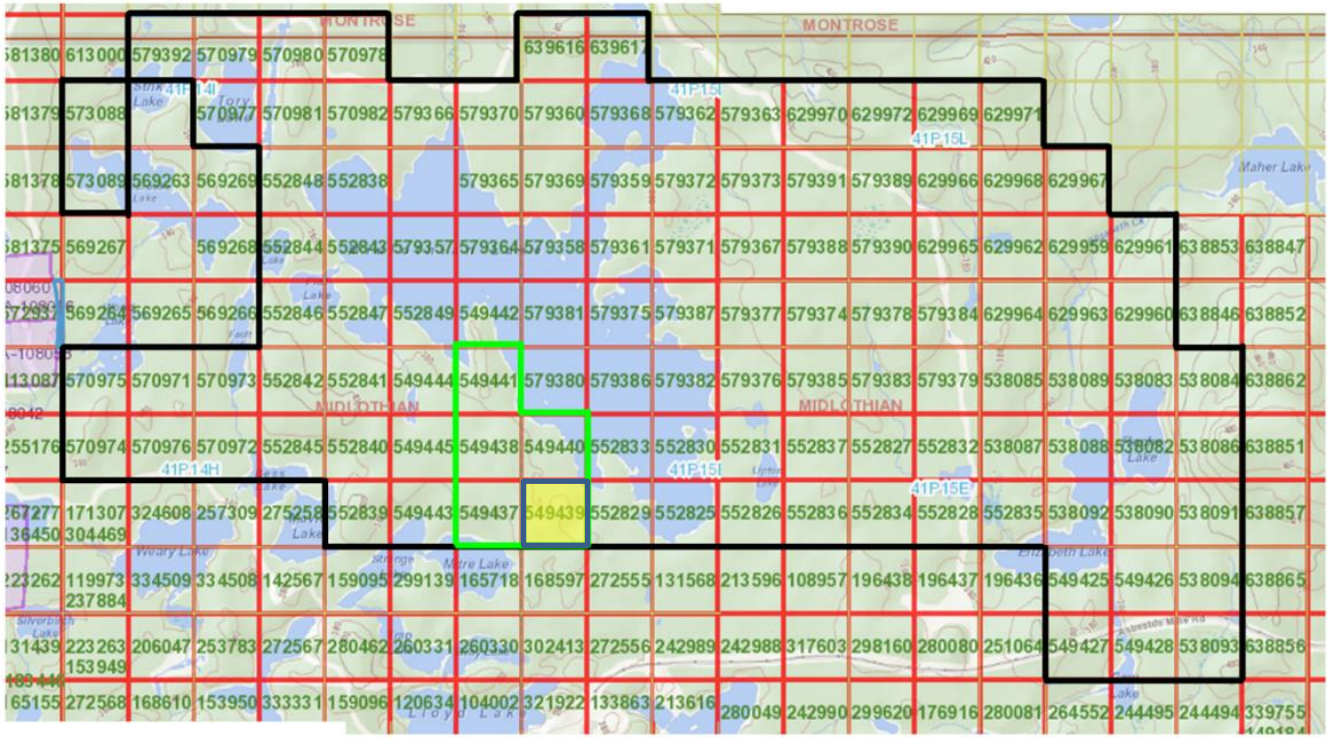

Figure 2.
Claim Map: Midlothian Lake Property
Midlothian Township, Ontario

Regional and Local Geology

The Midlothian Lake Property is located in the Halliday Dome area within the western portion of the Abitibi Subprovince of the Superior Province. The Halliday Dome consists mainly of calc- alkaline felsic and intermediate volcanic rocks with minor quantities of iron formation and basaltic rocks of the Tisdale Assemblage, unconformably overlain by younger Kinojevis Assemblage rocks, which are in turn unconformably overlain by sedimentary rocks of the Porcupine Assemblage.

Midlothian Township is located on the southeast quadrant of the dome and consists of intermediate to felsic volcanics, flows and pyroclastics, "Temiskaming" sediments and a series of mafic to ultramafic sills. The Coleman Member of the Gowganda Formation lies unconformably on top of the Archean volcanics and sediments. It is thought that the Larder Lake Break extends beneath the Gowganda Formation west of Matachewan and continues through the south portion of Midlothian Township. Surrounding geology in the Bannockburn Township area describes Neoarchean-age calc-alkaline intermediate to felsic volcanic rocks, mafic volcanic rocks, komatiitic basalt to dunite, silicate to sulphide iron formation, gabbro intrusions, and a series of sedimentary rocks including diamictite, arkose, and conglomerate (Préfontaine and Berger, 2005). Proterozoic-age (Huronian Supergroup) sediments (Cobalt Group - Gowganda Formation), composed mainly of clastic metasedimentary rocks such as conglomerate, sandstone, wackes and argillite, unconformably overlie the Archean supracrustal assemblages.

The area northeast of Midlothian Lake is underlain by arkose, sandstone and conglomerates of the Midlothian Formation dated 2688.5 Ma (Préfontaine and Robichaud, 2013). Rock units generally strike northwest to southeast and dip steeply to the north. The area has been intruded by north trending diabase dikes of the Matachewan Swarm dated 2454 Ma (Préfontaine and Robichaud, 2013). To the east, rocks of the Midlothian Formation and Matachewan diabase swarm are unconformably overlain by Huronian rocks consisting of conglomerates, argillite and greywacke of the Cobalt Group of the Gowganda Formation dated circa 2300 Ma (Préfontaine and Robichaud, 2013). Diabase dikes of the Sudbury Swarm dated 1238 Ma also have intruded rocks of the Midlothian Formation and cross the unconformity into the Cobalt Group.

Midlothian Township consists of intermediate to felsic volcanics, flows and pyroclastics, "Temiskaming" sediments and a series of mafic to ultramafic sills. The Coleman Member of the Gowganda Formation lies unconformably on top of the Archean volcanics and sediments. It is thought that the Larder Lake Break extends beneath the Gowganda Formation west of Matachewan and continues through the south portion of Midlothian Township.

The Midlothian Township Property is underlain by intermediate to felsic flows and pyroclastic rocks to the south. The north half of the property is underlain by "Temiskaming" type sediments: mostly conglomerates, greywackes and siltstone. Areas of carbonate and green mica alteration have been discovered on the property along the contact of the volcanics and sediments in the vicinity of Midlothian and Mitre Lakes.

Figure 3. Regional Geology

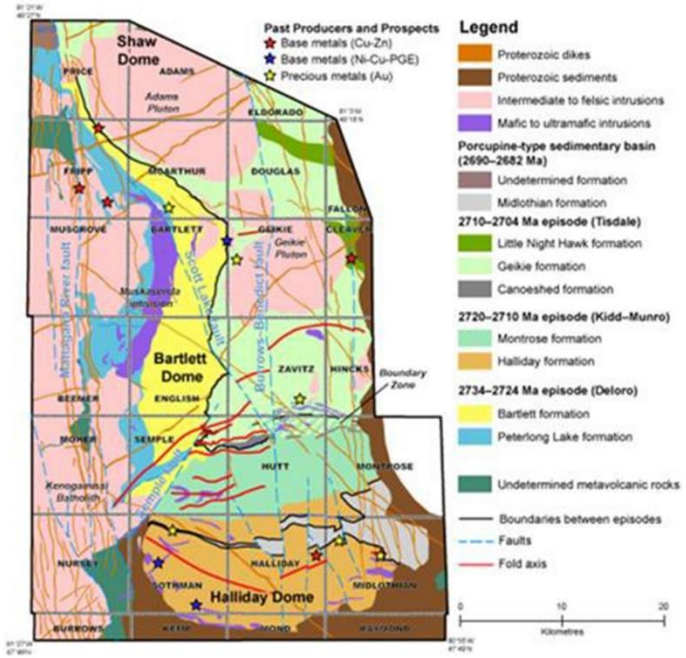

Figure 3. Schematic map of the study area depicting part of the Shaw Dome as well as the Bartlett and Halliday domes. The Bartlett and Halliday domes are further broken down into volcanic- and sediment-dominated episodes (assemblages) and formations. The green hatched pattern at the Zavitz–Hutt township boundary represents the boundary zone between the 2720–2710 Ma volcanic episode (Kidd–Munro) and the 2710–2704 Ma volcanic episode (Tisdale).

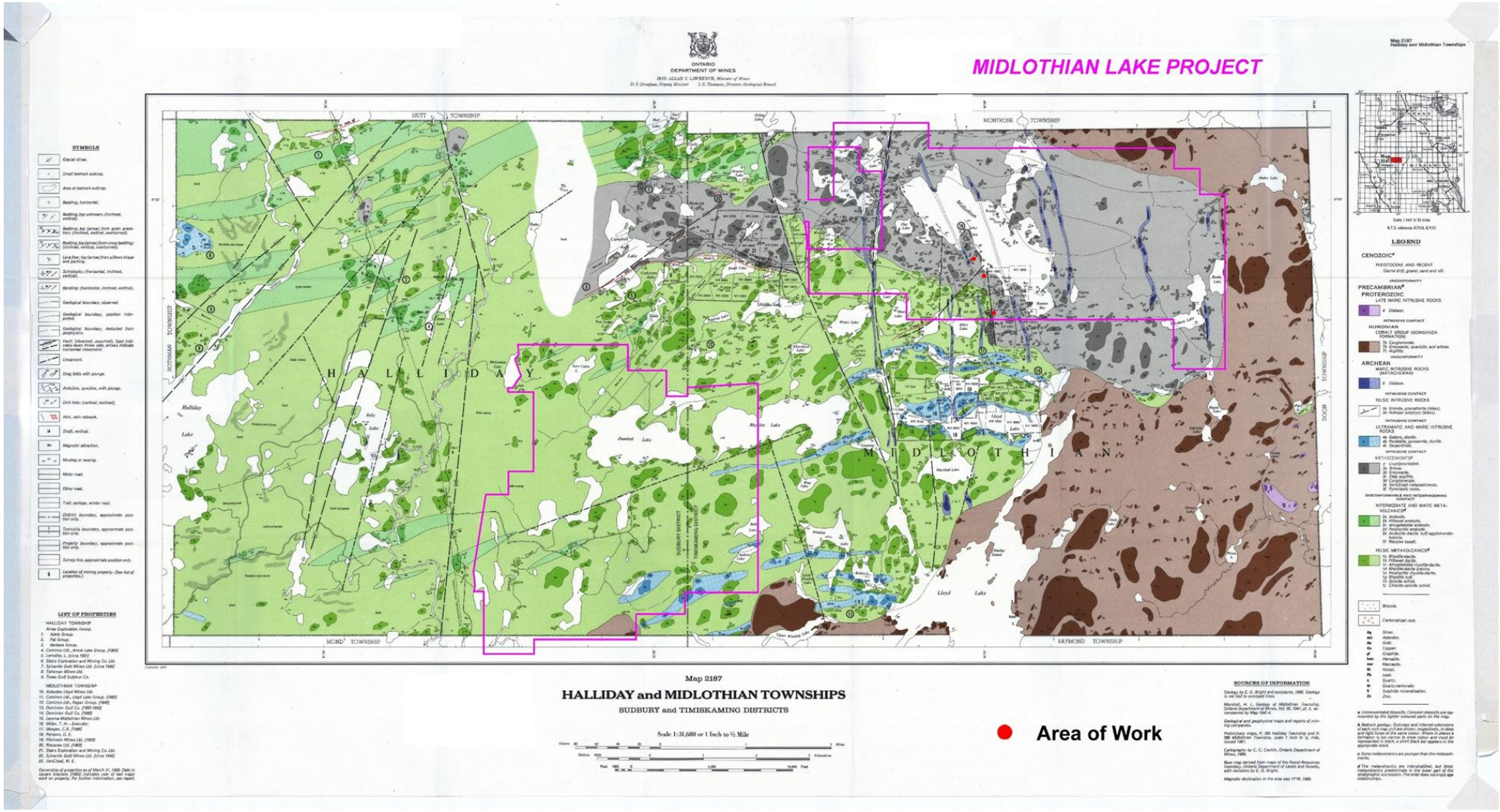

Figure 4: Geology of Halliday and Midlothian Townships ODM Map 2187

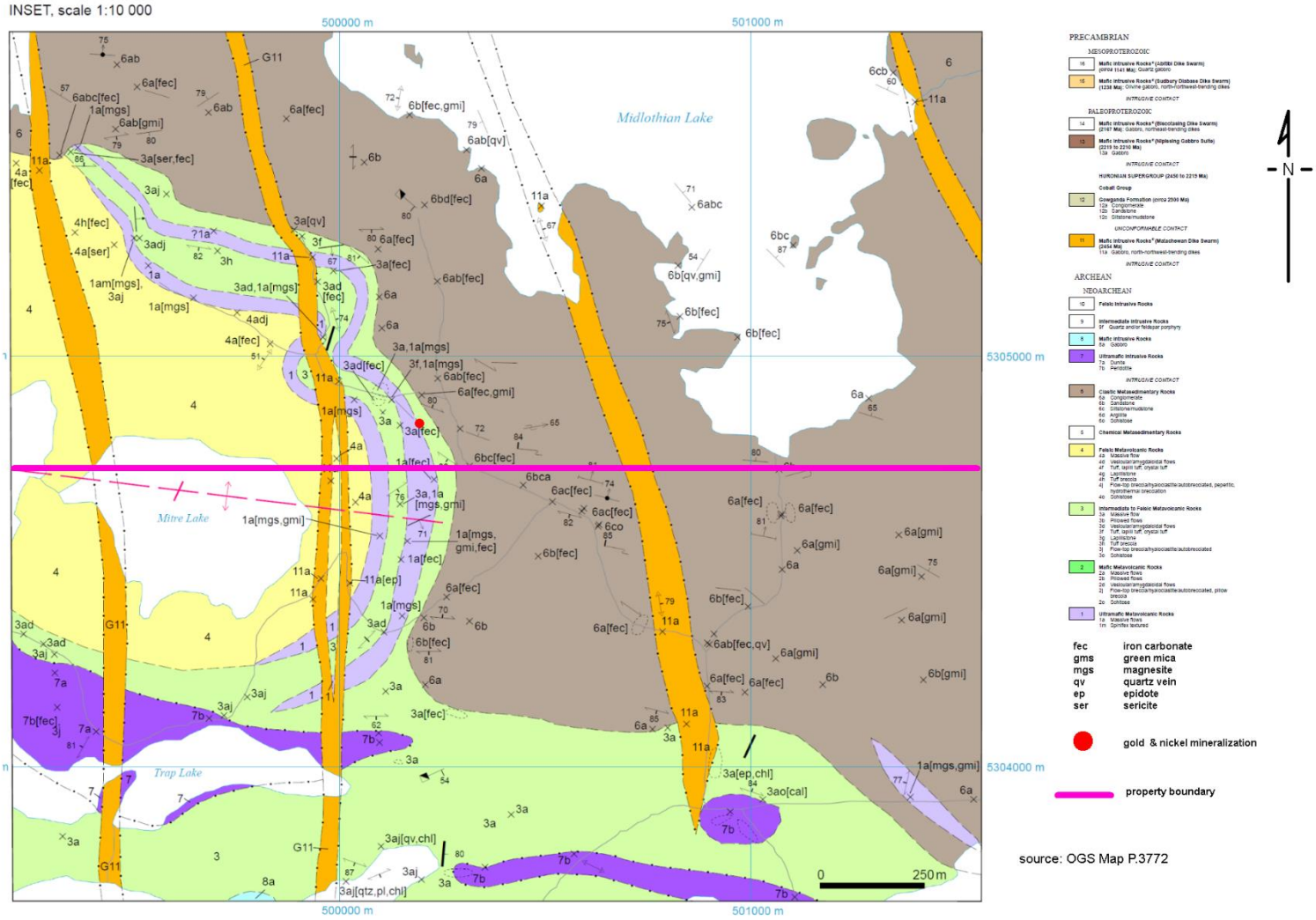

Figure 5. Mitre Lake Area, Midlothian Twp.

History of Exploration

Historic mineral exploration in Midlothian Township has occurred in several periods from as early as 1907 to present day. As a result, different sections of the property have been explored at various times. Historic exploration has led to the discovery of gold, copper, pyrite, graphite and marcasite on the property. The Halliday Dome area has been explored since the turn of the century, with increased activity in the 1960's. Gold exploration has gone through several cycles including the early 1900's, the 1930's and from 1940 to the early 1970's. An Indian land caution halted exploration in the area for over two decades. Savage (1963), a government geologist reported that gold was first found in Midlothian Township in 1909.

In 1946, H. I. Marshall created a detailed geological examination of Midlothian Township for the Ontario Department of Mines (Marshall, 1947) and in 1970 E.G. Bright mapped Halliday and Midlothian Townships reported in Geological Report 79. Montrose Township was presented as “Digital GIS Compilation: Bedrock Geology of Powell, Bannockburn and Montrose Townships”, Ontario Geological Survey, MRD 207 (Berger et al, 2006).

The following is a summary of recorded exploration near the property obtained through assessment filings from OGSEarth.

Historic Exploration: Midlothian Lake Property, Mitre Lake Area

Company	*Year*	*Work Description*
Stairs Exploration & Mining	1959 – 1964	21 DDH
Rio Tinto Mines	1963	1 DDH
Laroma Midlothian Mines Ltd.	1964	2 DDH
Laroma Midlothian Mines Ltd.	1964	3 DDH
Timiskaming Nickel	1968	1 DDH
Canadian Johns-Manville Co. Ltd.	1970	3 DDH
Dennison Mines Ltd.	1971	Geological Survey, Geochemical Survey, EM Survey and 2 DDH
Dennison Mines Ltd.	1971	2 DDH
John Hogan	1971	2 DDH
John Hogan	1971	1 DDH
International Trust Company	1972	4 DDH
Larche/Rosseau	1972	8 DDH
Allied Mining Corp.	1972	1 DDH
Allied Mining Corp.	1972	2 DDH
Tojaro Holdings Ltd.	1973	Magnetometer Survey
Stump Mines Ltd.	1973	2 DDH
United Asbestos Inc.	1973	3 DDH
Hanna Mining Company	1974	6 DDH
Hanna Mining Company	1974	6 Holes
Northrim Mines Inc.	1975	2 DDH
International Trust Company	1976	3 DDH
Falconbridge Copper Mines Ltd.	1978	7 DDH

Shield Geophysics Ltd.	1981	Airborne EM
Regal Goldfields Ltd.	1983	9 DDH
Goldteck Mines Ltd.	1987 – 1988	Geological Mapping, Mechanical Stripping, Magnetometer and Resistivity Surveys and 94 DDH
Tom Obradovich	1996	Mechanical Stripping
Orezone Resources Inc.	1996	Prospecting, Sampling (Laroma Showing)
Orezone Resources Inc.	2000	7 DDH
Canadian Arrow Mines Ltd.	2002	10 DDH
Mustang Minerals	2004	Airborne EM
Explor Resources	2008	Heli-VTEM
Explor Resources	2009	Ground Mag/IP/VLF
Explor Resource	2011	DDH (Montrose Property)
Dillman, Renaud	2020	Prospecting
Dillman, Renaud	2021	Prospecting

In terms of nickel mineralization in the area, historic details from assessments and suggest that the ultramafic and mafic sills and stocks in the rhyolitic strata are decent prospects. Peridotite and gabbro sills intrude the outer rhyolitic strata, and extend eastward from Sothman Township, east-northeastward into Halliday and Midlothian Townships. The nickel-copper bearing ultramafic sill of Kirkland Minerals Corporation Limited, in the southeast corner of Sothman Township averages 1.29 percent nickel, plus approximately 400,000 tons of 0.90 percent nickel (Survey of Mines, 1968, p. 153).

The following map is a snapped image of the Preliminary Map 983, Geochemical Distribution of Ni in Metavolcanics and Mafic |Intrusions in Halliday and Midlothian Townships (1974). The map illustrates the Ni-occurrences south of the Laroma prospect and south of Midlothian Lake toward Bray Lake where Ni values reach 1880 ppm Ni. The black dots illustrate Ni-content of assays in ppm.

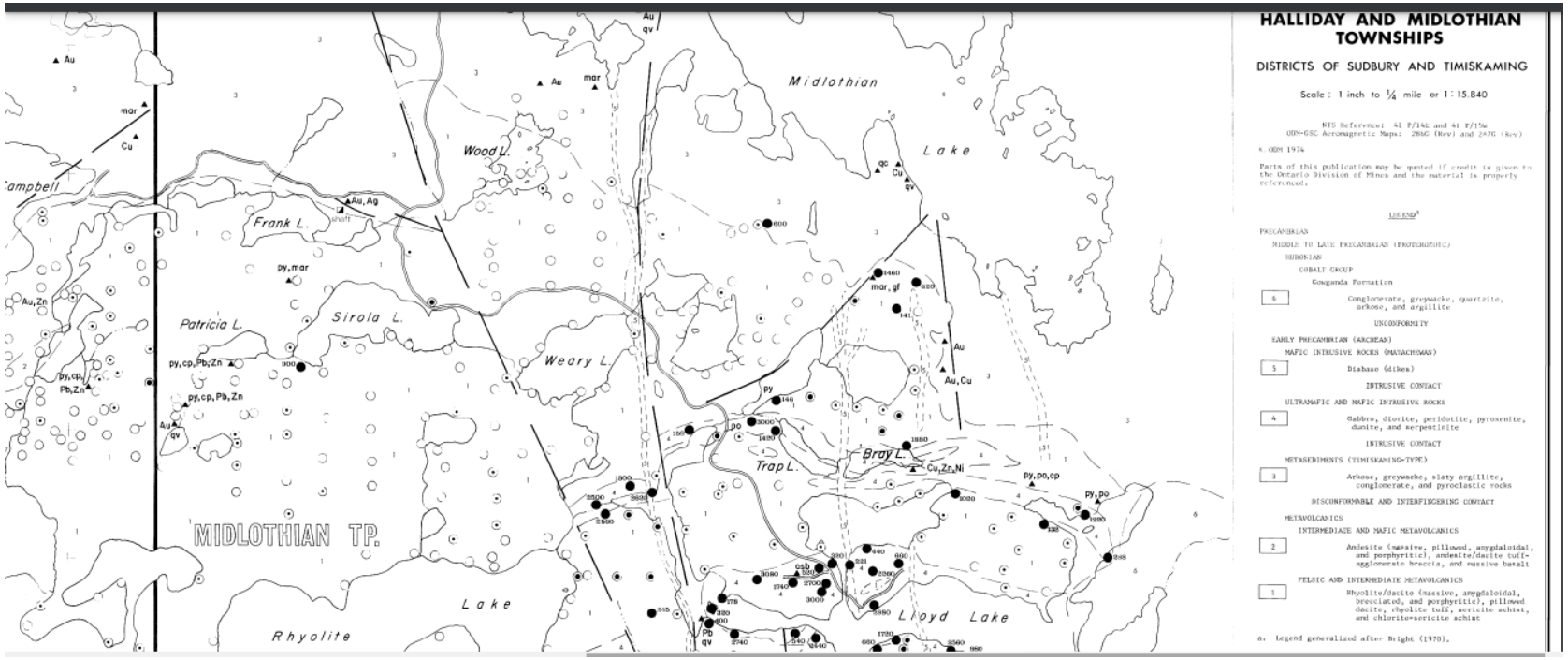

Figure 6. ODM Map P-938

Survey Dates and Personnel

The rocks samples examined in this report were collected as part during prospecting traverses on September 18, 2020 and June 13, 2021. The traverses were completed by: Jim Renaud of London, Ontario and Robert Dillman of Mount Brydges, Ontario.

Microprobe work was completed by the author, Dr. Jim Renaud at his facilities in London. Ontario. Rock samples were analyzed on December 2, 2021, January 24 and January 25, 2022. During this time, one day was devoted towards petrographic examination of the rocks.

Survey Logistics

Prospecting in the area between Midlothian Lake and Mitre Lake on the Midlothian Property was initiated to examine occurrences of gold in green mica- bearing units and quartz-carbonate alteration as reported in previous work. The traverse for September 18 2020 is plotted at a scale of 1:5,000 in Figure 7. After receiving favorable gold assays, the area was resampled on June 13, 2021 during a brief visit to this section of the property.

A compass and a Garmin GPS model GPSMAP 66st were used to navigate. The GPS unit was set to NAD83, Zone 17. Waypoints (WP) for the traverse were periodically recorded and are listed in Table 1.

All rock samples from the property were delivered to AGAT Laboratory for analyses. The lab is in Mississauga, Ontario. All rock samples were Fire Assayed for gold using a 50 gram charge and finished by Inductively Coupled Plasma – Optical Emission Spectroscopy (ICP-OES) to measure the gold concentration. Two samples were assay for gold using a Total Metallic Assay method. Assay certificates from the lab are appended to this report.

Rock sample locations, descriptions and assay results are also presented in Table 1 and plotted with geology and surface features on the appended map at a scale of 1 : 5,000.

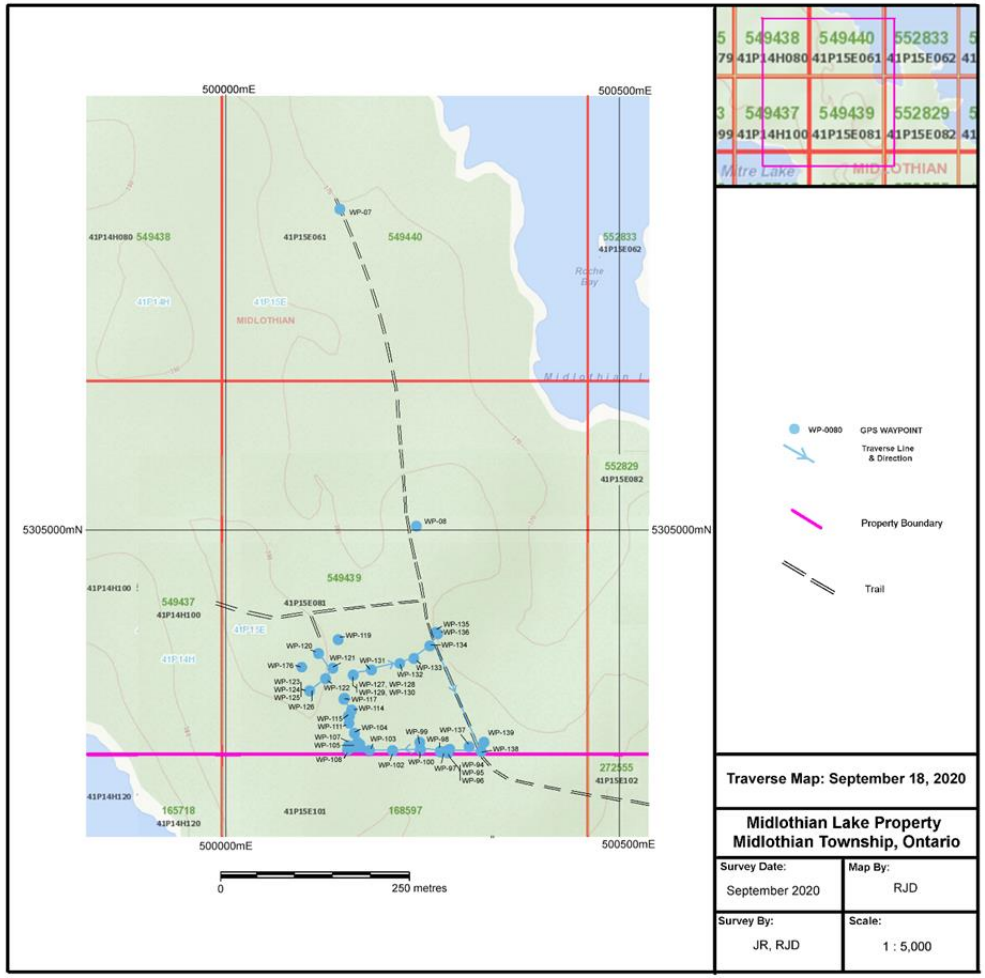

Figure 7. September 18, 2020 [WP-126 (SAMPLE ML-47), WP-128 (SAMPLE ML-49), WP-129 (SAMPLE ML-50), WP-130 (SAMPLE ML-51)]

Table 1. September 18, 2020 Traverse, Midlothian Lake Property

Waypoint	Easting	Northing	Claim, Cell	Rock Sample	Assay ppm	Notes
95	500290	5304728	549939, 41P15E081	ML-37	0.005	On slight rise. Grey quartz with FeC trace pyrite in conglomerate str. 118^0, dip 84^{0}E, mixed mature forest
96	500286	5304726	549939, 41P15E081	ML-38	0.007	On slight rise. Sheared conglomerate with fuch 1-5% py
97	500288	5304724	549939, 41P15E081			North end of conglomerate outcrop, FeC
98	500278	5304726	549939, 41P15E081			N-S gridline, moderate slope facing west
99	500252	5304728	549939, 41P15E081			On slope, sheared sericite with fuchsite Tr. py
100	500253	5304726	549939, 41P15E081			Tr. py in grey quartz + carbonate in quartzite beside schist
102	500217	5304727	549939, 41P15E081			Mylonite, FeC + fuch, top of hill, moderate slope west, E – W gridline L11S, 24+25E
103	500188	5304726	549939, 41P15E081			Draw N – S, 10 m wide, schist east side str. 154^0, dip 78^{0}E
104	500178	5304694	549939, 41P15E081			Schist, FeC spheres steep slope E
105	500176	5304734	549939, 41P15E081			Schist, FeC spheres, Steep slope E
106	500172	5304737	549939, 41P15E081			Quartz boulder, steep slope E
107	500172	5304729	549939, 41P15E081			Qtz dolomite, steep hill E
108	500160	5304729	549939, 41P15E081			Grey quartz + fuchsite, boulder, steep slope E
109	500160	5304727	549939, 41P15E081			Grey quartz + fuchsite, boulder, steep slope E
110	500161	5304733	549939, 41P15E081	ML-39	0.018	Moderate green carb with grey quartz outcrop, steep slope E, boulder.
111	500169	5304748	549939, 41P15E081	ML-40	0.002	Conglomerate with fuchsite pebbles, Tr. pyrite, boulder in draw
112	500169	5304748	549939, 41P15E081	ML-41	0.006	Sheared mafic with 5% pyrite, qtz & carbonate, big boulder
113	500161	5304770	549939, 41P15E081	ML-42	0.005	Quartz + FeC boulders, side of hill
114	500165	5304777	549939, 41P15E081	ML-43	0.377	1.4 cm wide pyrite seam in carb-sheared conglomerate boulder, top of hill
115	500162	5304770	549939, 41P15E081	ML-44	0.010	5cm wide qtz-FeC vein in green carbonate tr. py
117	500156	5304792	549939, 41P15E081			Conglomerate.
118	500155	5304791	549939, 41P15E081			E – W grid line
119	500148	5304865	549939, 41P15E081			North end of old trench, old road
120	500122	5304848	549939, 41P15E081			FeC in sandstone, old stripped area
121	500141	5304830	549939, 41P15E081			South end of old trench, old road FeC sandstone with white quartz
122	500132	5304818	549939, 41P15E081			Small trench, 5m E - W

Table 1. September 18, 2020 Traverse, Midlothian Lake Property (continued)

Waypoint	Easting	Northing	Claim, Cell	Rock Sample	Assay ppm	Notes
123	500111	5304802	549939, 41P15E081			West end of trench 4 x4 x 2.5 m
124	500111	5304803	549939, 41P15E081	ML-45	0.074	Quartz + strong green carbonate, 1% pyrite in pit
125	500111	5304803	549939, 41P15E081	ML-46	0.108	Strong green carbonate with qtz stringers with 5% 2cm blebs of pyrite , loose beside pit
126	500113	5304803	549939, 41P15E081	ML-47	0.527 FA 0.469 g/t TMA	White to pink Qtz – carb – fuch stringers, Tr, -2% cubic pyrite, loose beside pit. Fire Assay & Total Metallics Assay.
127	500167	5304821	549939, 41P15E081	ML-48	0.074	5 cm quartz stringers + carb in green carbonate, E pit at end of long trench. South face 4 x 4 x 4, on contact green carb west, quartzite? east
128	500167	5304820	549939, 41P15E081	ML-49	0.072	Qtz + fuch + black tourmaline 1-5% fine pyrite, loose by pit E side
129	500165	5304821	549939, 41P15E081	ML-50	>10.0 FA 14.5 g/t TMA	Quartz stringers/ veins in green carbonate, NW corner bottom of pit, chips 1m. Fire Assay & Total Metallic Assay.
130	500163	5304822	549939, 41P15E081	ML-51	0.104	Grab at top W side of big pit, quartz + FeC + white quartz in green carb wallrock, 1-5% py, tr. cpy.
131	500190	5304828	549939, 41P15E081			Gentle slope east from pit Loose schist, spruce, cedar, overburden into low
132	500226	5304836	549939, 41P15E081			Conglomerate outcrop, base of west facing hill. Qtz-fuch float
133	500245	5304842	549939, 41P15E081			Top of hill, conglomerate.
134	500265	5304858	549939, 41P15E081			Top of hill, steep east facing hill. Conglomerate FeC outcrop
135	500272	5304874	549939, 41P15E081			Outcrop, conglomerate
136	500275	5304873	549939, 41P15E081			Road
137	500315	5304732	549939, 41P15E081			Conglomerate str 300^0, crossed by carb stringers
138	500330	5304727	549939, 41P15E081			Road
139	500334	5304737	549939, 41P15E081			Argillite outcrop, no alteration

Highlighted samples are those investigated in the attached petrographic report below

Petrographic and Electron Microprobe Methods

The samples were cut and 4 polished thin section were made. Samples were subsequently carbon coated and examined in transmitted and reflected light with a Zeiss petrographic microscope. Regions of interest were photographed using the petrographic microscope and circled with a diamond scribe to enable relocation of the selected areas when in the microprobe. Samples were examined in detail using the Oxford Instrument Energy Dispersive System (EDS) on the microprobe and relevant minerals analyzed using the EDS system. Backscattered electron detector images of relevant and interesting mineralogical and textural relationships were collected digitally. For each backscatter image a scale bar in microns is located at the bottom of each image which is useful in evaluating the grain sizes of the various minerals. All minerals were analyzed using a JEOL JXA 733 electron microprobe equipped with a Tracor Northern EDS and five wavelength spectrometers.

Results

Although the proposed intention of the investigation was to evaluate gold-bearing species, no gold was found in the polished thin section samples. Assays results for these samples report gold mineralization with values ranging 0.072 ppm Au to 14.5 ppm (14.5 g/t) Au. All the samples were collected in the vicinity of the Laroma Prospect. The samples consisted of strong green carbonate alteration/ fuchsite with white and grey quartz stringers and traces of very minor fine to rarely coarse pyrite.

Interestingly, the samples contain a wide array of Ni-Sb-Co-Te-As-bearing phases which changes the tenor of the Laroma Prospect. Below are details of the four rocks analyzed with photomicrographs, backscatter electron images, EDS spectra, and some EDS analyses. Some of the sulphide grains show an O-peak due to the fine-grained nature of some of the sulphide-species resulting in beam spill-over onto adjacent oxide phases. Closer evaluation of the

geology of the area suggests that the property sits on the western extension of the Larder Lake Break which provides structure, faulting and shearing, permitting hydrothermal sfluid migration into rocks around the Laroma Prospect.

Discussion

The presence of Cr-bearing fuchsitic mica (Cr-paragonite) suggests the precursor rock was likely a Cr-bearing ultramafic rock (i.e. komatiite). The green mica, fuchsite, and the compositionally zoned dolomite-ankerite solid solution carbonates are the most abundant minerals in this rock. Fuchsite occurs as contorted linear zones and as clots intergrown with quartz and zoned carbonates. Textural evidence suggests that the Cr-paragonite represent late stage hydrothermal solution and alteration of a mafic Cr-rich volcanic protolith. The fuchsite contains Cr substituted in the muscovite structure for octahedral Al. A mafic or ultramafic source is suggested for the inclusion of Cr in muscovite.

Carbonate is also relatively important in these samples. There are differernt carbonate series recognized in the samples: (1) dolomite-ankerite s.s., (2) dolomite, and (3) calcite. The carbonates demonstrate chemical zonation from core to margin evident by dark and bright compositional variations in backscatter. Interestingly, the dolomite-ankerite s.s. carbonate are associated with coarse domains of feathery Cr-green fuchsite + quartz + chromite + fine-medum grained disseminations of sulphides.

This mineralogical association of the different carbonate species is suggestive of bulk rock control and possible hydrothermal fluid influx. The dolomite-ankerite s.s. carbonates associated with Cr-paragonite and chromite suggests derivation from an ultramafic precursor. The later stage carbonate and quartz veinlets and Ni-sulphide species are associated with a later hydrothermal event. The significance of Cr-paragonite in these strained fuchsite-carbonate rocks are 2-fold: (a) Cr-bearing fractured, brecciated, and strained carbonate-quartz-fuchsite domains suggests the introduction of these elements from an external source. It is suggested that the source of Cr was probably a mafic or ultramafic intrusion at some depth. Because Cr is an immobile element, it is unlikely to have moved far from its source (the mafic-ultramafic intrusion), (b) Cr-rich micas are known to be associated with some Archean gold deposits

such as Dome, Kerr Addison and Aquarious mines, where Cr has been derived from the host ultramafic rocks. Late metamorphic fluids also remobilized Cr from the ultramafic

rocks at the Kidd Creek VMS deposit (Timmins, Ontario) and deposited it in the contact rhyolite as fuchsite (Schandl, 1989; Schandl and Wicks, 1993; Smith et al.,1993).

The fuchsite grains are paragonitic and indeed have a persistent and elevated content of sodium around 8 wt% Na2O. End-member paragonite is defined as the most aluminous of all micas in that the octahedral sites are occupied essentially by aluminum only and does not contain either octahedral site Ti, Mg, Fe, Mn, and Cr. Thus, the mica compositions from analyzed by EDS on these samples from the Midlothian Property do indeed contain analyses with elevated sodium. In this regard, it would be of some interest to establish the specific geological situation of the samples in the suite that approach true paragonitic muscovite that have only a minimal occupancy of cations in the octahedral site in addition to aluminum. It is not uncommon for a zone of paragonitic muscovite to be present at the direct margin of large gold deposits of hydrothermal origin. Known examples are the Ridgeway Gold deposit in South Carolina and the Con Mine in Yellowknife. In both situations, there is a rather significant zone of either true paragonite or paragonitic muscovite or both across a miscibility gap, at the direct interface between altered host rocks and domains of fluid-dominated hydrothermal assemblages and mineralization. The presence of Cr-paragonite muscovite in samples from the Laroma Prospect area might well be evidence that similar processes were operative in the area.

In terms of providing a rock name for the current suite of rocks investigated, the most appropriate name would be a Listwanite. Listwanite (listvenite, listvanite, or listwaenite) is a rock type that forms when the groundmass of ultramafic rocks (ex. Peridotites), is altered to carbonate minerals and cut by ubiquitous carbonate veins containing one or more of magnesite, calcite, dolomite, ankerite, and/or siderite. The original mafic minerals in the peridotite are commonly altered to Mg- or Ca-carbonate and hydrous Mg-silicates. Complete carbonate alteration of the pre-cursor rock means that every single atom of magnesium and calcium as well as some of the iron atoms have combined with CO2 to form secondary carbonates like magnesite, calcite, and siderite, while

the remaining silica, are found in quartz, serpentine, and talc. Thus, in terms of bulk mineralogy, listwanites consist primarily of quartz (often of a rusty red colour), carbonate, serpentine, talc, ± mariposite/fuchsite (i.e., Cr-muscovite) ± gold.

As explained in some detail by Buckman et al. (2010), Listwanites are host to world-class gold deposits, such as McLaughlin's Mine in California. Alteration commonly develops along faults that intersect bodies of serpentinized ultramafic rocks. Listwanites form as a result of the chemical reaction between serpentinite and CO2-rich fluids. These fluids usually migrate along faults or fractures along the contact of serpentinite and the adjacent country rocks. Freshly broken listwanites have a green-orange colour due to the presence of fuchsite and ferro-magnesium carbonates respectively. The weathered surface of listwanites usually has a gossanous boxwork texture and a brown-red colour due to the preferential breakdown of the ferro-magnesium carbonates. Other, less abundant minerals, commonly found in silica-carbonates include chlorite, fuchsite (Cr-rich mica), talc, fluorite, residual serpentine and chromite, and sulfides such as pyrite, chalcopyrite and arsenopyrite.

Buckman et al. (2010) also explain that ultramafic rocks (upper mantle peridotites) are believed to be the main source of gold (Pipino, 1980), which is contained within the accessory opaque minerals (sulfides, chromite, and magnetite). Gold contents in serpentinized mantle peridotite range between 3 and 5 ppb. Large-scale hydrothermal systems operating during the late stages of tectonic emplacement leach gold from the opaque minerals and transport it in a CO2-S-As-Cl-Na-K-B-rich solution as arsenic complexes. The hydrothermal fluids are focussed along tectonic contacts. As the system evolves the acid gold-bearing solutions precipitate silica-pyrite-arsenides and gold when entering into the reducing and alkaline carbonatized rocks. Silica-carbonates are on average 5 – 20 times more enriched in gold (average 0.02 – 0.1 ppm Au) than the surrounding ultramafic rocks (between 0.001-0.010 ppm) (Buisson and Leblanc, 1987). Economic grades of gold are usually associated with sulfides, sulfarsenides or arsenides (Buisson and Leblanc, 1987). The gold is usually bound to the sulfides, pyrite and Co-arsenides. Trace element analyses show strong positive correlations between Au and As, and quite commonly K. Elements such as Ba, Sb, B, Bi, Ag, and Cu may also be associated with high gold values.

Although the samples investigated in this study did not contain gold or silver in the polished sections, the Laroma Prospect has been investigated by several property holders for its gold content with many assays returning elevated Au. Interestingly, historic assessment reports have only ever documented gold grade and not base metal nor PGE potential. There were a number of differernt Ni-sulphides encountered through the investigation including: Ni-S (vaesite), As-Ni-Sb-S, As-Ni-Co-Sb-S, Sb-Ni-As-S, and Ni-As-S. Once these Ni-sulphides and sulphosats were determined with the microprobe, the hand samples were tested with Dimethylglyoxime (Ni-testing powder) to confirm the observations. When the Dimethylglyoxime was added to the rock surface, there was an instant reaction which is evident by the purple-pink tinge shown in the following images. Samples which have reacted with the powder have been plotted on the map presented in Figure 8.

Cobalt and nickel mineralization has been noted in the Bou Azzer ophiolite in Moracco which contains listwanite formed along the margin of a large serpentinite unit wth quartz-carbonate lenses hosting cobalt-nlckel arsenide mineralization. It represents a type of listwanitic cobalt-nickel deposit with accessory gold (Leblanc, 1986). A type of Co- Ni arsenide deposit with accessory gold and no silver can be recognized in ultrarnafic massifs of upper mantle origin. They consist of quartz -carbonate lenses with Co (Ni -Fe) arsenides where gold is related to skutterudite (Co-Ni-As) and gold content increases and correlates with the Co arsenide concentration (Leblanc, 1986).

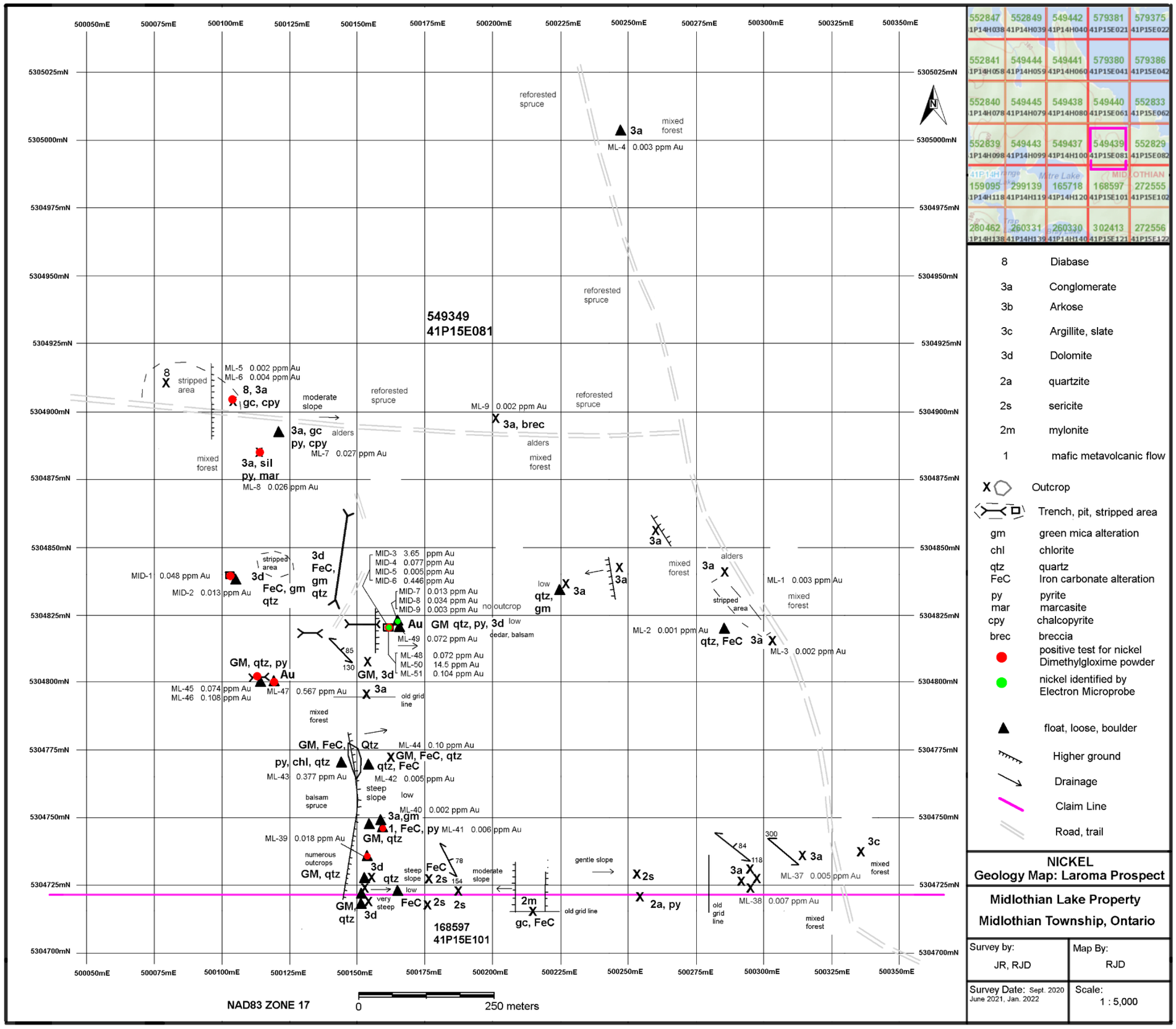

Figure 8: Locations with Ni-sulphides identified by Electron Microprobe and Dimethylglyoxime (Ni-testing) powder.

Conclusions

(1) The Laroma Prospect and the Midlothian Property should be considered for its Ni-Co-Sb-As content in addition to its gold tenor.

(2) Co-Ni arsenide deposit without much silver but with gold may be hydrothermal products derived from ultramafic rocks of mantle origin.

(3) Literature states gold-bearing arsenide deposits are located along suture/fault zones. The Midlothian Property and the Laroma Prospect are located along the western extension of the Larder Break.

(4) The host rocks containing dominantly carbonate-quartz and Cr-paragonite on the Midlothian Property can be referred to as Listwanites.

Recommendations

In addition to further prospecting, ground magnetics, and VLF surveys, it is recommended that a further study of the carbonate and Cr-paragonite mineralogy be undertaken. A comprehensive investigation of the micas and the Cr-paragonite to establish if there are differeing compositions including Cr-phengitic muscovite and whether there may be an association to the gold. Also interrogating the carbonate species may help vector toward higher grade Ni-Co-Sb contents and possibly gold.

A budget for the proposed work includes:

Budget

Prospecting (2 Geologists)……$20,000
Assays and Geochemistry……15,000
Ground Magnetometer Survey……25,000
VLF Survey……25,000
Petrographic Investigation of Micas and Carbonates……20,000
Line Cutting……20,000

$125,000

Respectfully Submitted, Dr. Jim Renaud, P.Geo

January 30, 2022

References

Bright, E. G. 1970. Geology of Halliday and Midlothian Townships. Geological Report 79. Ontario Department of Mines.

Buckman, Solomon & Ashley, Paul, 2010. Silica-Carbonate (Listwanites) Related Gold Mineralization Associated with Epithermal Alteration of Serpentinite Bodies.

Buisson, G., and Leblanc, M., 1987. Gold in mantle peridotites from Upper Proterozoic ophiolites in Arabia, Mali, and Morocco. Economic Geology, 82, 2091-2097.

Dillman, R.J., and Renaud, R., 2022. Report on a Prospecting Traverse, Midlothian Lake-Mitre Lake Area Midlothian Lake Property: Larder Lake Mining Division Midlothian Township, Ontario.

Leblanc, M., 1986. Co-Ni Arsenide Deposits, with Accessory Gold, in Ultramafic Rocks from Morocco; Canadian Journal of Earth Sciences, Volume 23, pages 1592-1602.

Pipino, G., 1980. Gold in Ligurian ophiolites, Italy. In: A. Panayiotou (ed.), Ophiolites; Proceedings, International Ophiolite Symposium, Cyprus Ministry of Agriculture and Natural Resources Geological Survey Department, Nicosia, Cyprus, pp. 765-773.

Préfontaine, S. and Robichaud, L. 2013. Precambrian geology of Midlothian Township; Ontario Geological Survey, Preliminary Map P.3772, scale 1:20 000.

Prefontaine, S., 2011. Geology and mineral potential of Midlothian Township, Halliday Dome, Abitibi greenstone belt; in Summary of Filed work and other activities 2011, Ontario Geological Survey, Open File Report 6270, p 4-1 to 4-12.

Smith, P.E., Schandl, E.S. and York, D, 1993. Timing Of Metasomatic Alteration Of The Kidd Creek Massive Sulphide Deposit, Ontario, Using 40Ar739Ar Laser Dating Of Single Crystals Of Fuchsite. Economic Geology, Special Issue: Abitibi Ore Deposits in A Modern Context, v. 88, p. 1636-1645.

Specimen Notes for 'ML-50'

The rock is dominated by ankerite solid carbonate 60% dolomite-solution 10% intergrown with quartz and 25% polycrystalline paragonite Cr-bearing also fine-mica. There are disseminations grained barite of apatite hosting rock has been inclusions. The coarse-grained cut by late stage quartz veins. polycrystalline sample appear Areas of the Cr-mica growth to have clots of carbonate sealed by the possibly groundmass

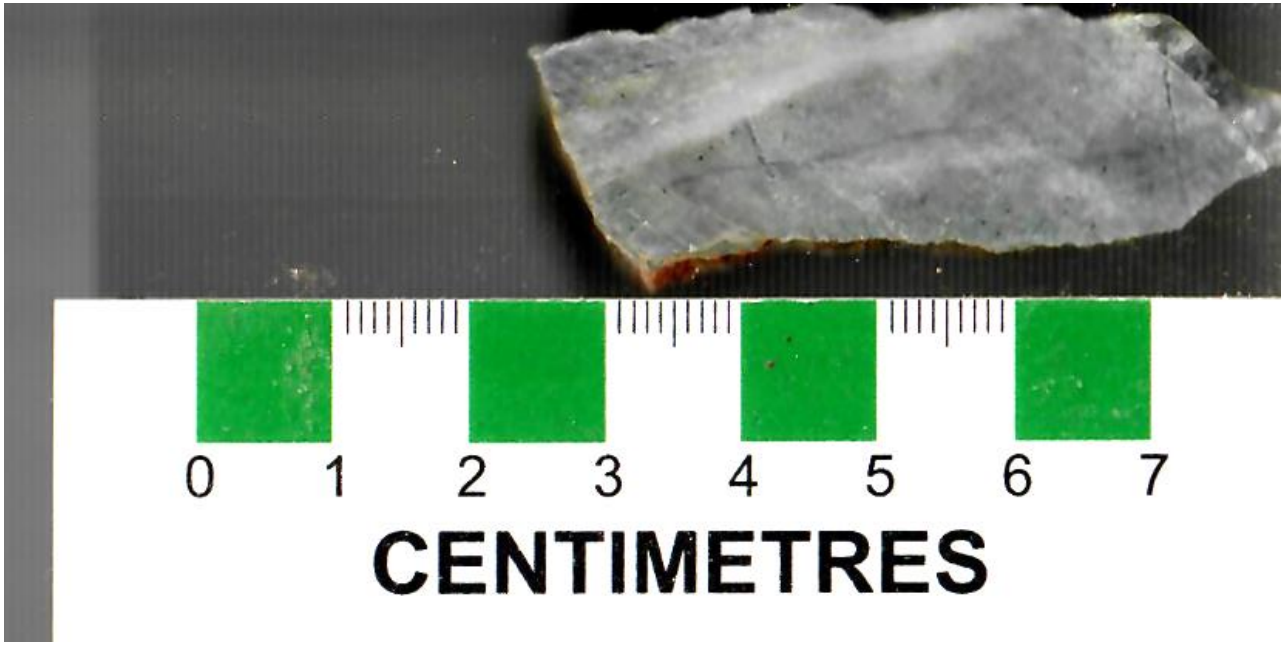

suggesting some brecciation and sealing. There appears to be evidence of the As-Ni-Sb-Co-S mineral growth on the periphery of the Cr-mica clots suggesting a possible hydrothermal growth scenario for both the Cr-mica and sulphides. The sulphide inventory of the rock consists of minute grains of Pb-Sb-oxide, galena, Fe-sphalerite, and zoned grains of As-Ni-Sb-S (possibly Sb-Gersdorffite) and As-Ni-Co-Sb-S (possibly Co-Gersdorffite) minerals.

Handspecimen of sample ML-50

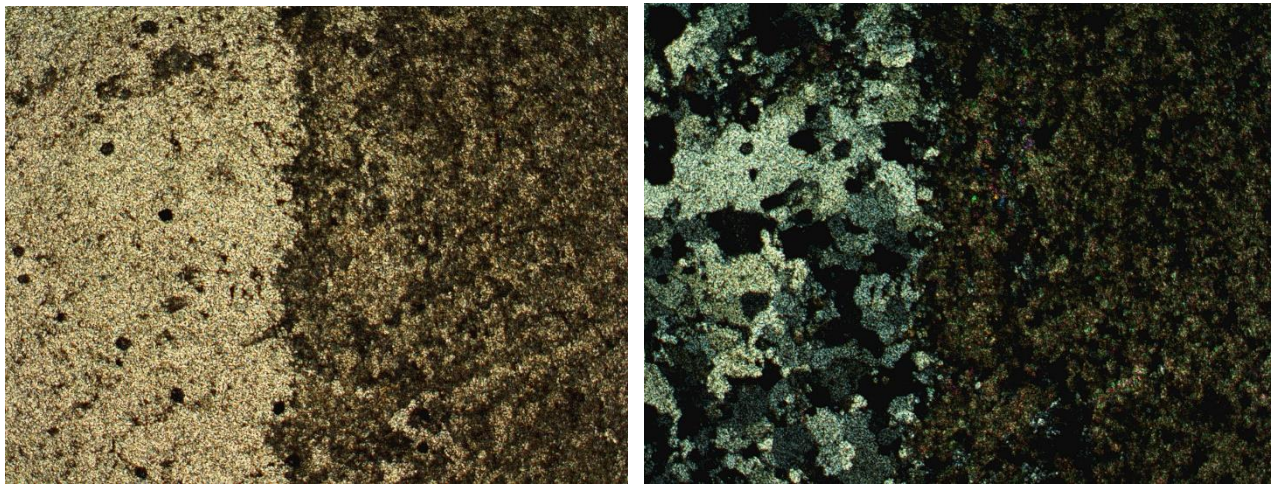

Plane light photomicrograph (left) and crossed polarized image (right) illustrating the dominant carbonate groundmass in the rock intergrown with Cr-paragonite mica (right side of image) cut by a later coarser-grained polycrystalline quartz vein (left side of image). Field of View = 9mm

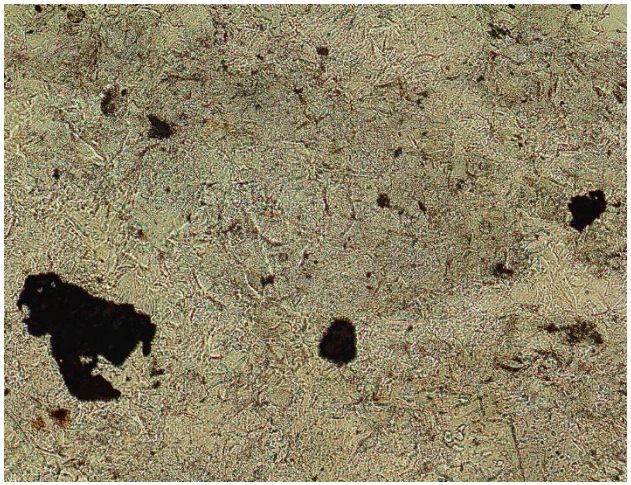

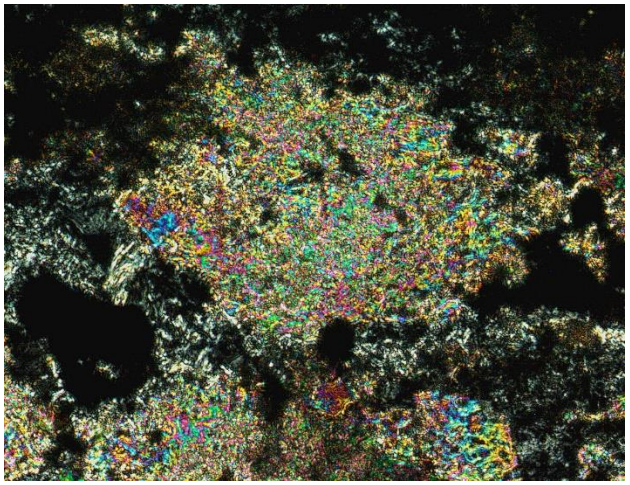

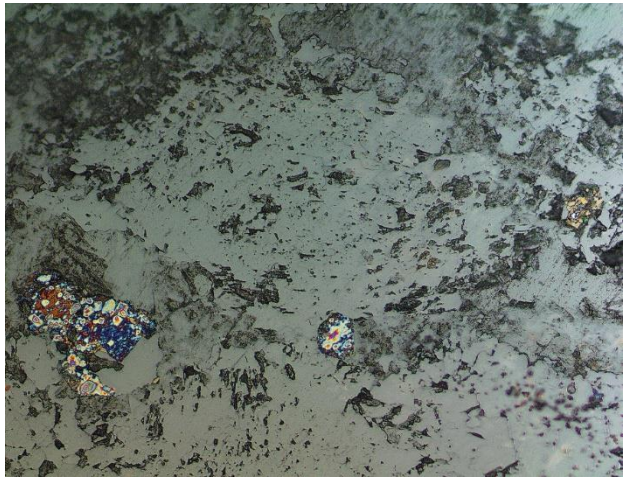

Plane light image (top left) and crossed polarized image (top right) illustrating clots of highly birefringent Cr-paragonite mica sealed within a quartz, Cr-paragonite, dolomite-ankerite solid solution groundmass. The reflected light image (bottom) illustrates three grains of the complicated As-Ni-Sb-Co-S grains growing on the margin of the mica domain suggesting a possible hydrothermal origin for the sulphides and Cr-micas. Field of view = 2.2mm

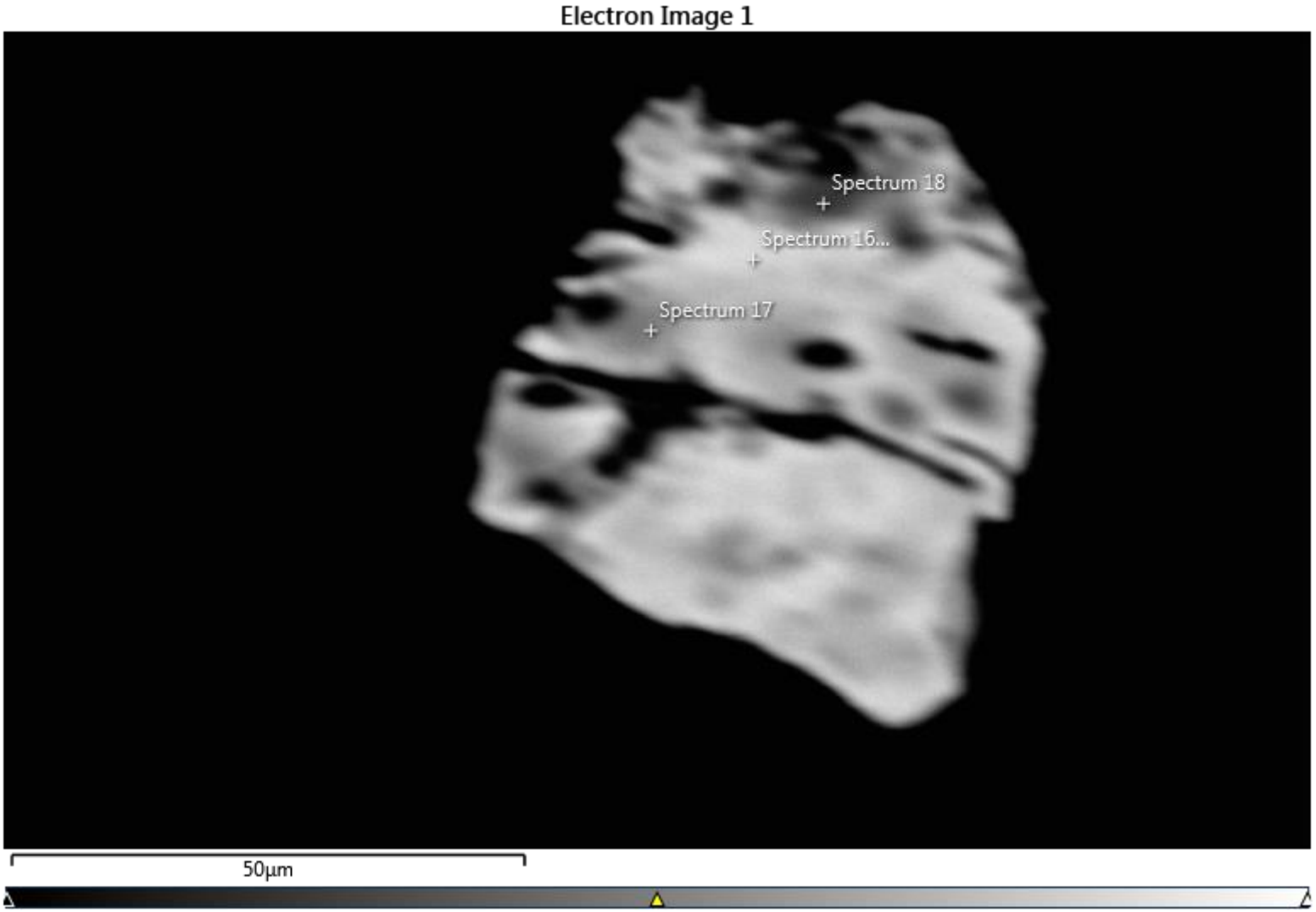

Backscatter image of a domainally zoned grain of As-Ni-Sb-S (spectrum 16), As-Ni-Co-Sb-S (spectrum 17), Fe-Ni-As-Co-Cu-S (spectrum 18).

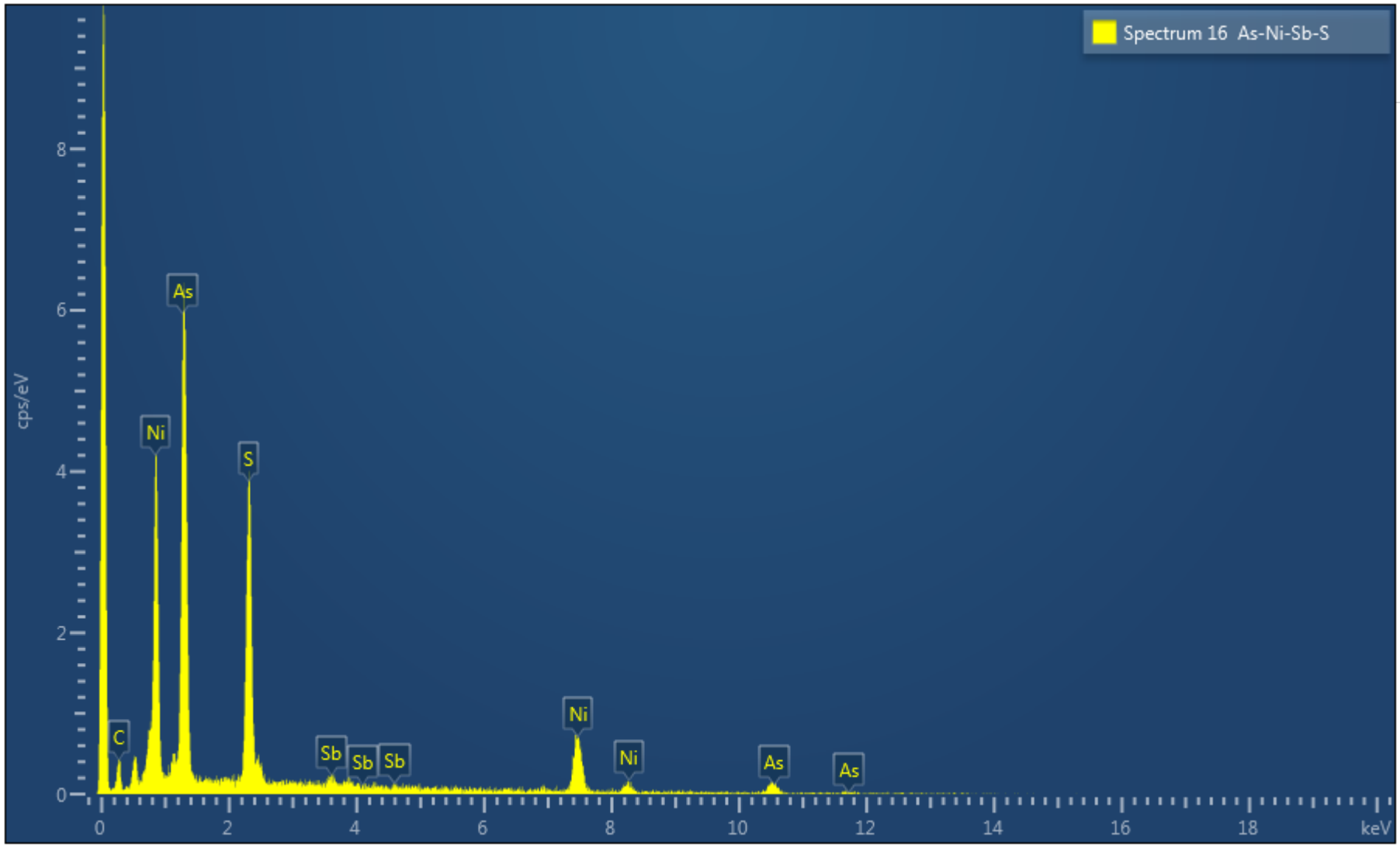
Spectrum 16 As-Ni-Sb-S
cps/eV
0
2
4
6
8
C
Ni
As
S
Sb
Sb
Sb
Ni
Ni
As
As
0
2
4
6
8
10
12
14
16
18
keV

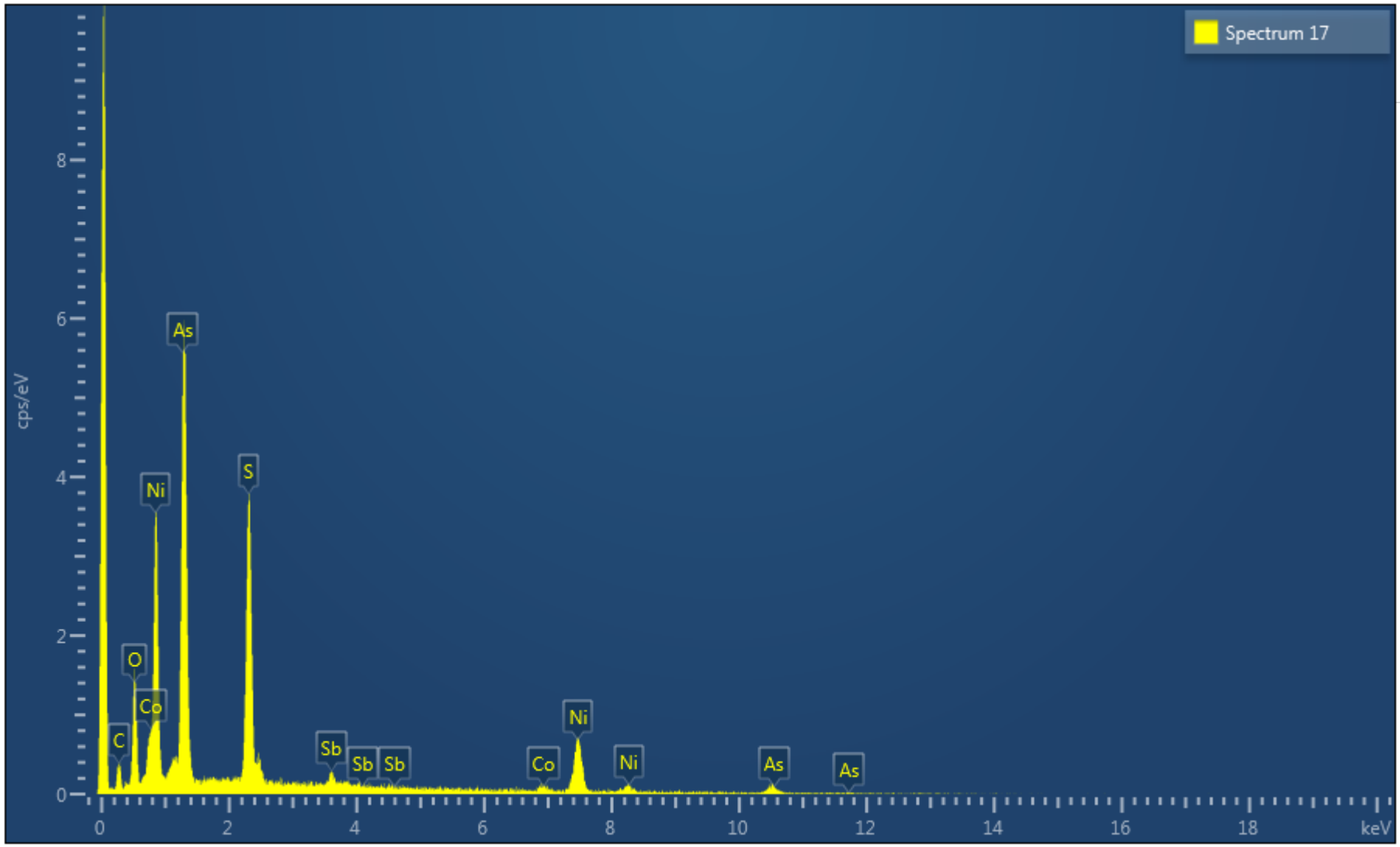
Spectrum 17
cps/eV
0
2
4
6
8
0
2
4
6
8
10
12
14
16
18
keV
C
O
Co
Ni
As
S
Sb
Sb
Sb
Co
Ni
Ni
As
As

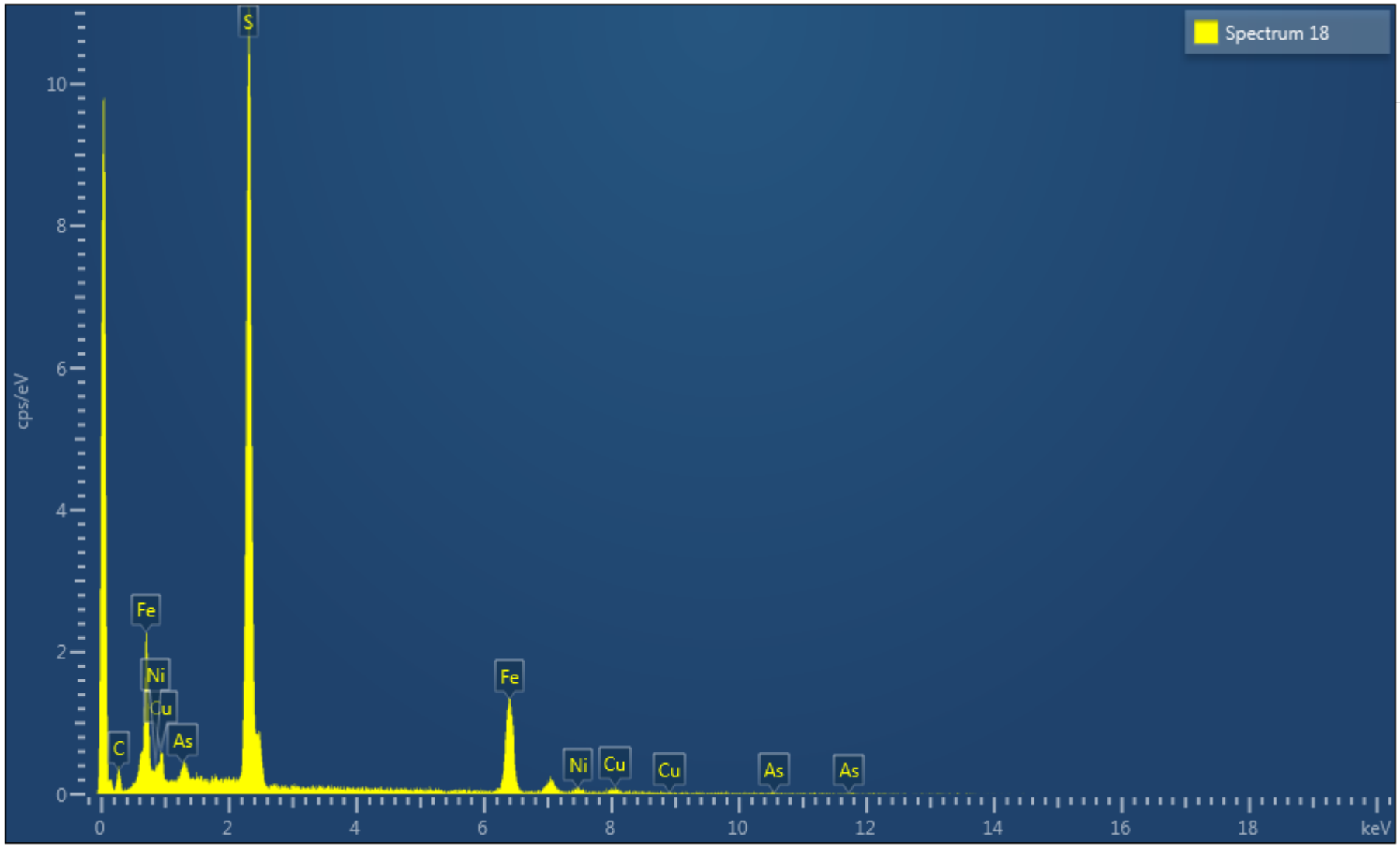
Spectrum 18
cps/eV
keV
S
Fe
Ni
Cu
As
C
Fe
Ni
Cu
Cu
As
As
0
2
4
6
8
10
12
14
16
18

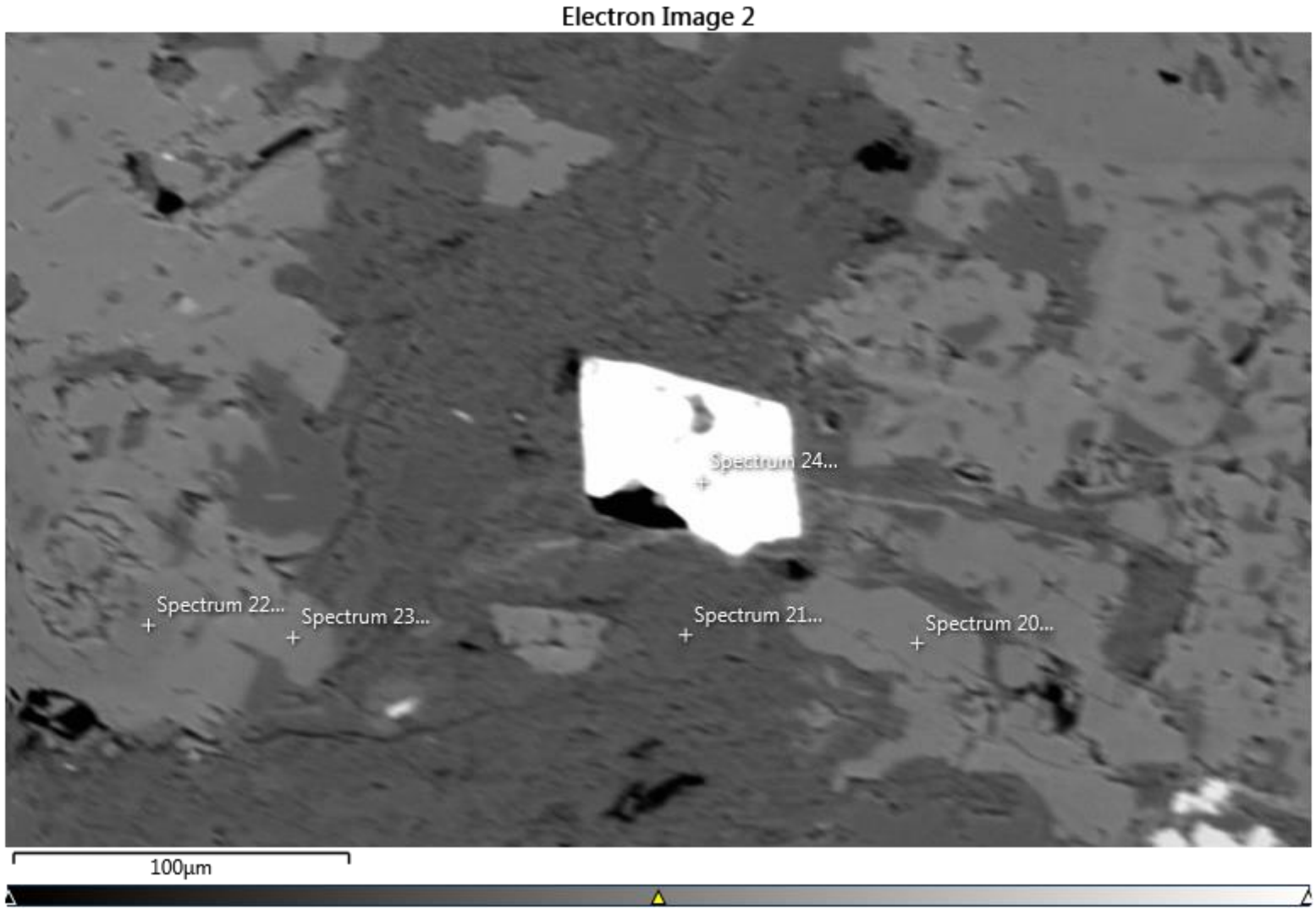

Backscatter image illustrating compositionally zoned dolomoite-ankerite solid solution carbonate (spectrum 20) intergrown with coarse Cr-paragonite mica (spectrum 21) hosting a coarse grain of As-Ni-Sb-S (spectrum 24).

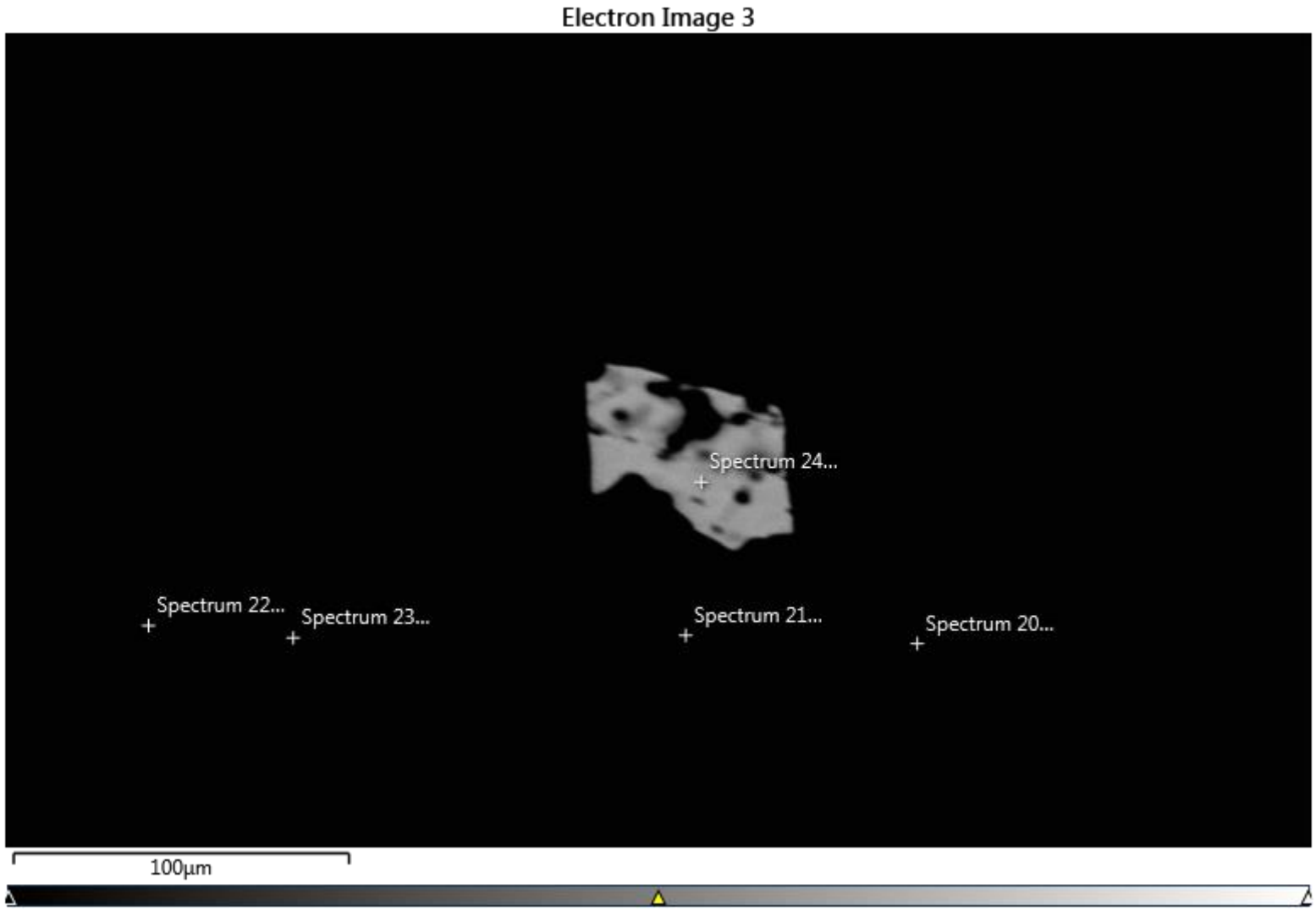

Same backscatter image as above with brightnest intensity reduced to illustrate the dark and bright compositional variation in the As-Ni-Sb-S grain (spectrum 24).

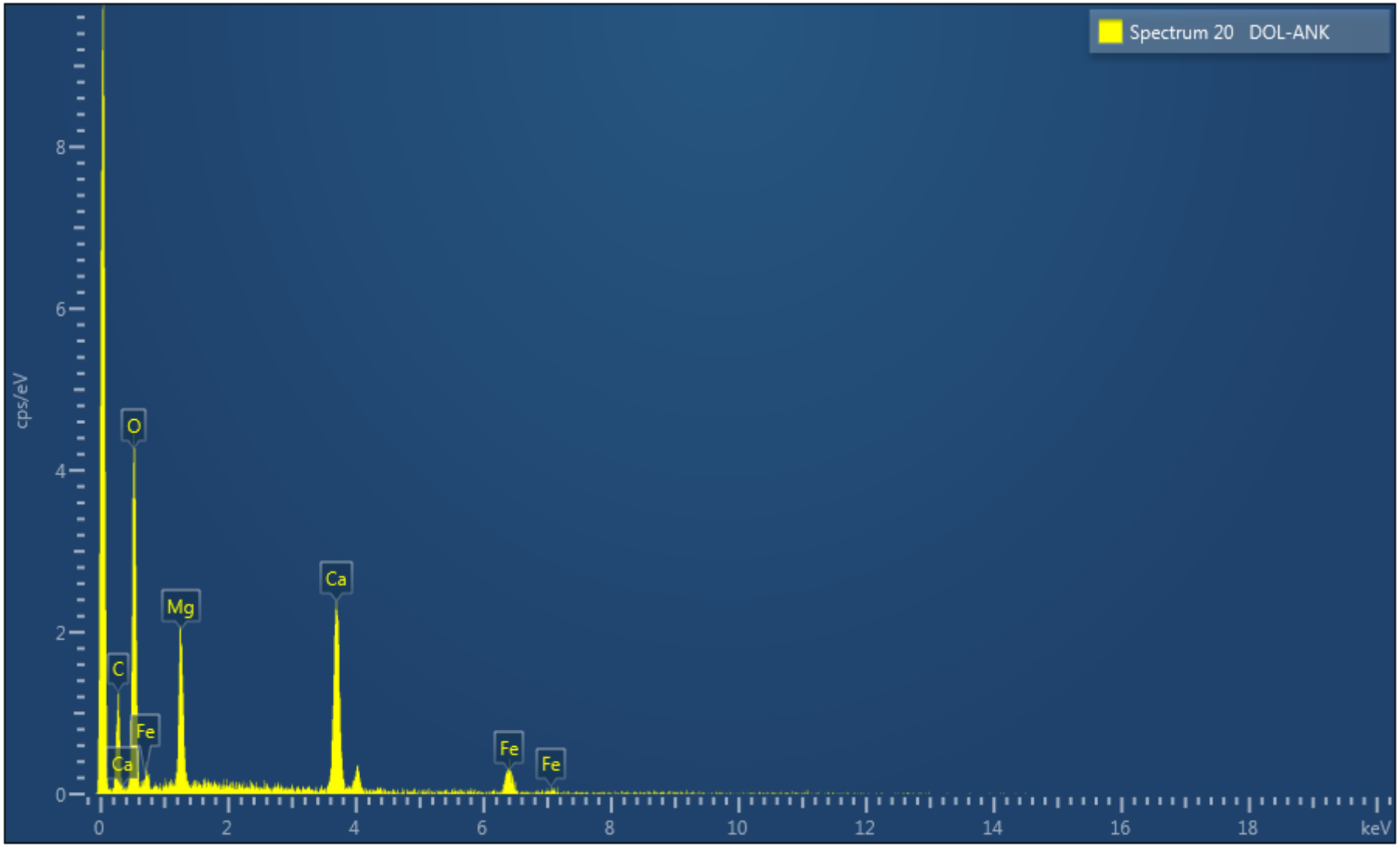
Spectrum 20 DOL-ANK
cps/eV
0
2
4
6
8
O
C
Ca
Fe
Mg
Ca
Fe
Fe
0
2
4
6
8
10
12
14
16
18
keV

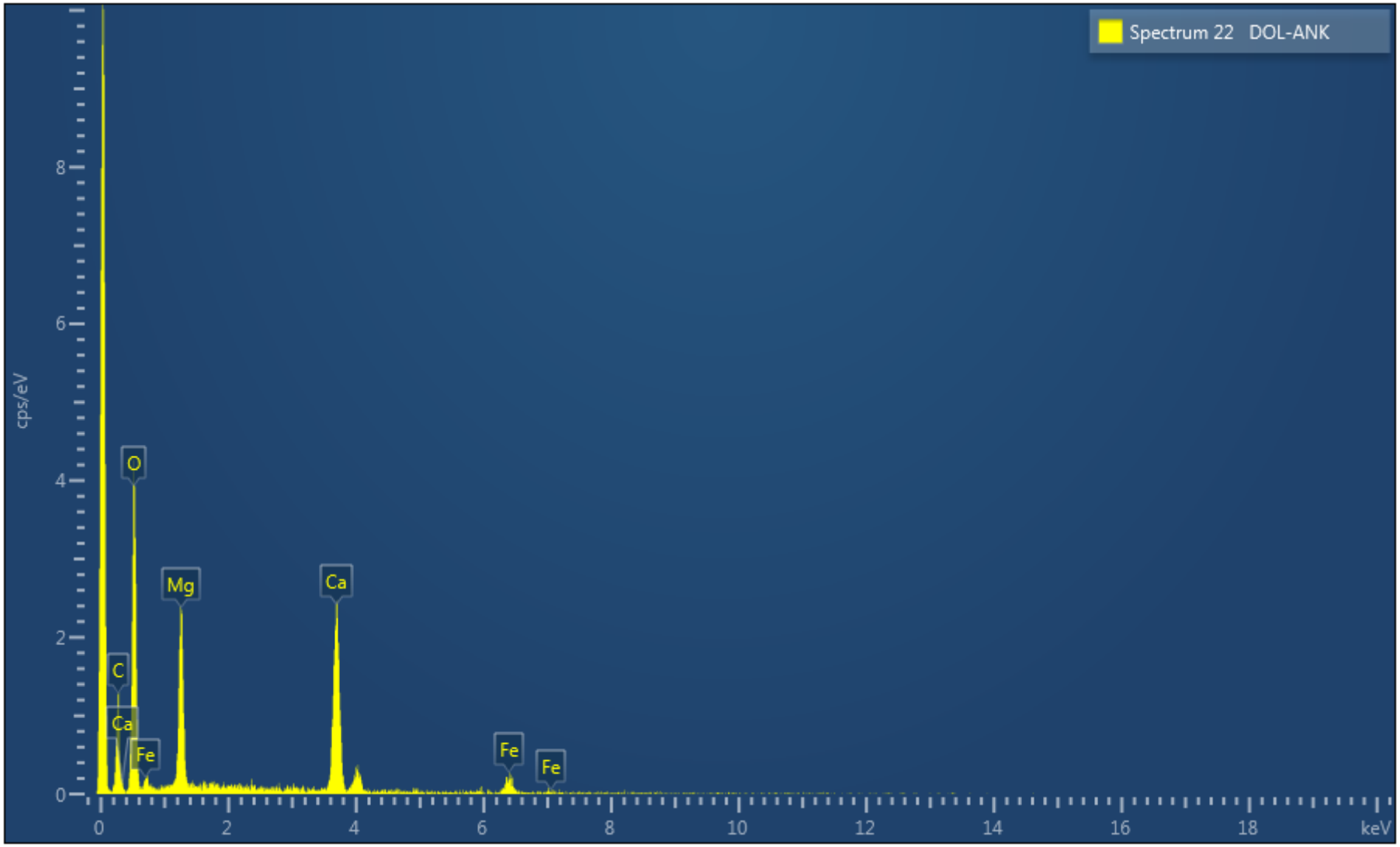
Spectrum 22 DOL-ANK
cps/eV
0
2
4
6
8
O
C
Ca
Fe
Mg
Ca
Fe
Fe
0
2
4
6
8
10
12
14
16
18
keV

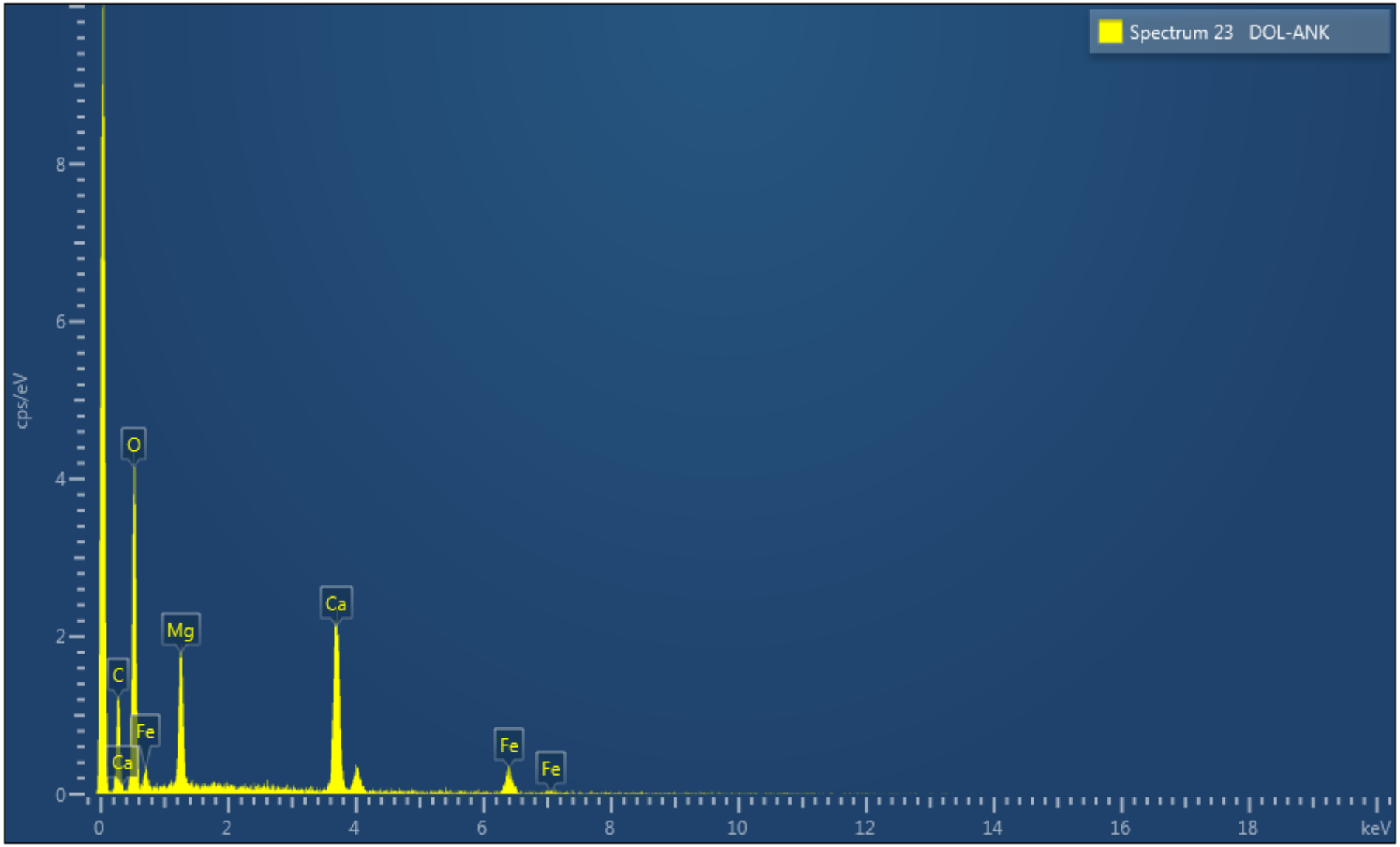
Spectrum 23 DOL-ANK
cps/eV
0
2
4
6
8
O
C
Fe
Ca
Mg
Ca
Fe
Fe
0
2
4
6
8
10
12
14
16
18
keV

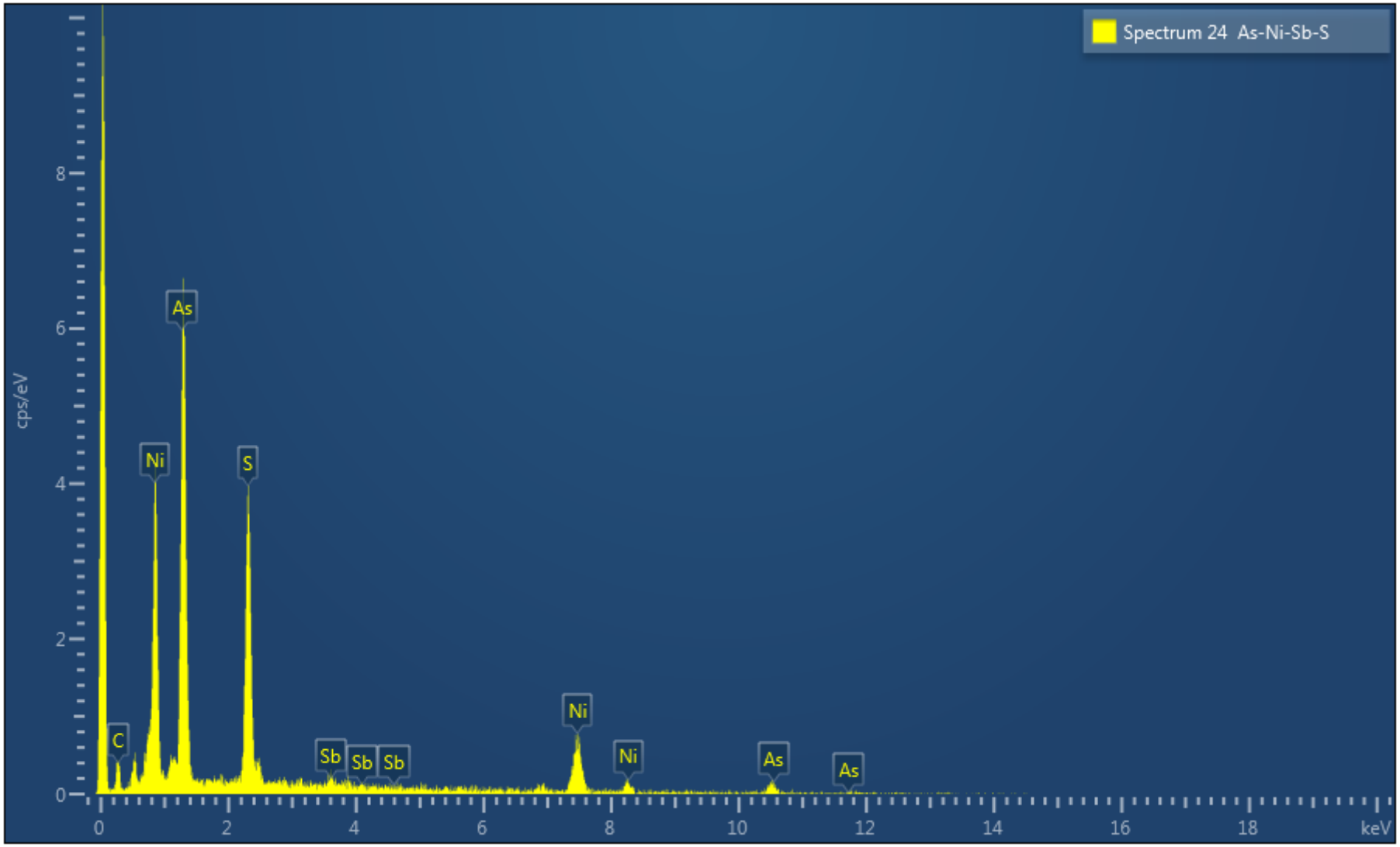
Spectrum 24 As-Ni-Sb-S
cps/eV
0
2
4
6
8
C
Ni
As
S
Sb
Sb
Sb
Ni
Ni
As
As
0
2
4
6
8
10
12
14
16
18
keV

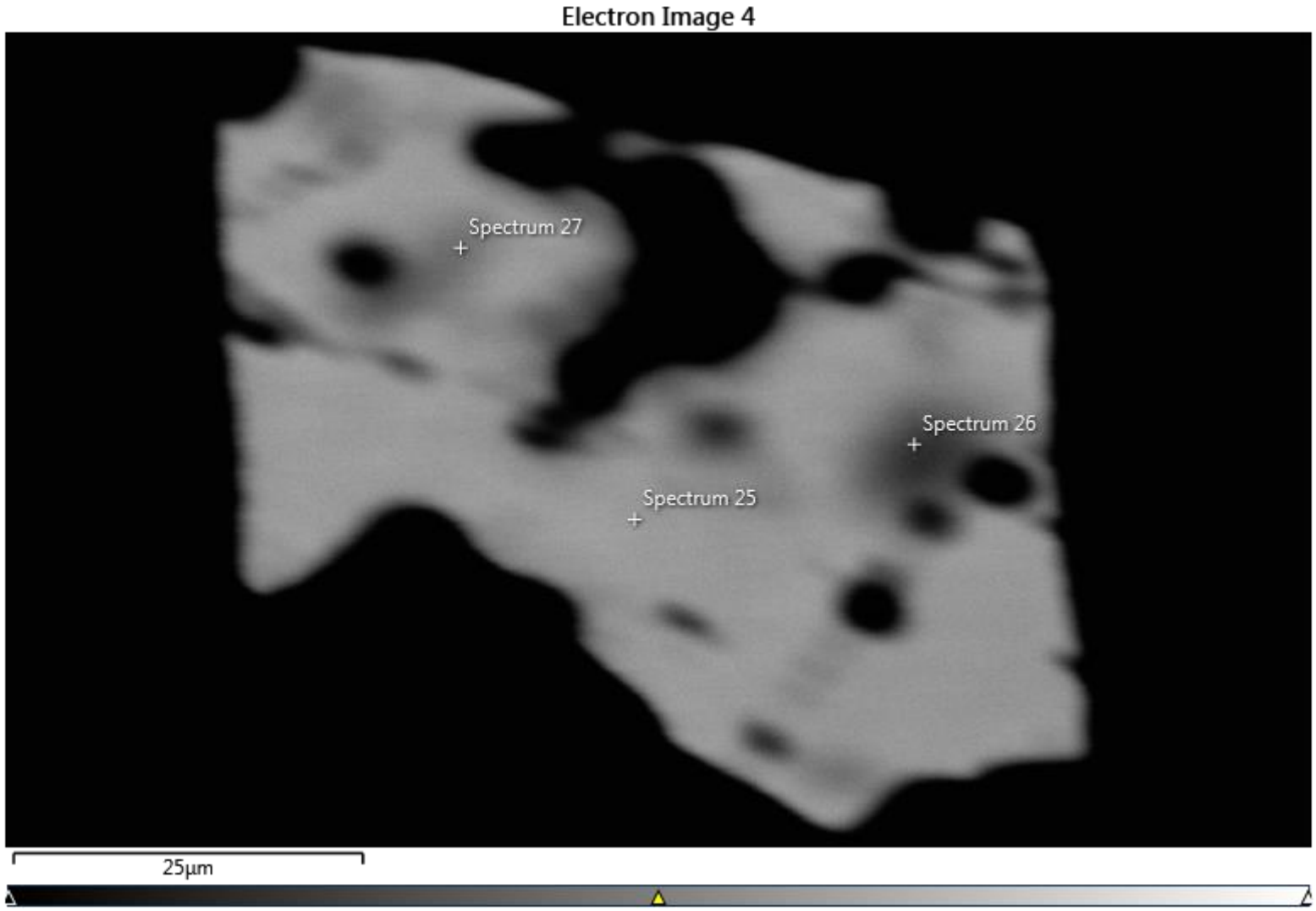

Backscatter image of a compositionally complex grain of Ni-As-S (spectrum 25), Ni-As-Sb-Co-S (spectrum 26), and As-Ni-Sb-Co-S (spectrum 27).

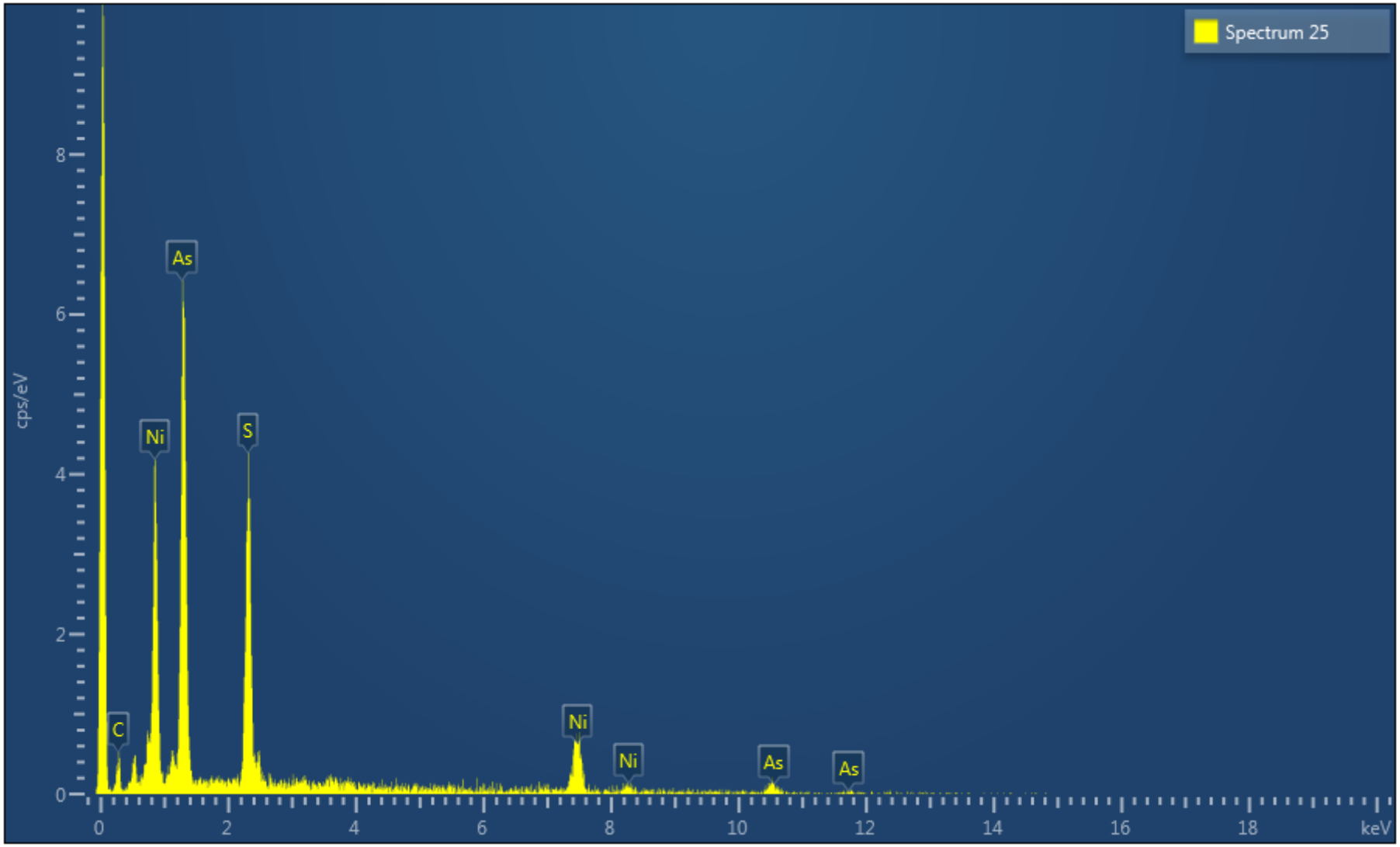
Spectrum 25
cps/eV
0
2
4
6
8
C
Ni
As
S
Ni
Ni
As
As
0
2
4
6
8
10
12
14
16
18
keV

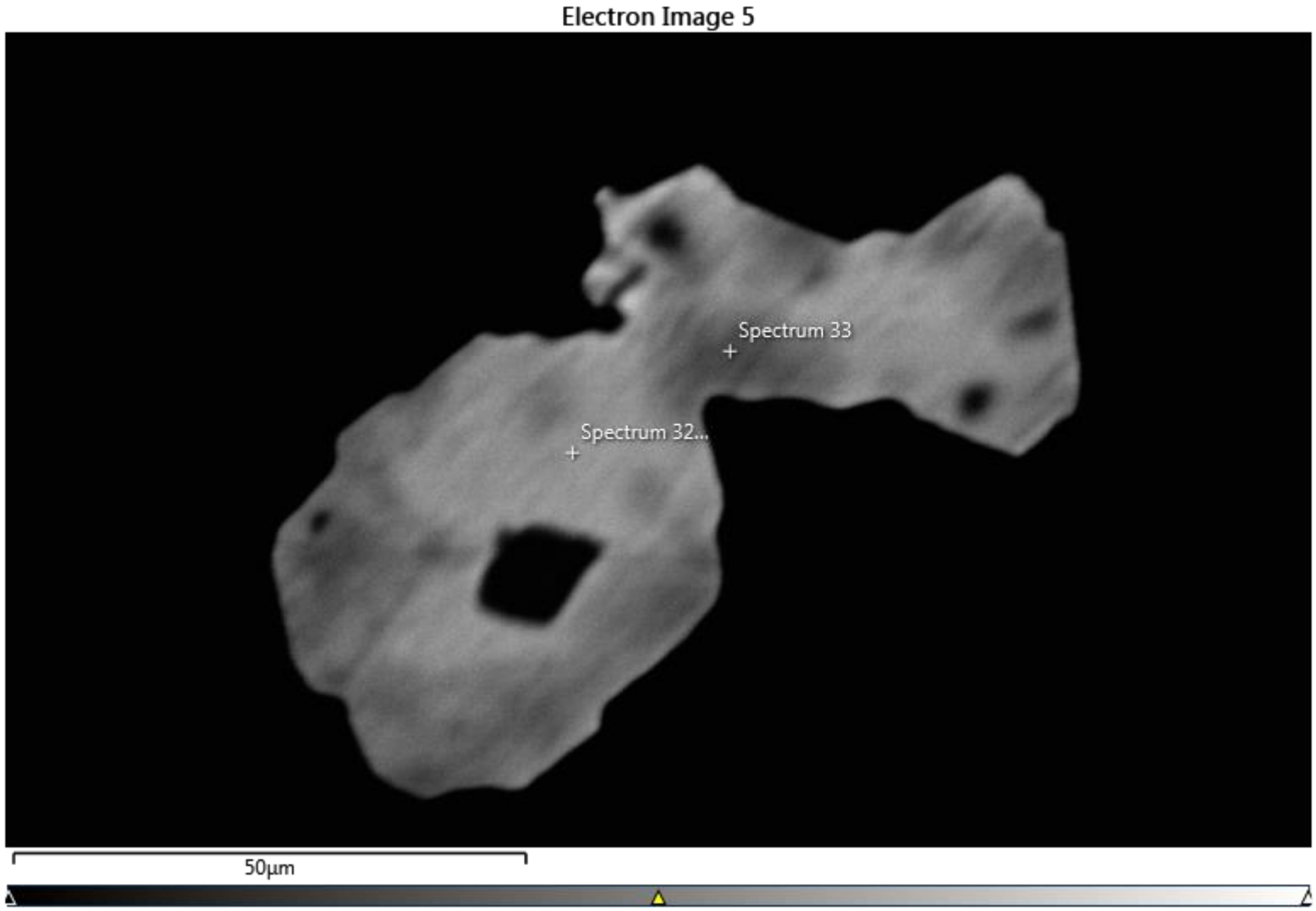

Backscatter image of a grain of As-Ni-Sb-S showing dark and bright compositional variation as a function of the amount of Sb present.

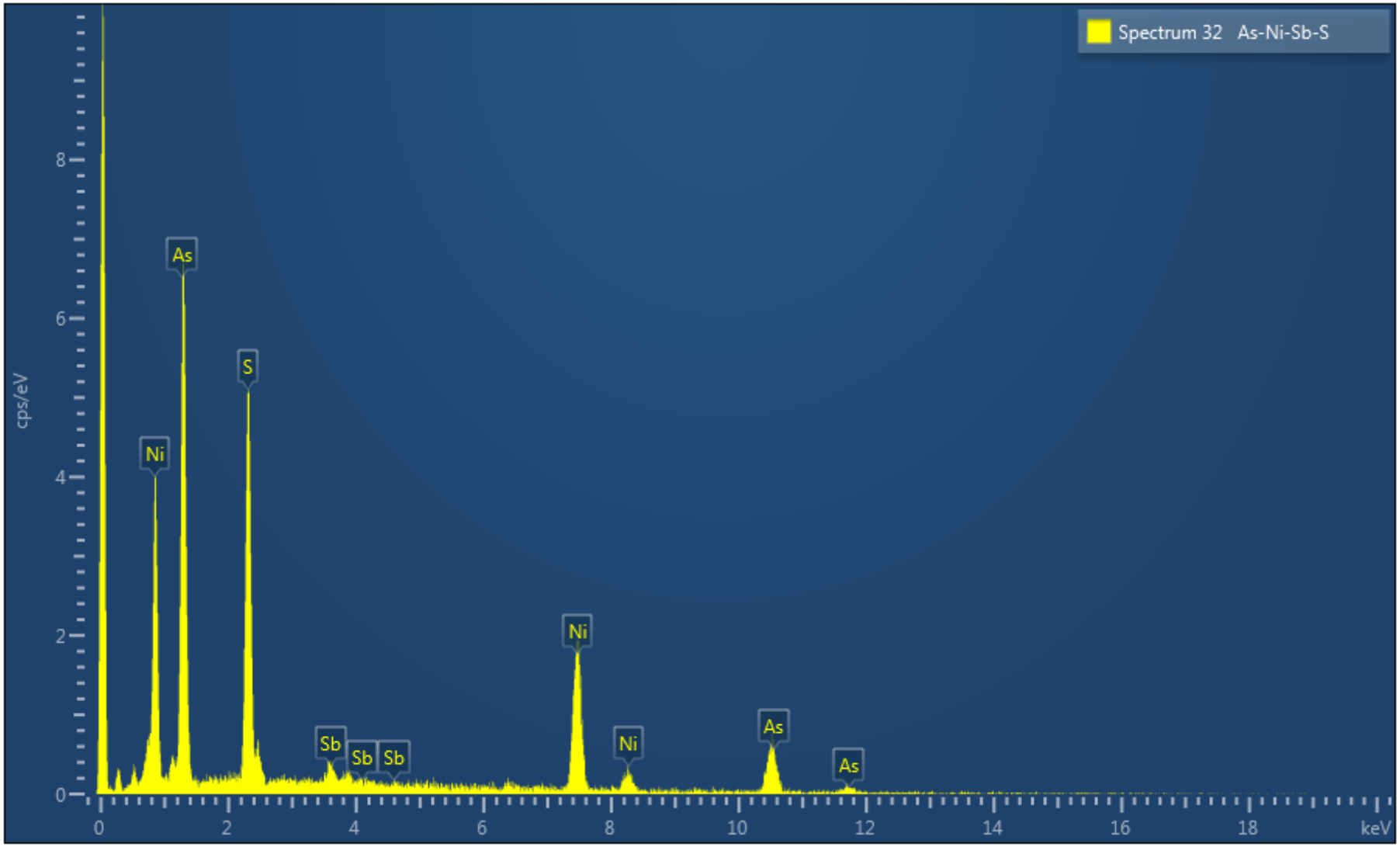
Spectrum 32 As-Ni-Sb-S
cps/eV
0
2
4
6
8
Ni
As
S
Sb
Sb
Sb
Ni
Ni
As
As
0
2
4
6
8
10
12
14
16
18
keV

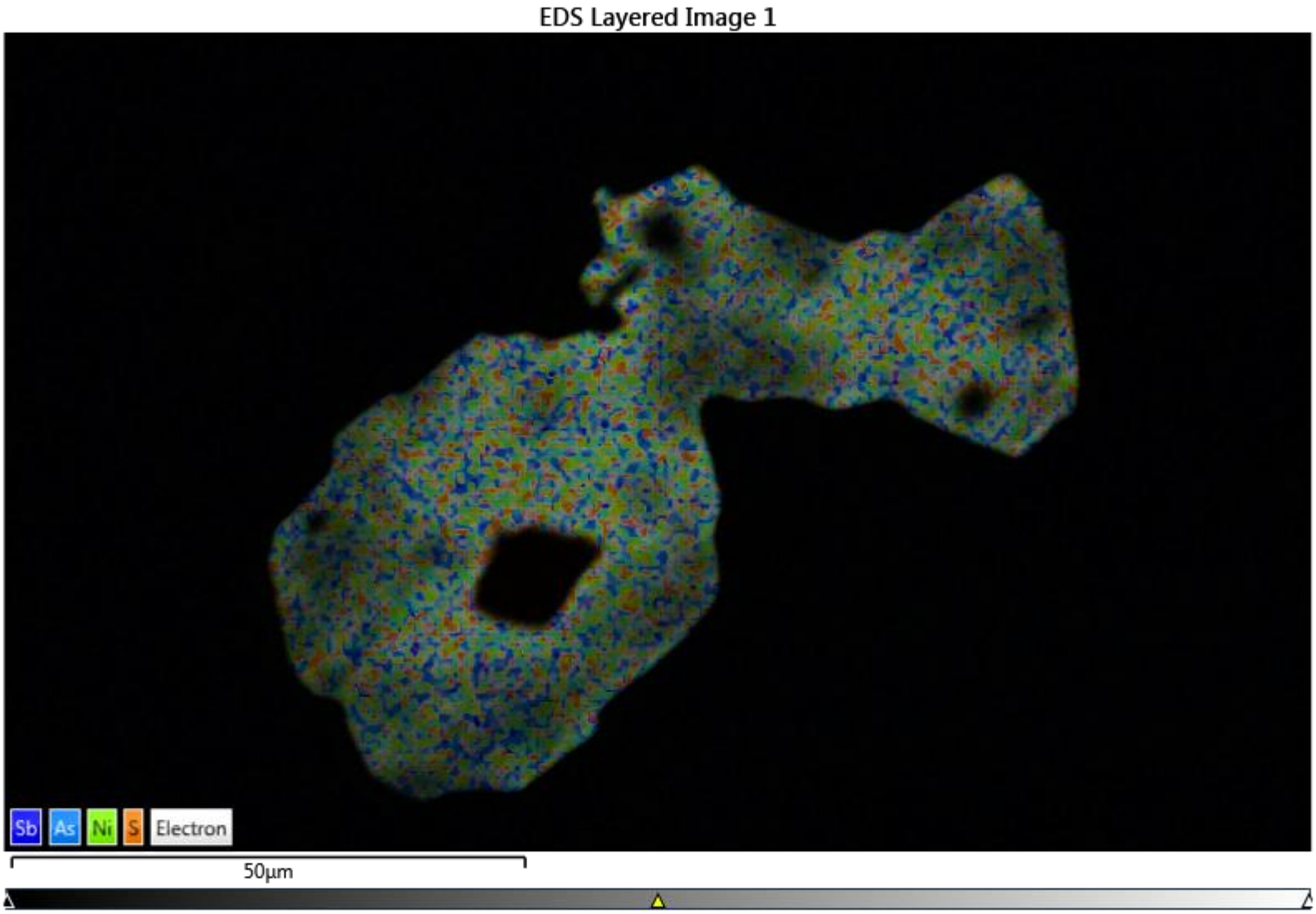

Mineral dot maps illustrating the distribution of the various elements within the grain. Individual maps are presented below.

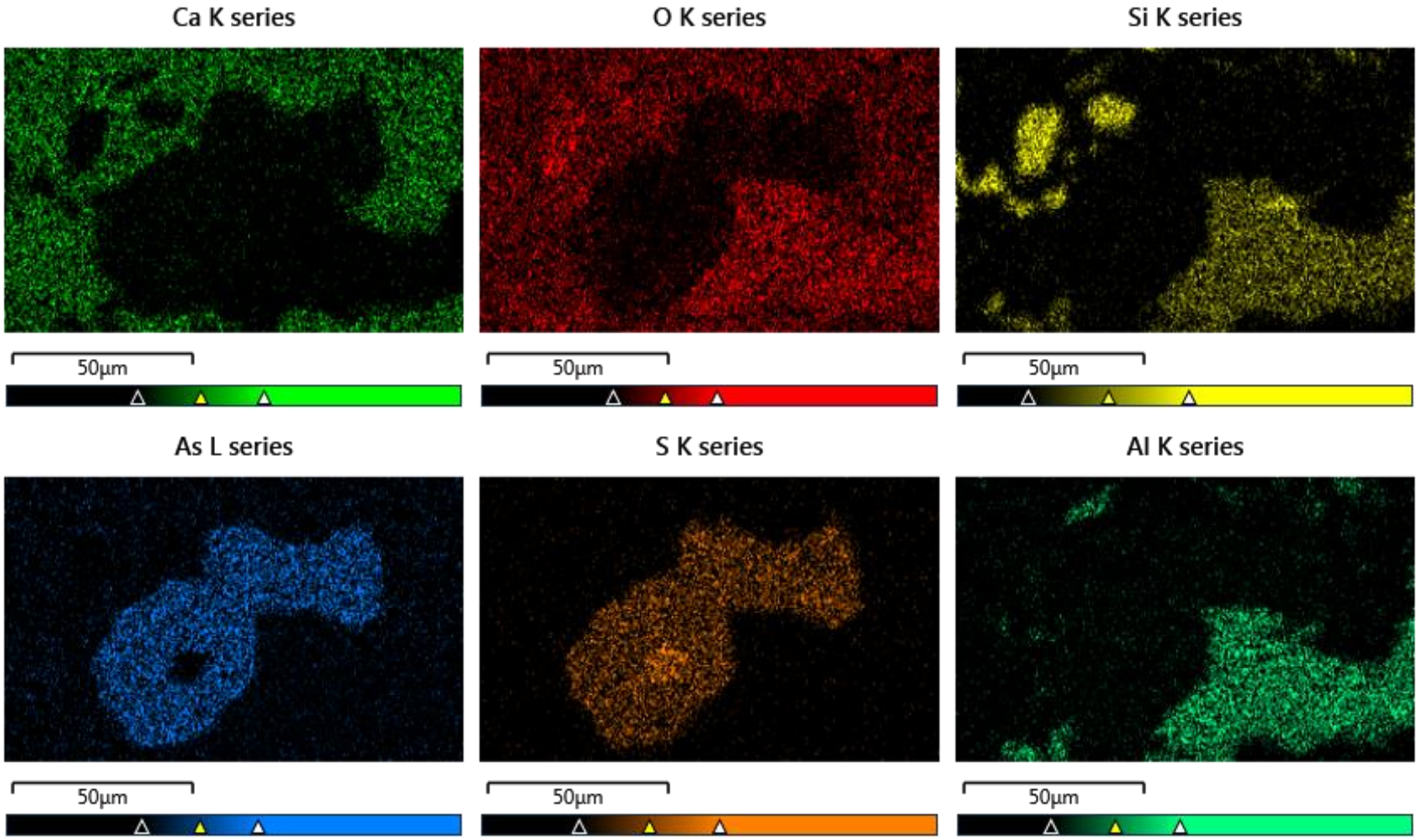
Ca K series
O K series
Si K series
50µm
50µm
50µm
As L series
S K series
Al K series
50µm
50µm
50µm

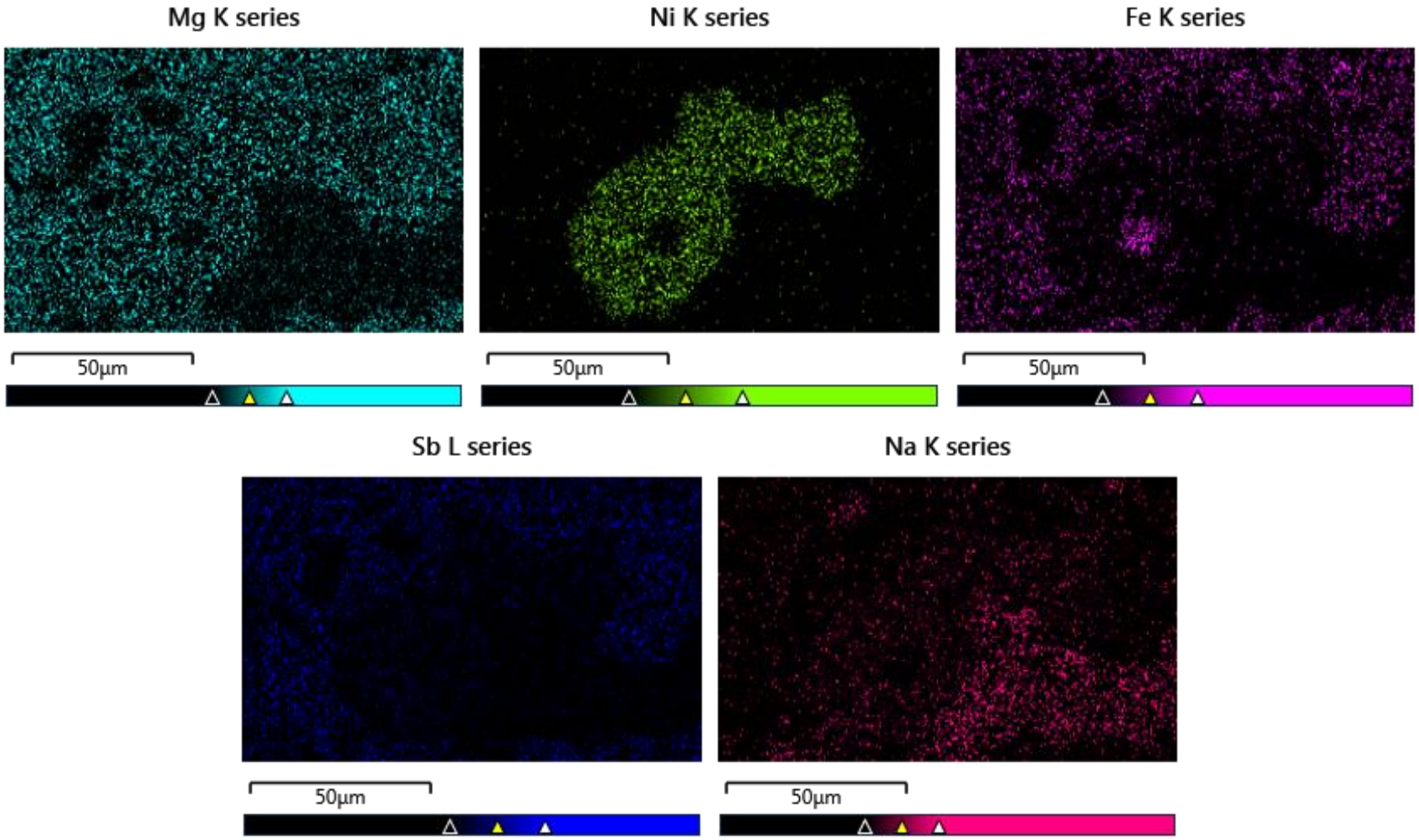
Mg K series
50µm
Ni K series
50µm
Fe K series
50µm
Sb L series
50µm
Na K series
50µm

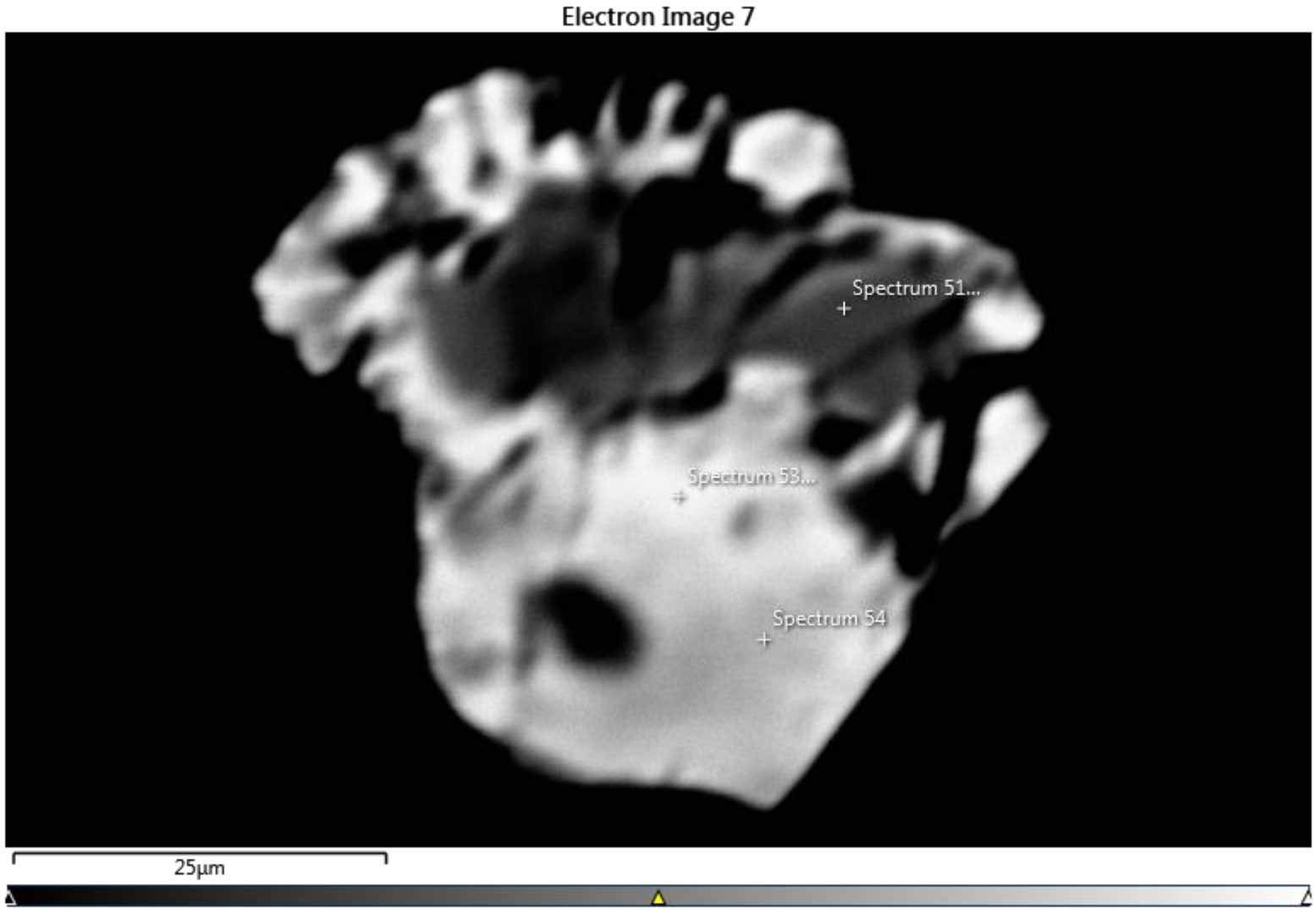

Backscatter image illustrating the complex intergrowth of chalcopyrite (spectrum 51), As-Ni-Co-Sb-S (spectrum 53), and As-Ni-Sb-Co-S (spectrum 54).

Electron Image 8

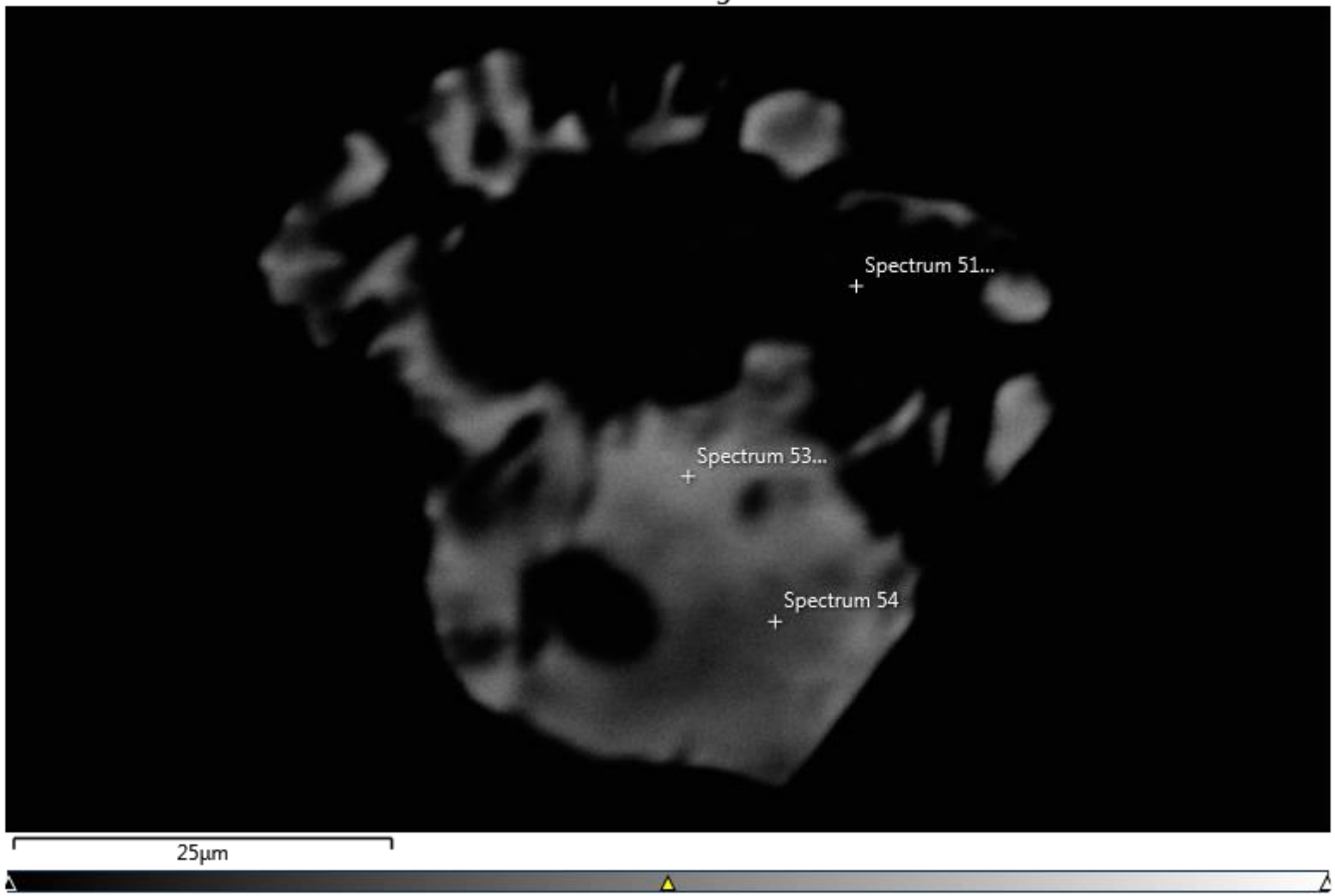

Same image as above with backscatter brightness reduced to better illustrate the compositional zoning within the grain.

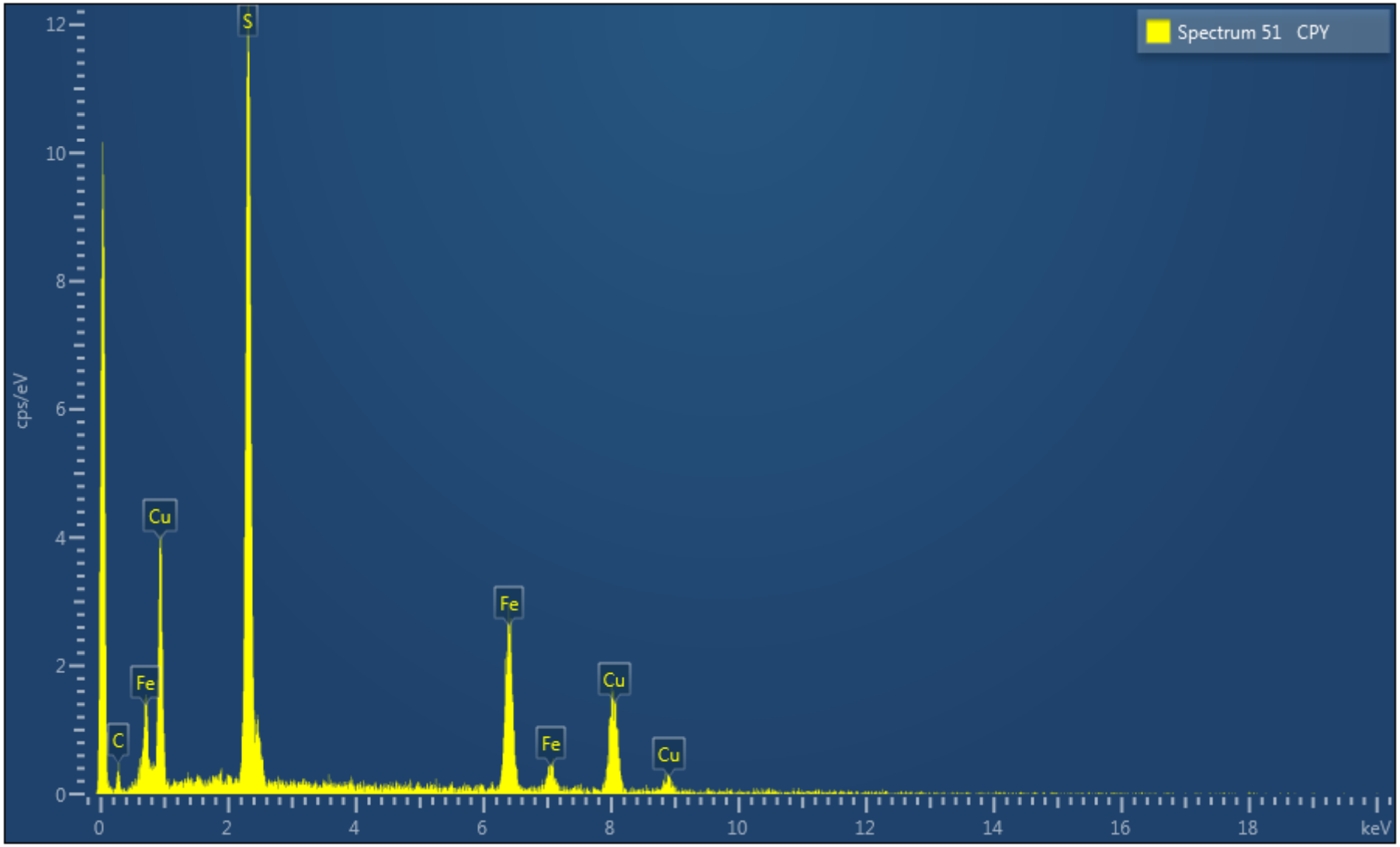
Spectrum 51 CPY
cps/eV
keV
S
Cu
Fe
C
Fe
Fe
Cu
Cu
0
2
4
6
8
10
12
14
16
18
0
2
4
6
8
10
12

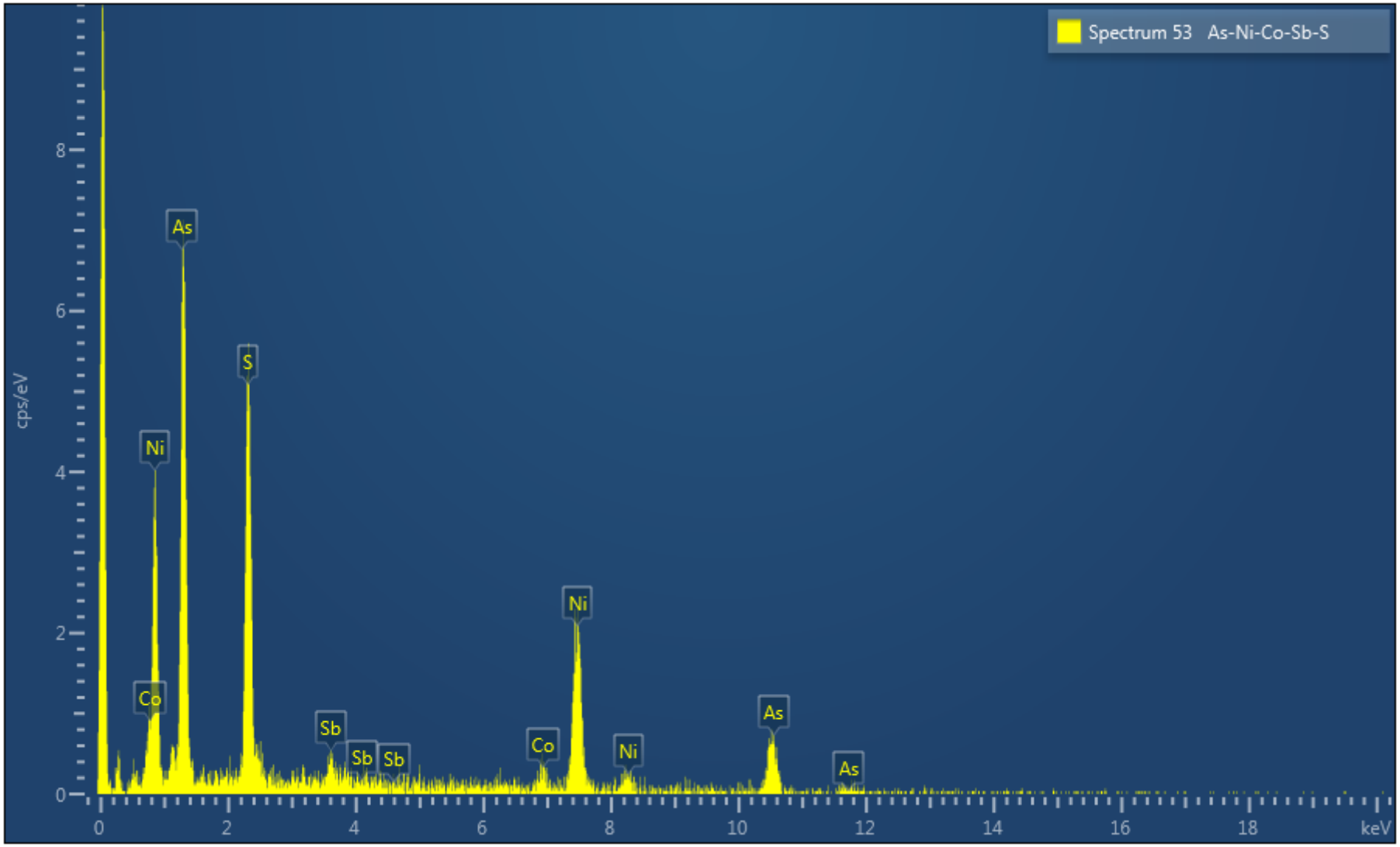
Spectrum 53 As-Ni-Co-Sb-S
cps/eV
keV
As
Ni
S
Co
Sb
Sb
Sb
Co
Ni
Ni
As
As
0
2
4
6
8
10
12
14
16
18

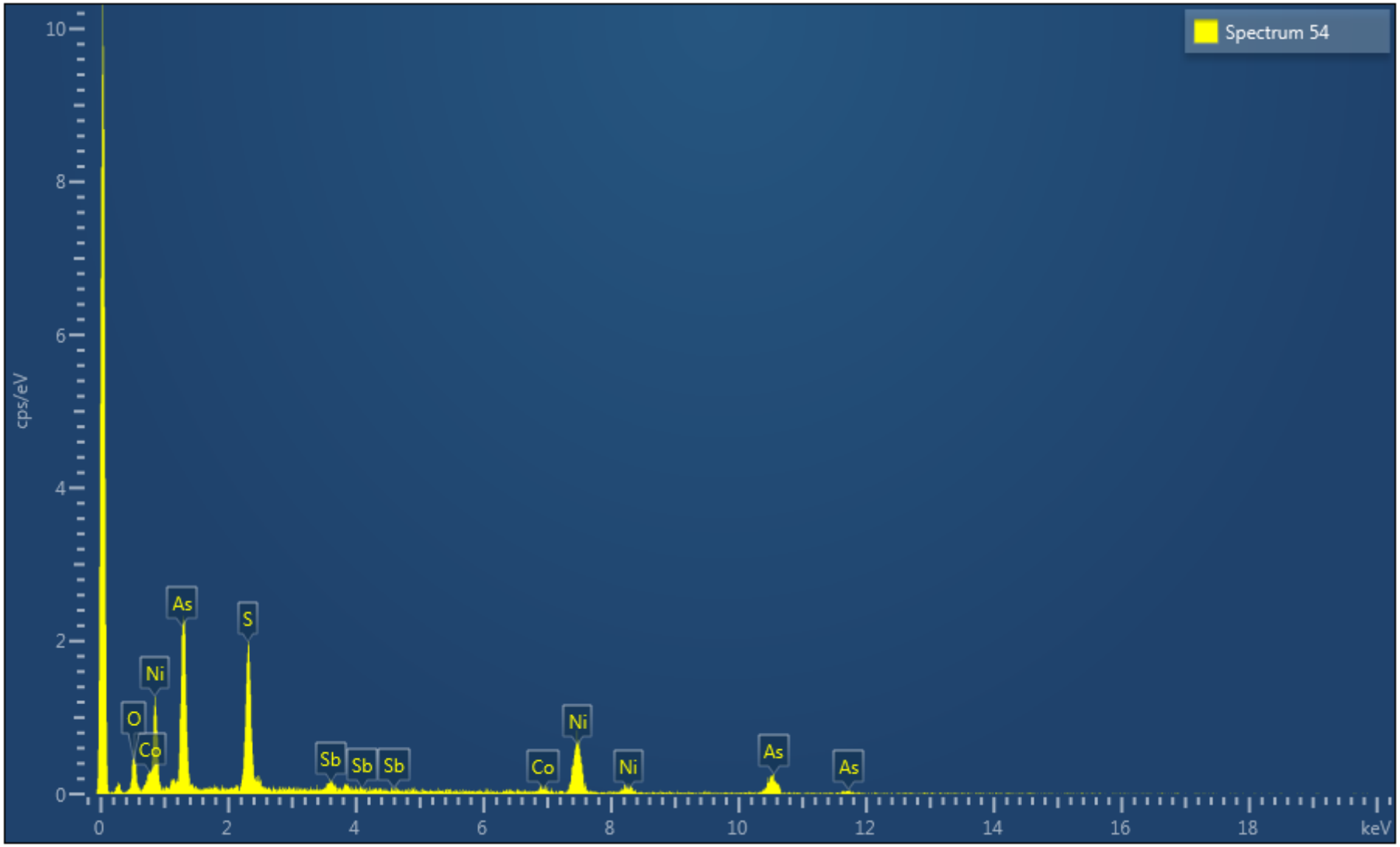
Spectrum 54
cps/eV
10
8
6
4
2
0
0
2
4
6
8
10
12
14
16
18
keV
O
Co
Ni
As
S
Sb
Sb
Sb
Co
Ni
Ni
As
As

Specimen Notes for 'ML-51'

The rock is dominated by 50% dolomite-ankerite solid solution carbonate intergrown with 10% polycrystalline quartz and 40% Cr-bearing paragonite mica. Areas of the sample appear to show the intergrowth of Cr-paragonite with the various carbonate species and some areas have clots of Cr-mica growth sealed by the carbonate groundmass. Some of the Cr-micas have bright areas which appear to carry a hint of Ni. There As-Ni-Sb-S grains with inclusions of Sb-Ni-As-S. There are grains of Ni-S (possible vaesite) with rinds of As-Ni-Sb-S. The sulphide inventory also hosts grains of Sb-Ni-As-Te-S within the complicated carbonate groundmass.

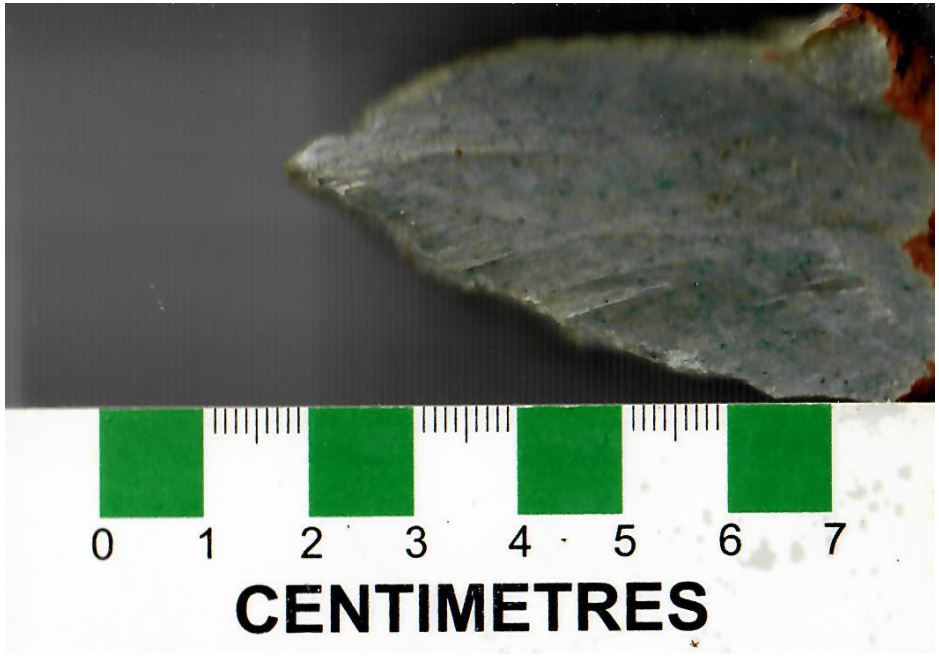

Handspecimen of ML-51.

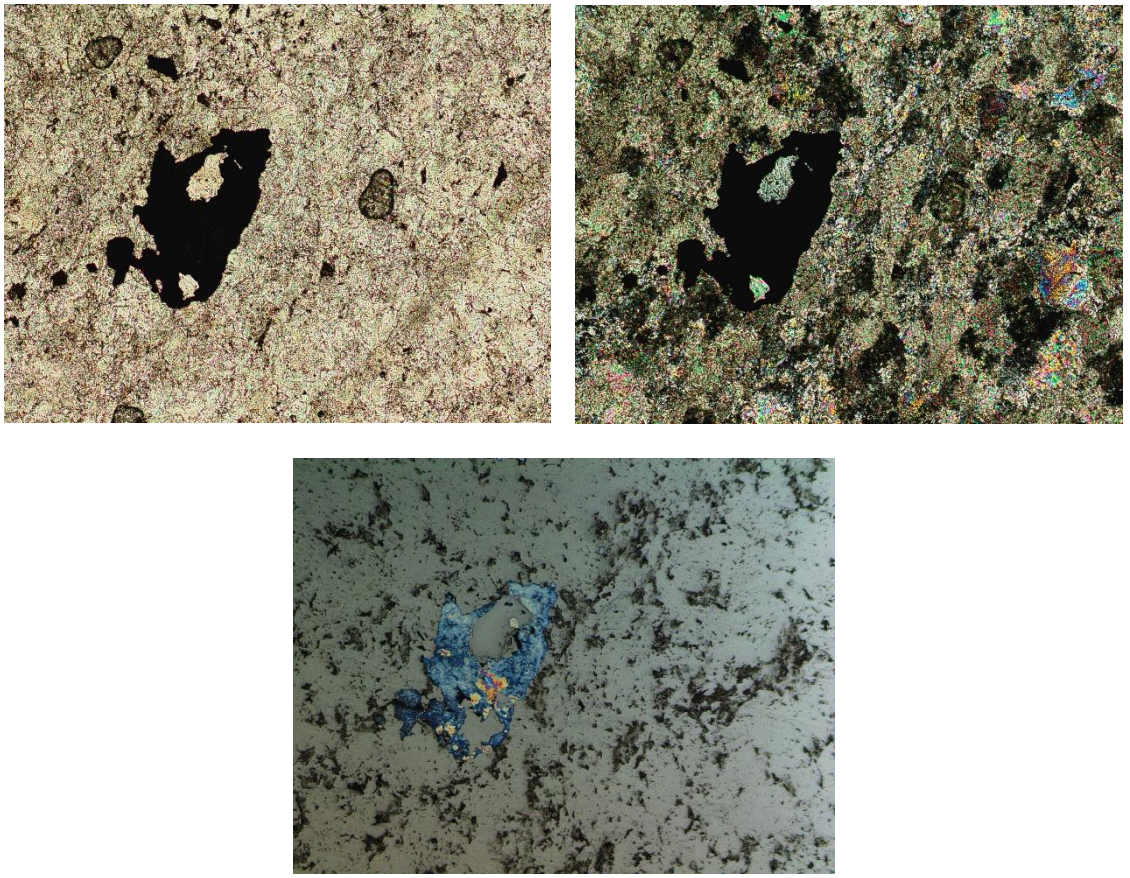

Plane light image (left) and crossed polarized image (right) illustrating a dominantly carbonate-rich rock intergrown with highly birefringent Cr-paragonite grains. The lower image is a coarse grain of Ni-As-S intergrown with Ni-Sb-As-Te-S (see backscatter images below). Field of View = 2.2mm

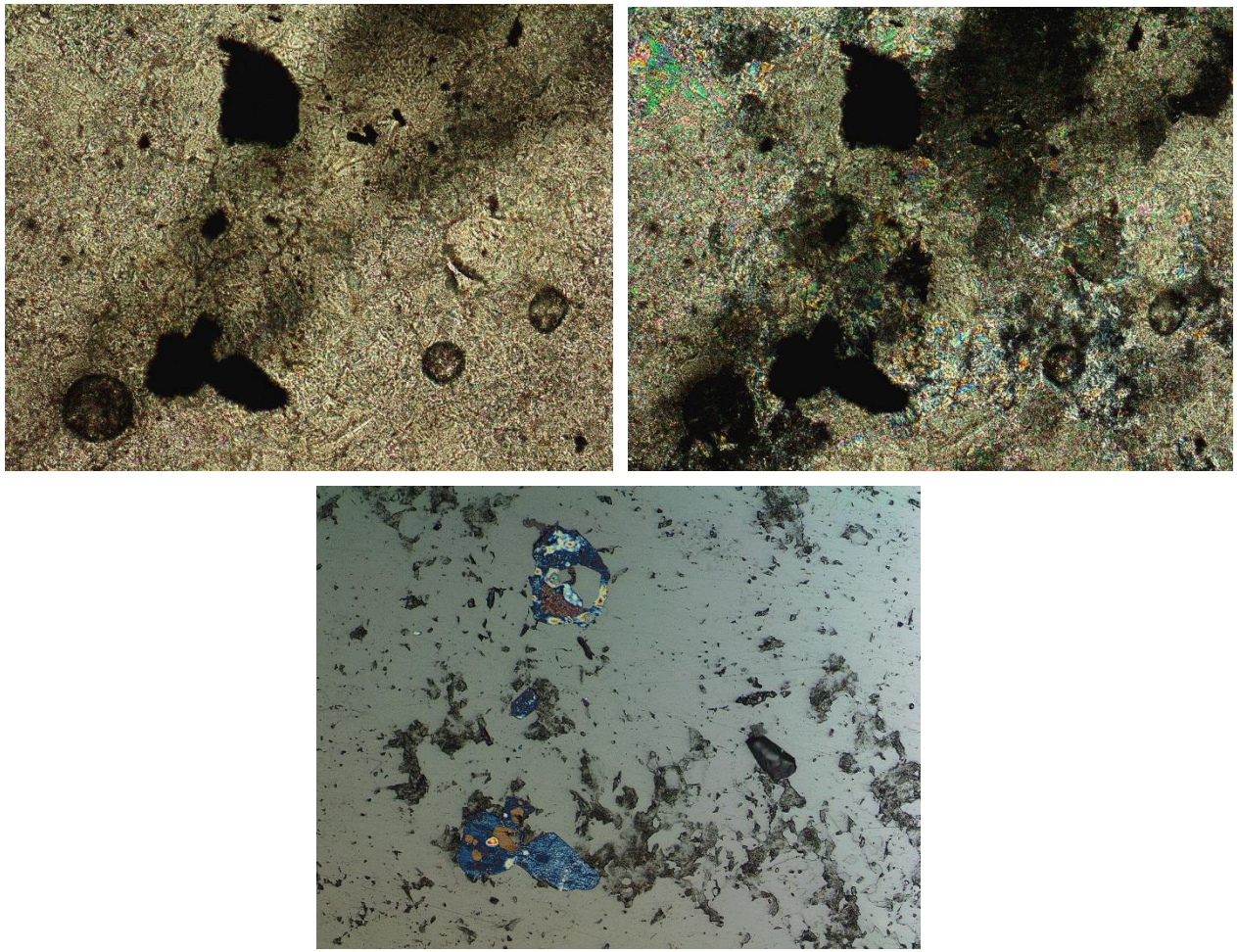

Plane light image (top left) and crossed polarized image (top right) illustrating a dominantly carbonate-rich rock intergrown with highly birefringent Cr-paragonite grains. The reflected light image (bottom) shows a number of coarse grain of Ni-As-S intergrown with Ni-Sb-As-Te-S. Field of View = 2.2mm

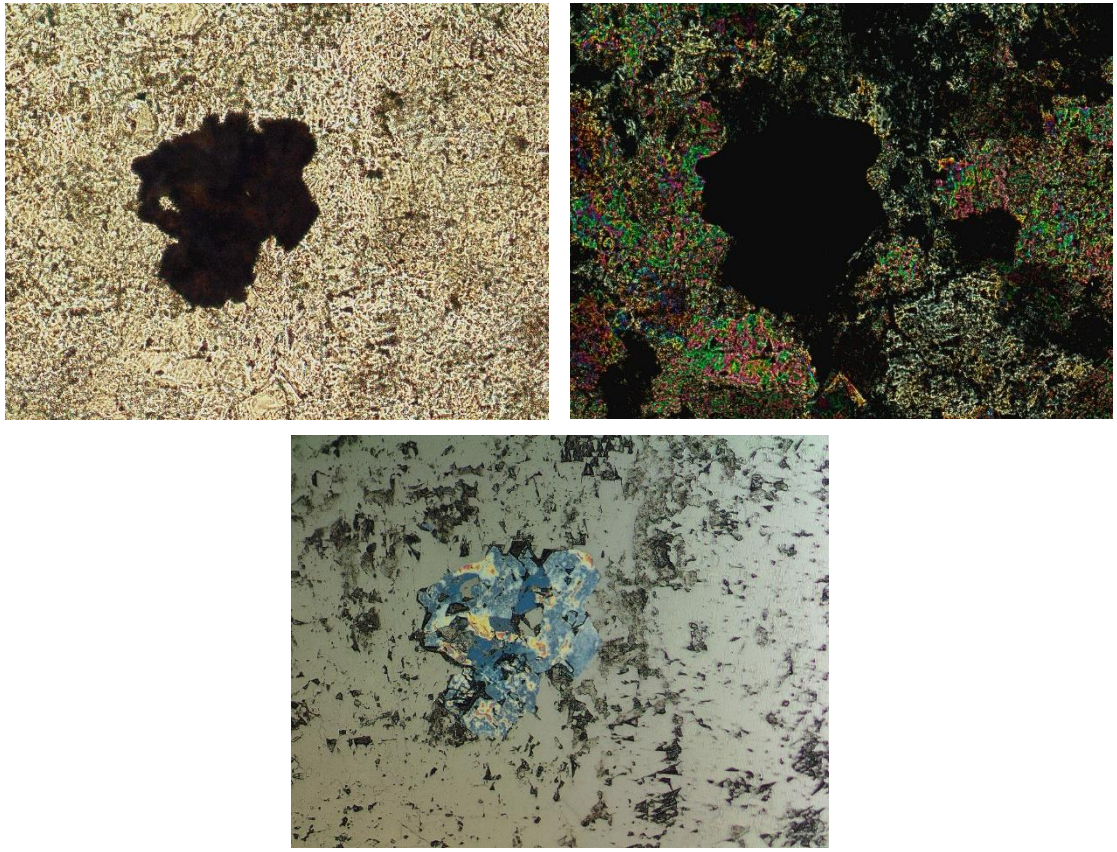

Plane light image (top left) and crossed polarized image (top right) illustrating a dominantly carbonate-rich rock intergrown with highly birefringent Cr-paragonite grains. The reflected light image (bottom) shows a coarse grain of Ni-As-S intergrown with Ni-Sb-As-Te-S. Field of View = 1.2mm

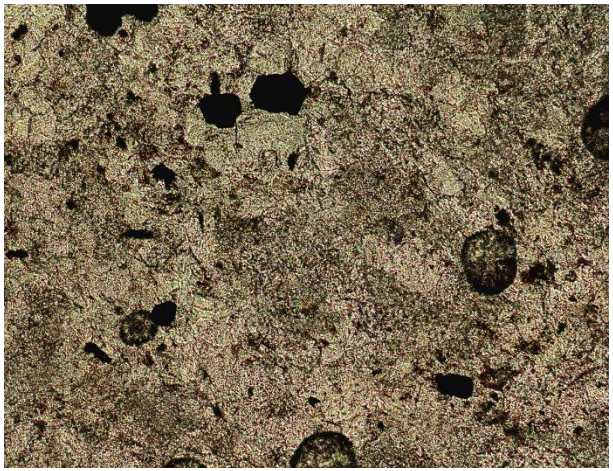

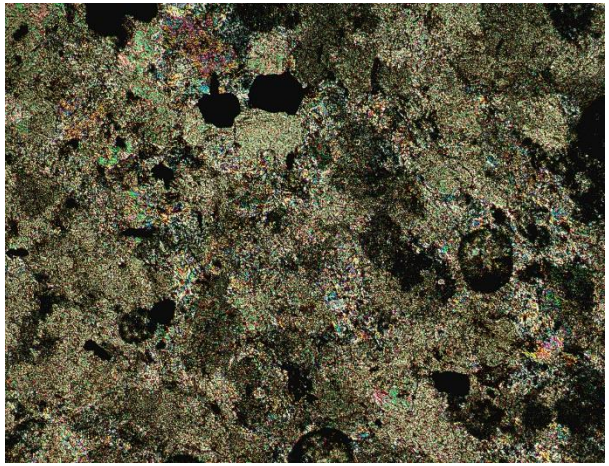

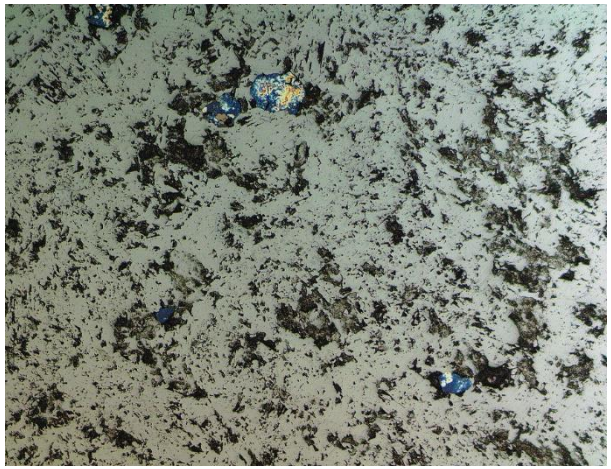

Plane light image (top left) and crossed polarized image (top right) illustrating a dominantly carbonate-rich rock intergrown with highly birefringent Cr-paragonite grains. The reflected light image (bottom) shows disseminated grains Ni-As-S intergrown with Ni-Sb-As-Te-S. Field of View = 2.2mm

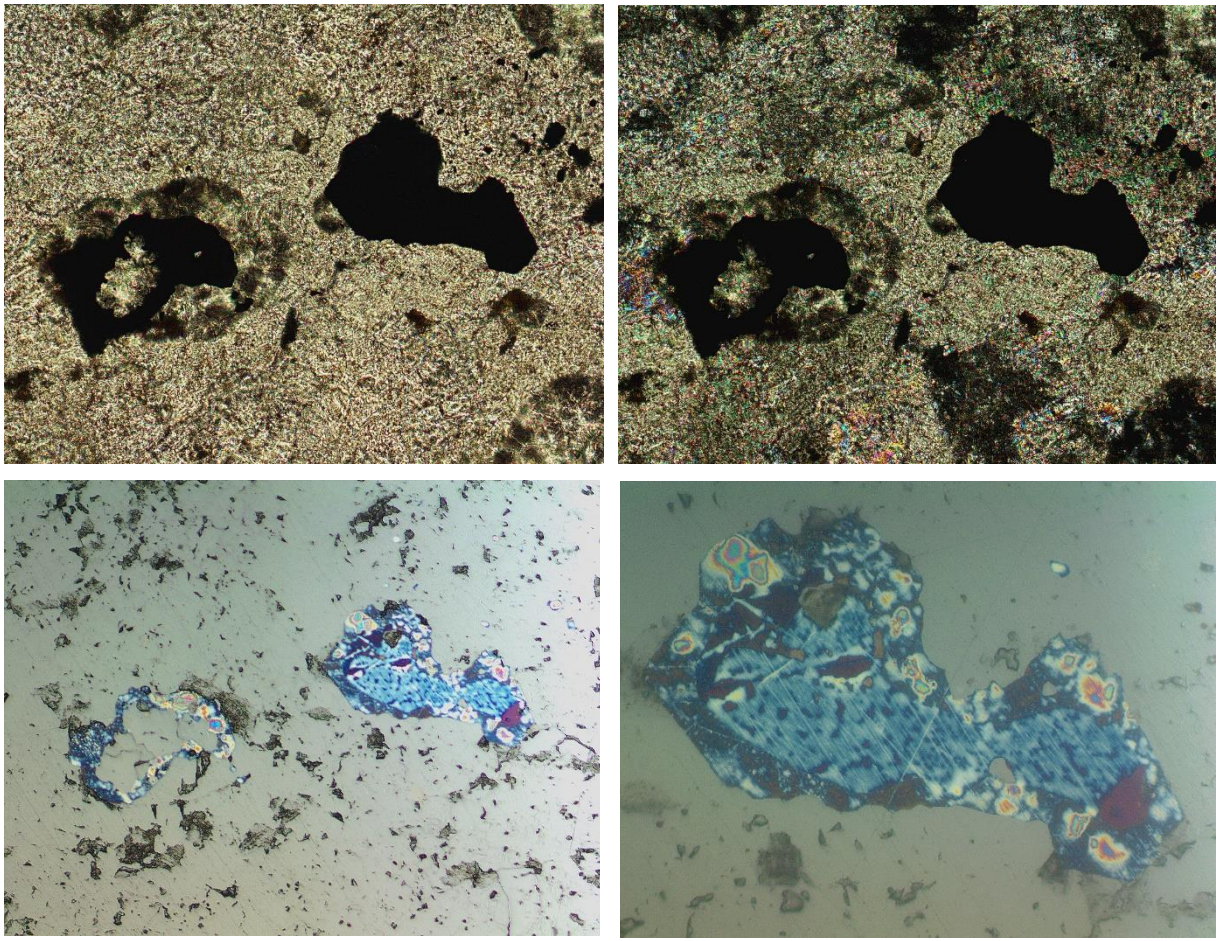

Plane light image (top left) and crossed polarized image (top right) illustrating a dominantly carbonate-rich rock intergrown with highly birefringent Cr-paragonite grains. The lower left image is reflected light showing a coarse grain of Ni-S intergrown with As-Ni-Sb-S (see backscatter images below). Field of View = 2.2mm. The lower right image is a higher magnification of the coarse sulphide grain. Field of View = 6mm. See backscatter image below.

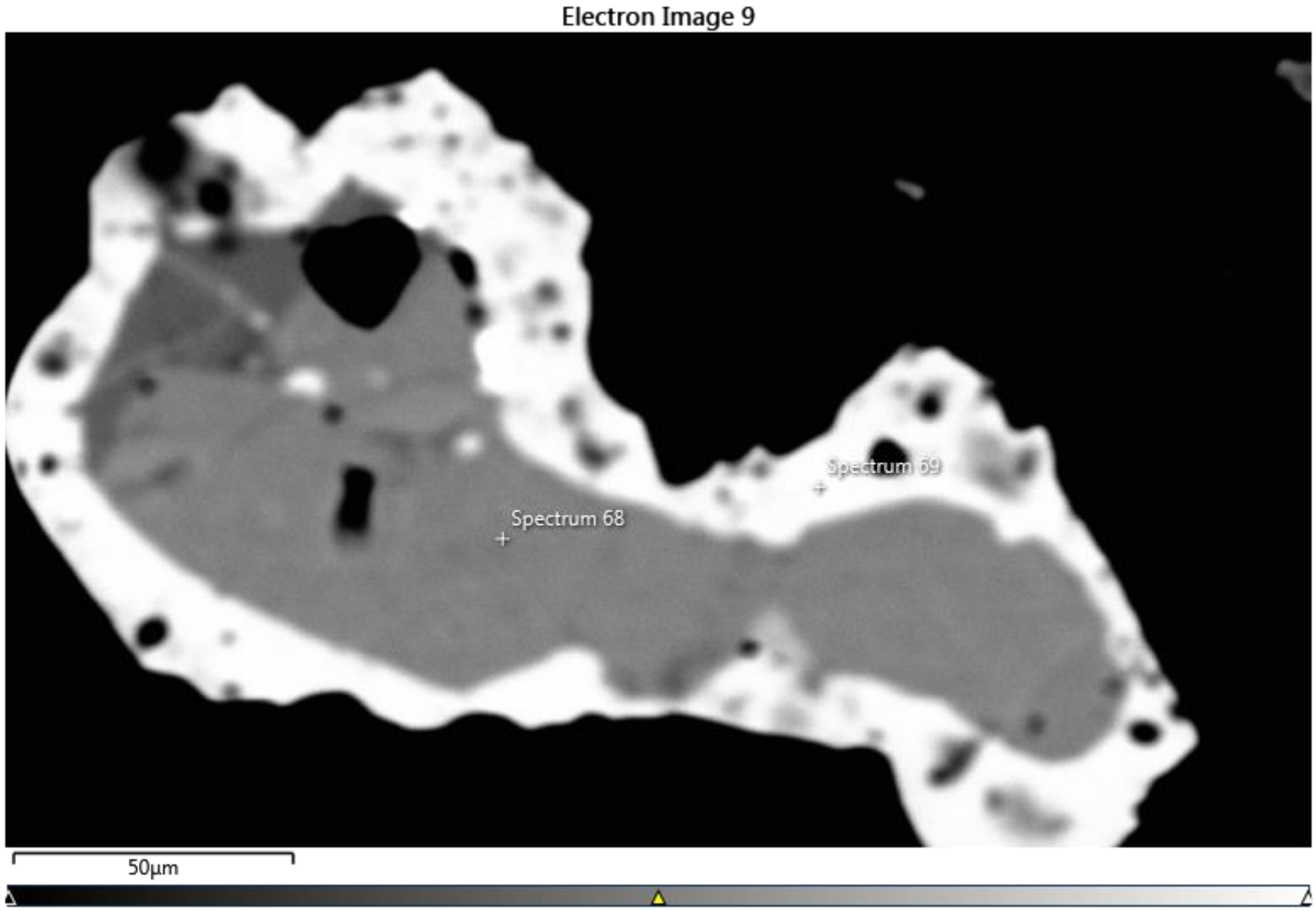

Backscatter image illustrating the complex zoning and intergrowths of Ni-S (Vaesite - spectrum 68) and As-Ni-Sb-S (possible Sb-Gersdorffite - spectrum 69).

Electron Image 10

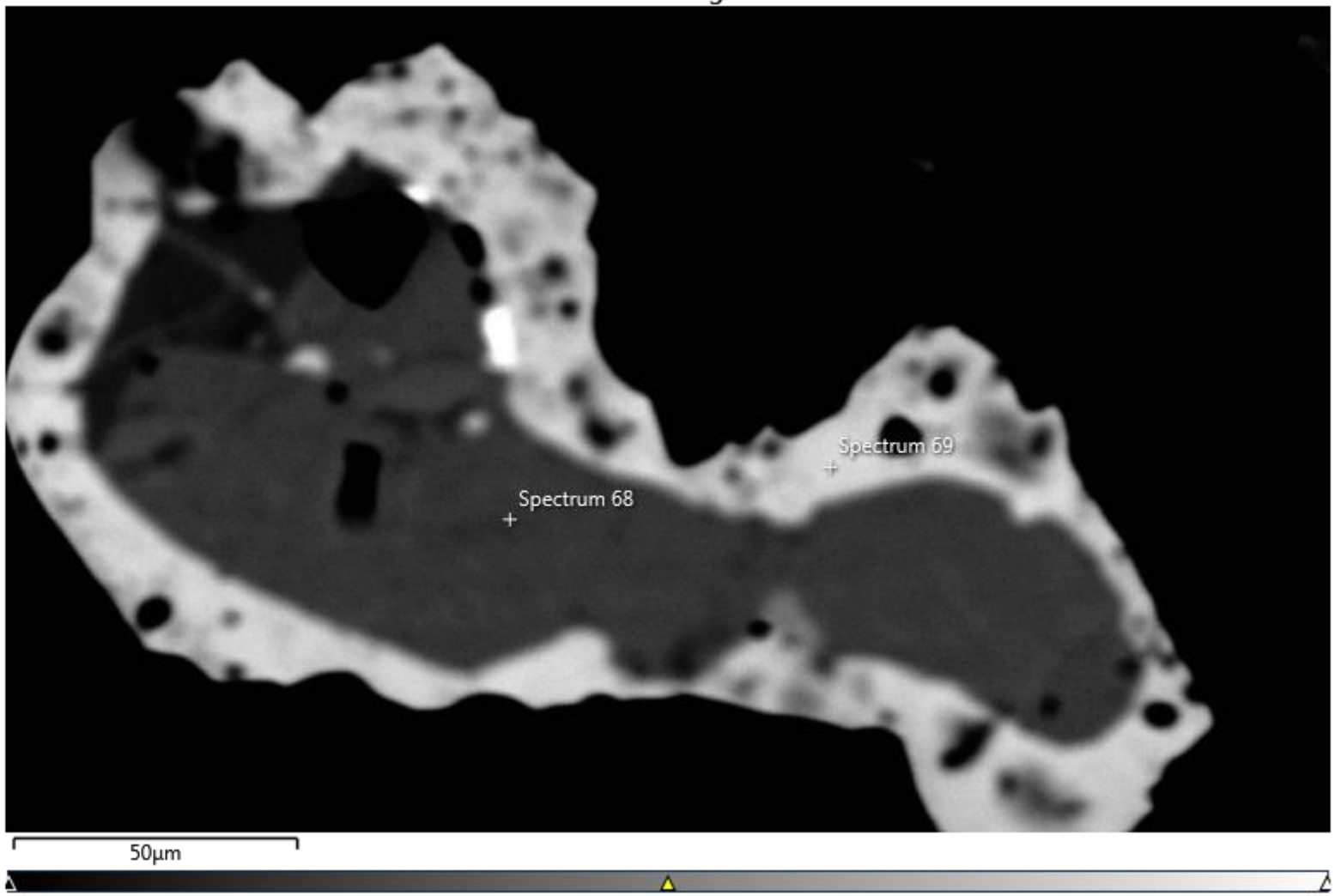

Same image as above with backscatter intensity reduced to illustrate the different phases.

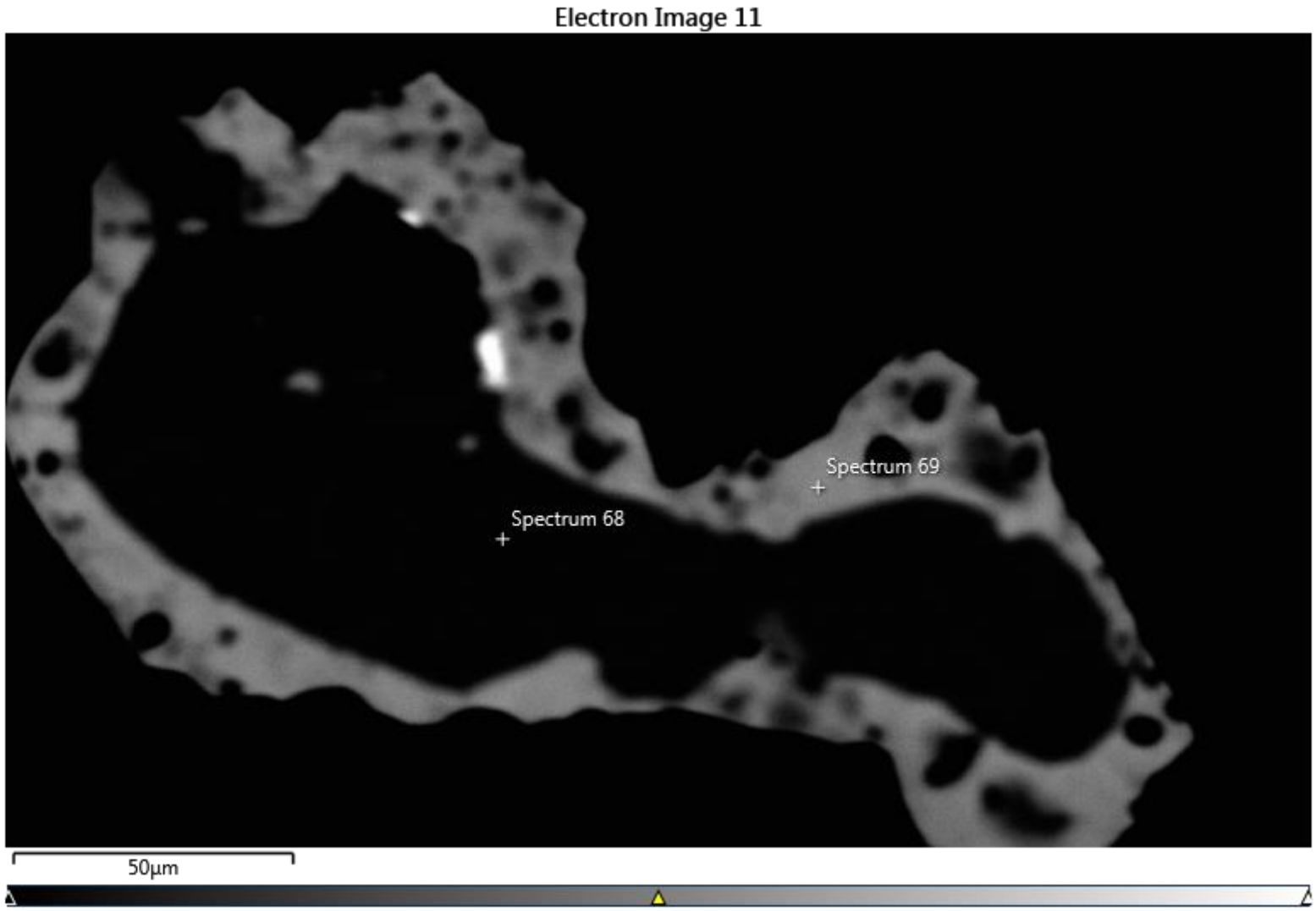

Backscatter intensity reduced further to illustrate the different phases.

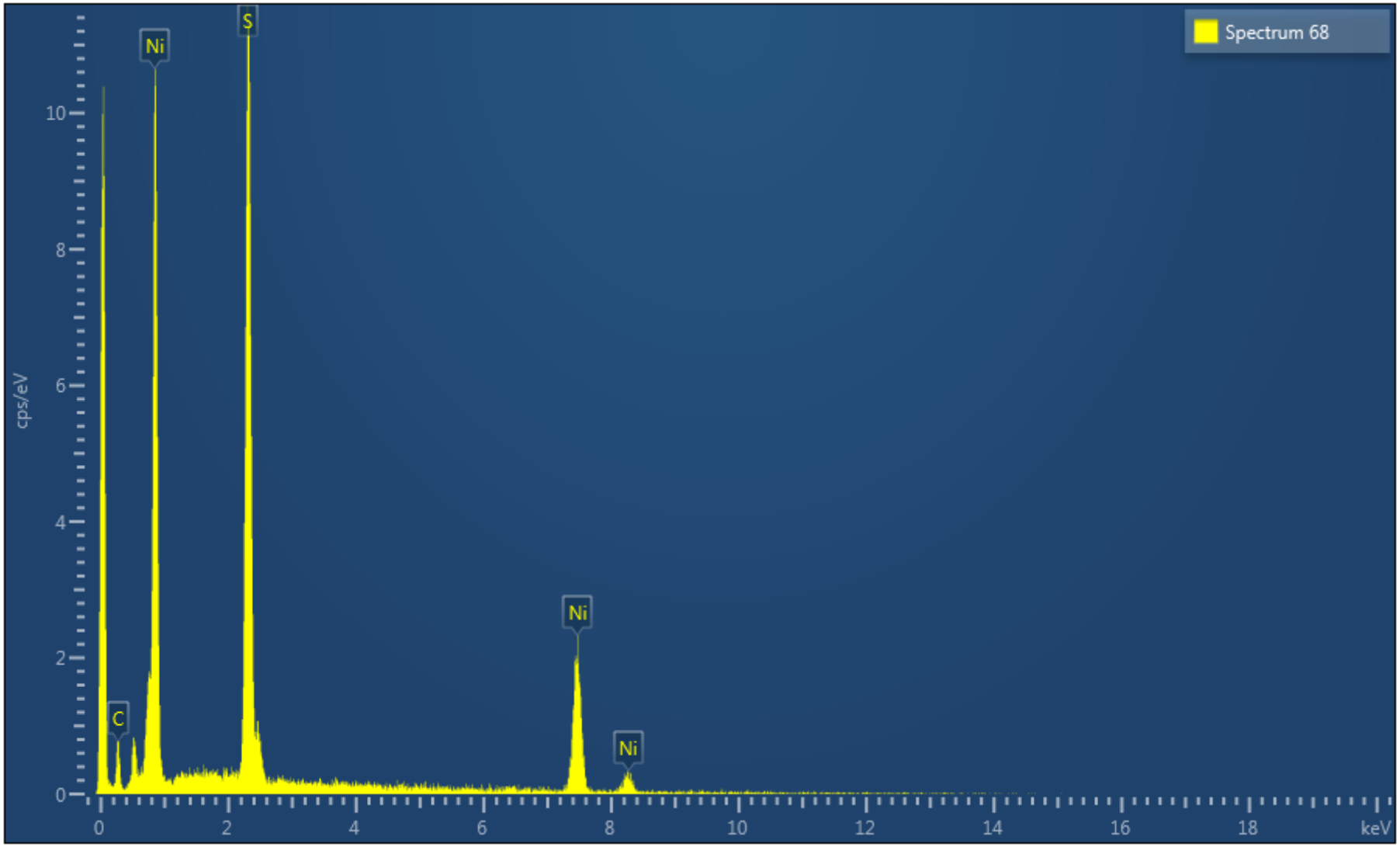
Spectrum 68
Ni
S
C
Ni
Ni
cps/eV
0
2
4
6
8
10
0
2
4
6
8
10
12
14
16
18
keV

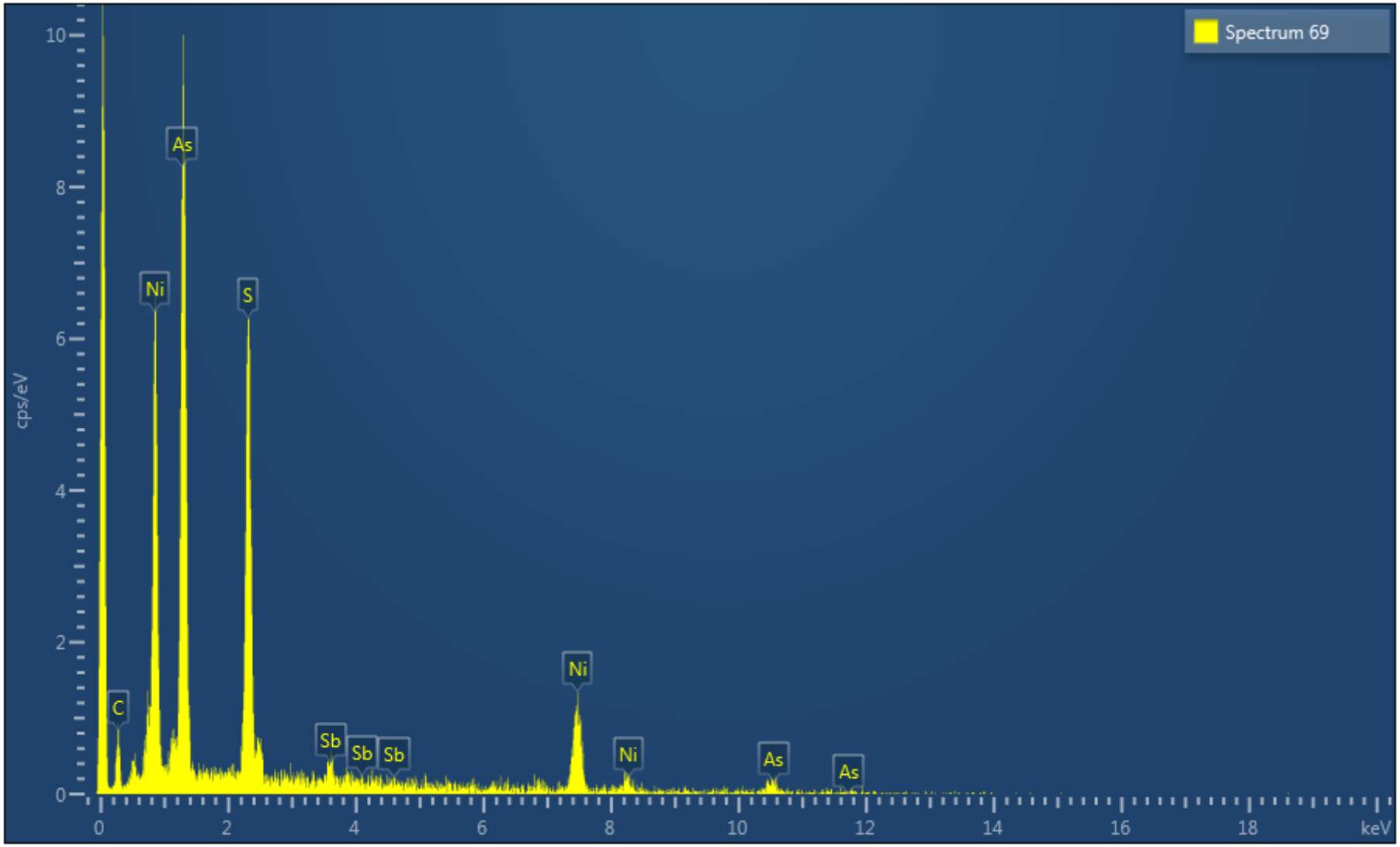
Spectrum 69
cps/eV
keV
C
Ni
As
S
Sb
Sb
Sb
Ni
Ni
As
As

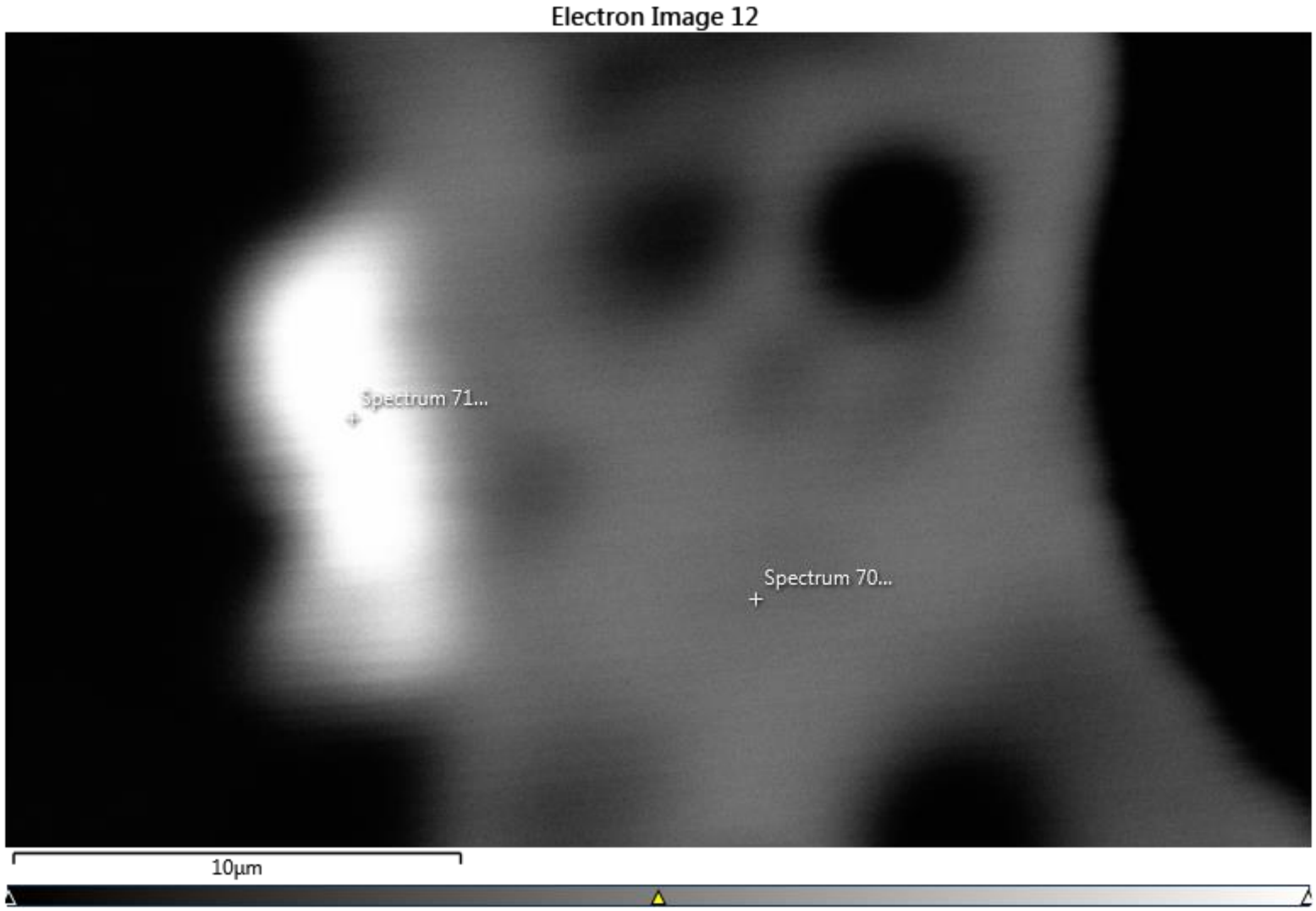

Higher magnification of the brightest phase from the images above showing As-Ni-Sb-S (spectrum 70) and Sb-Ni-As-S (spectrum 71).

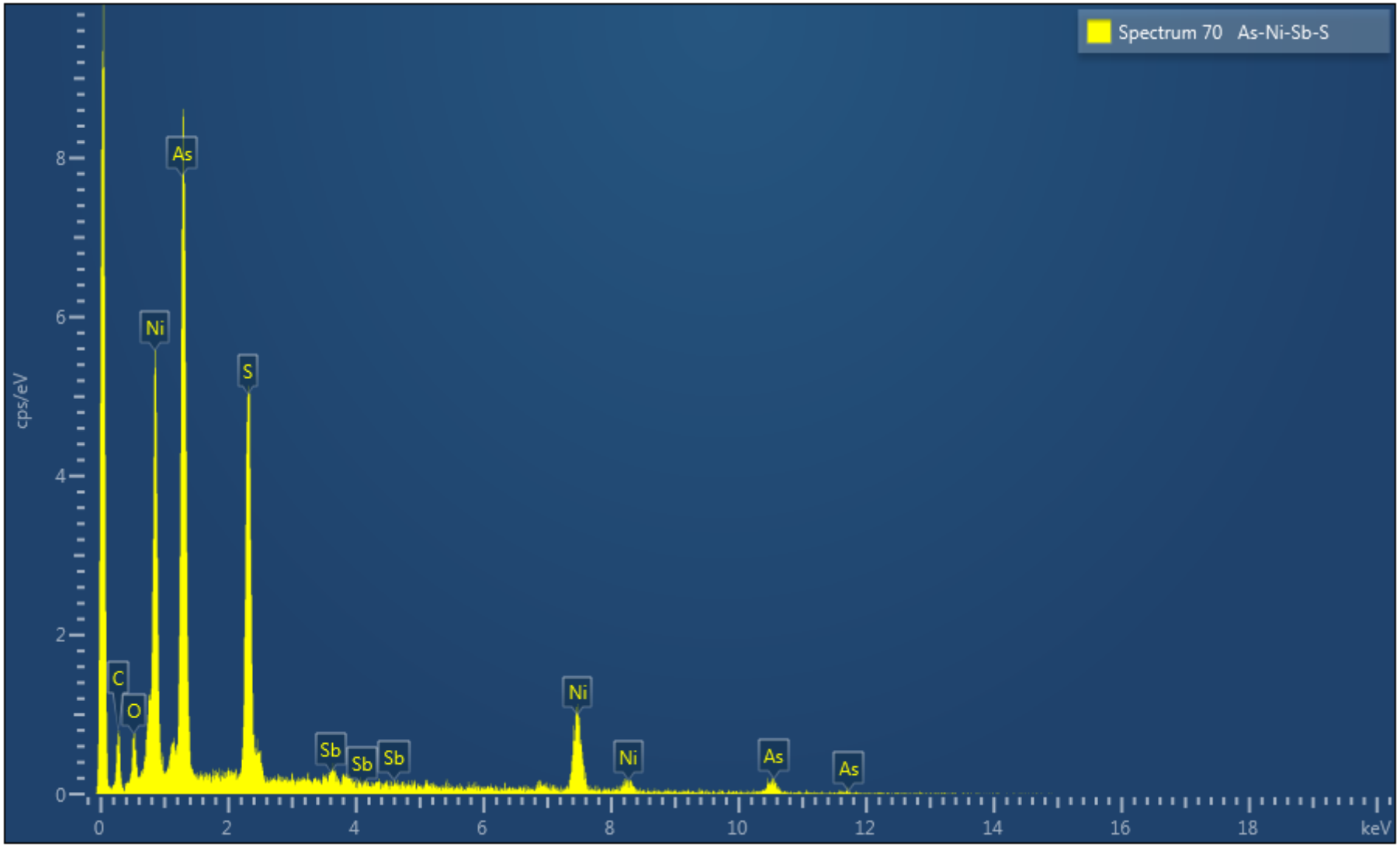
Spectrum 70 As-Ni-Sb-S
cps/eV
0
2
4
6
8
C
O
Ni
As
S
Sb
Sb
Sb
Ni
Ni
As
As
0
2
4
6
8
10
12
14
16
18
keV

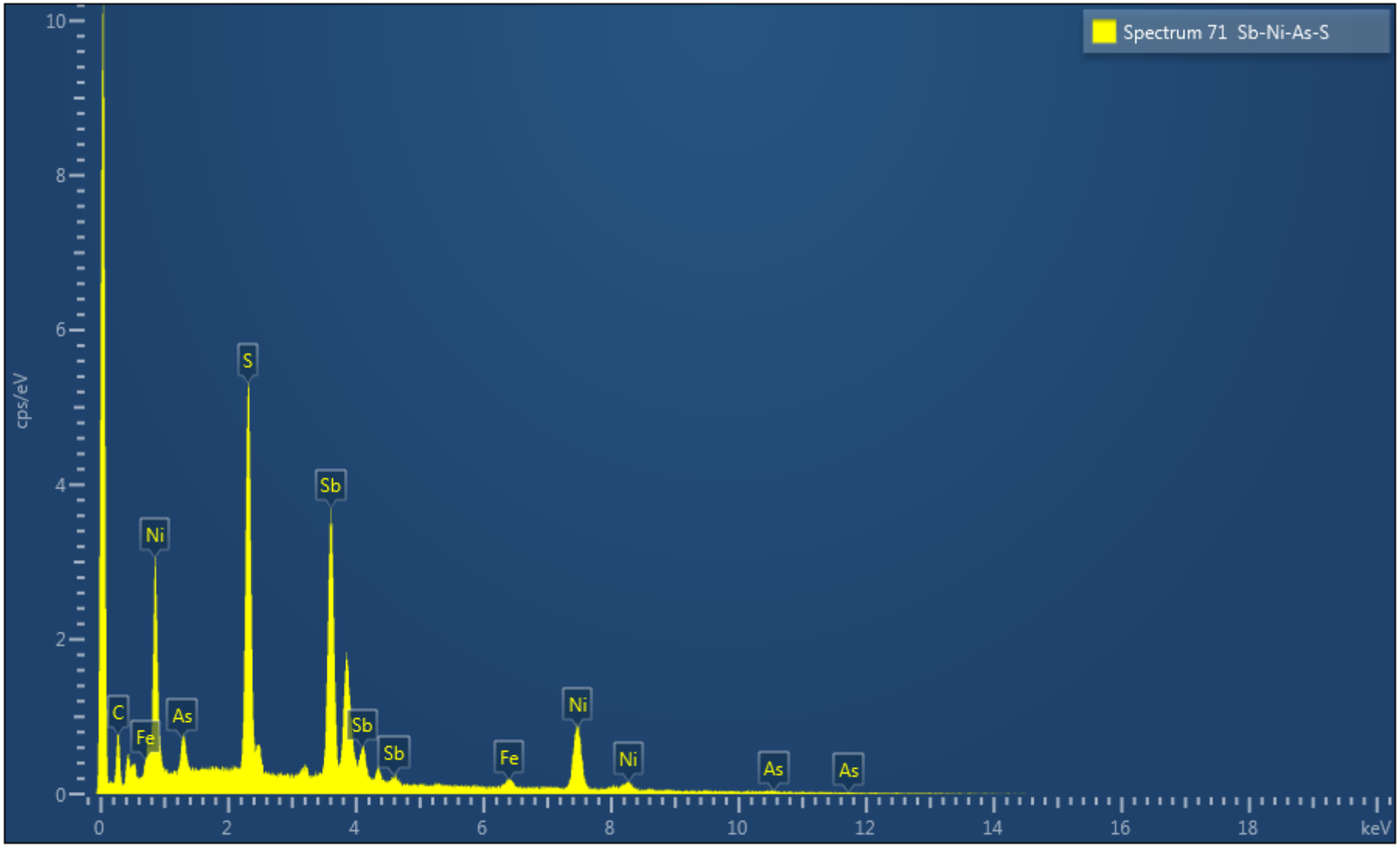
Spectrum 71 Sb-Ni-As-S
cps/eV
keV
C
Fe
Ni
As
S
Sb
Sb
Sb
Fe
Ni
Ni
As
As

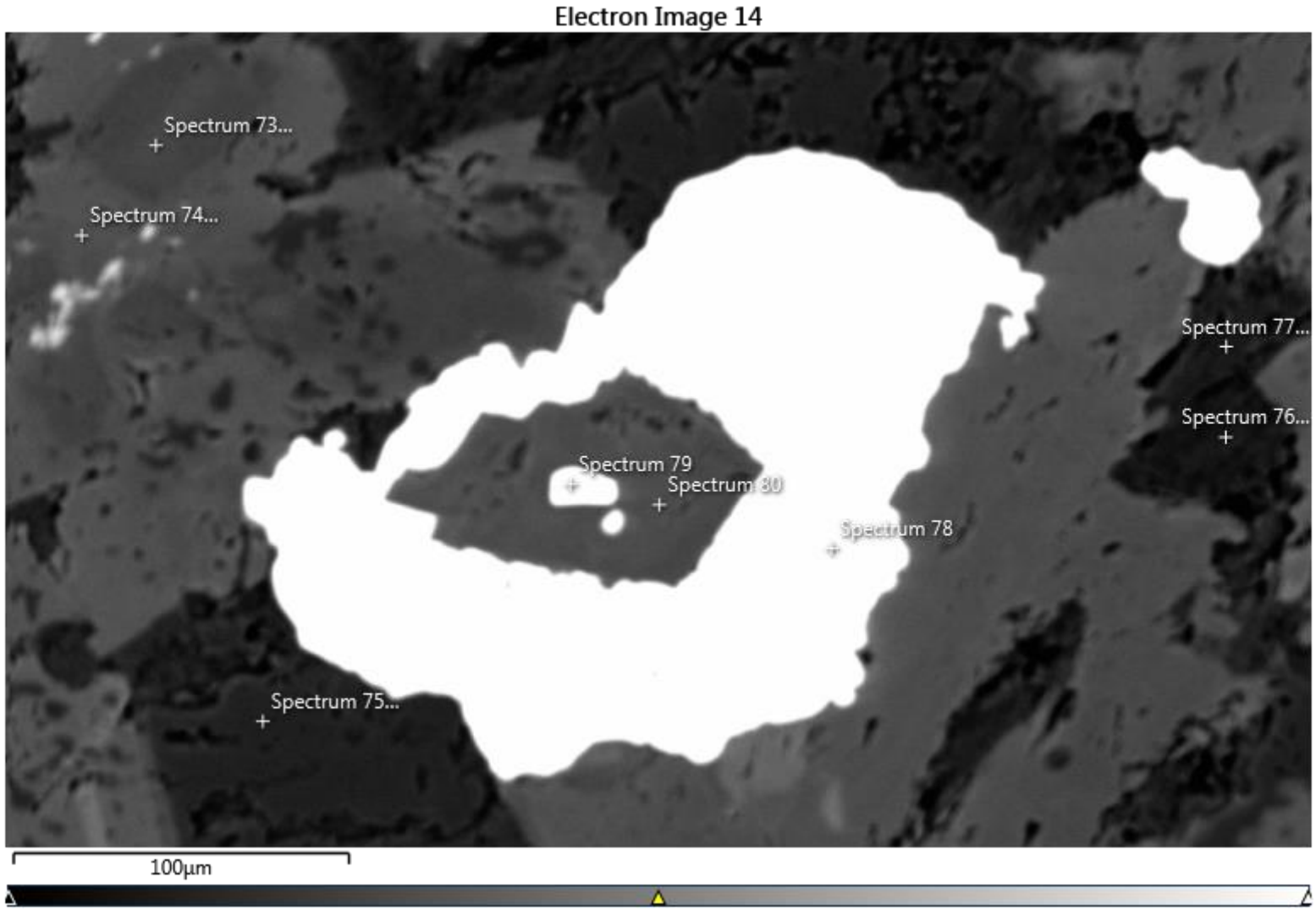

Backscatter image showing a groundmass of compositionally zoned dolomite-ankerite solid solution carbonates (spectrum 73-74, 80), quartz (spectrum 75), and Cr-paragonite mica (spectrum 76-77). The bright sulphide grains are Ni-As-S (spectrum 78) and Ni-Sb-As-Te-S (spectrum 79).

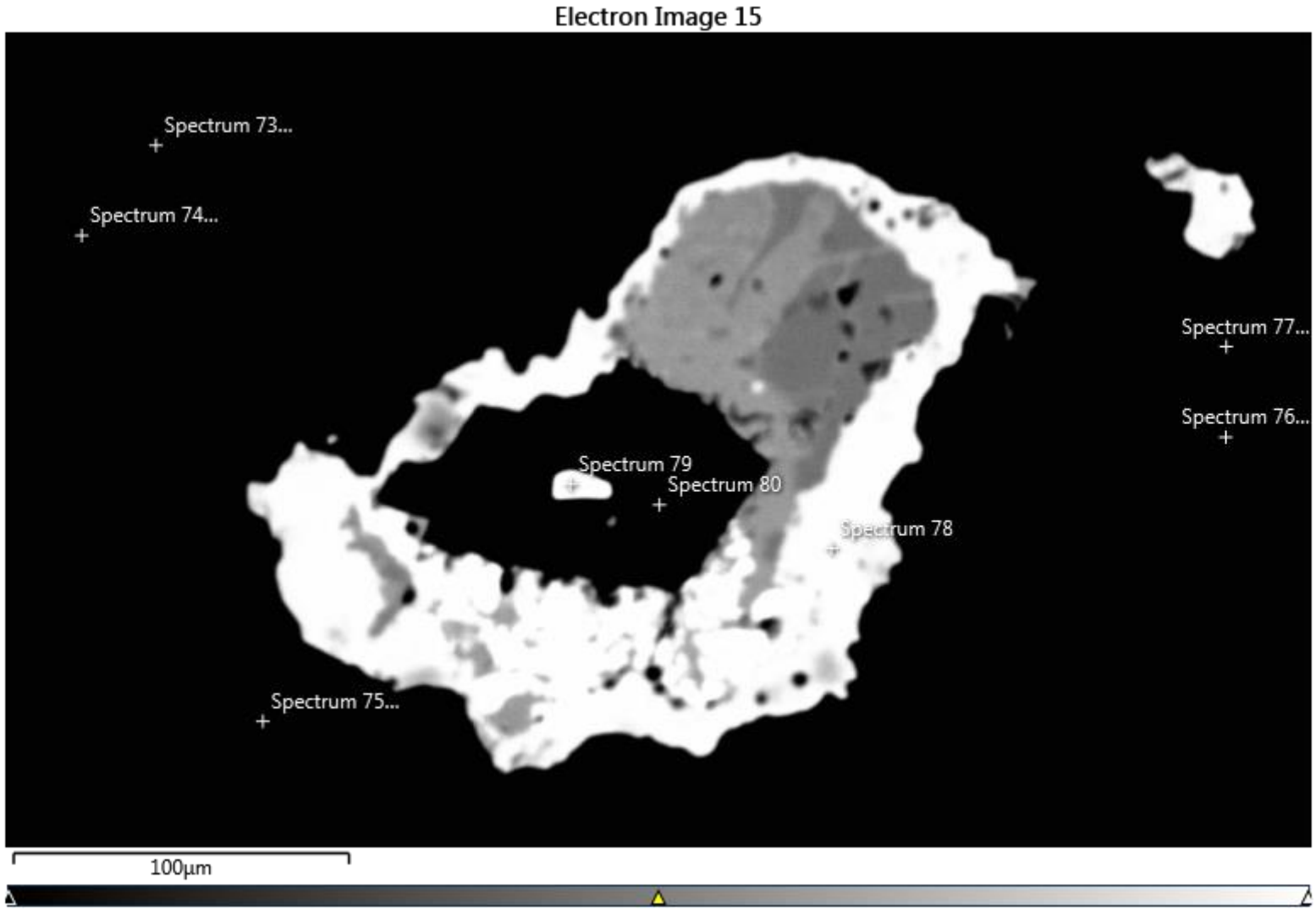

Same image as above with brightness reduced to illustrate the different domains.

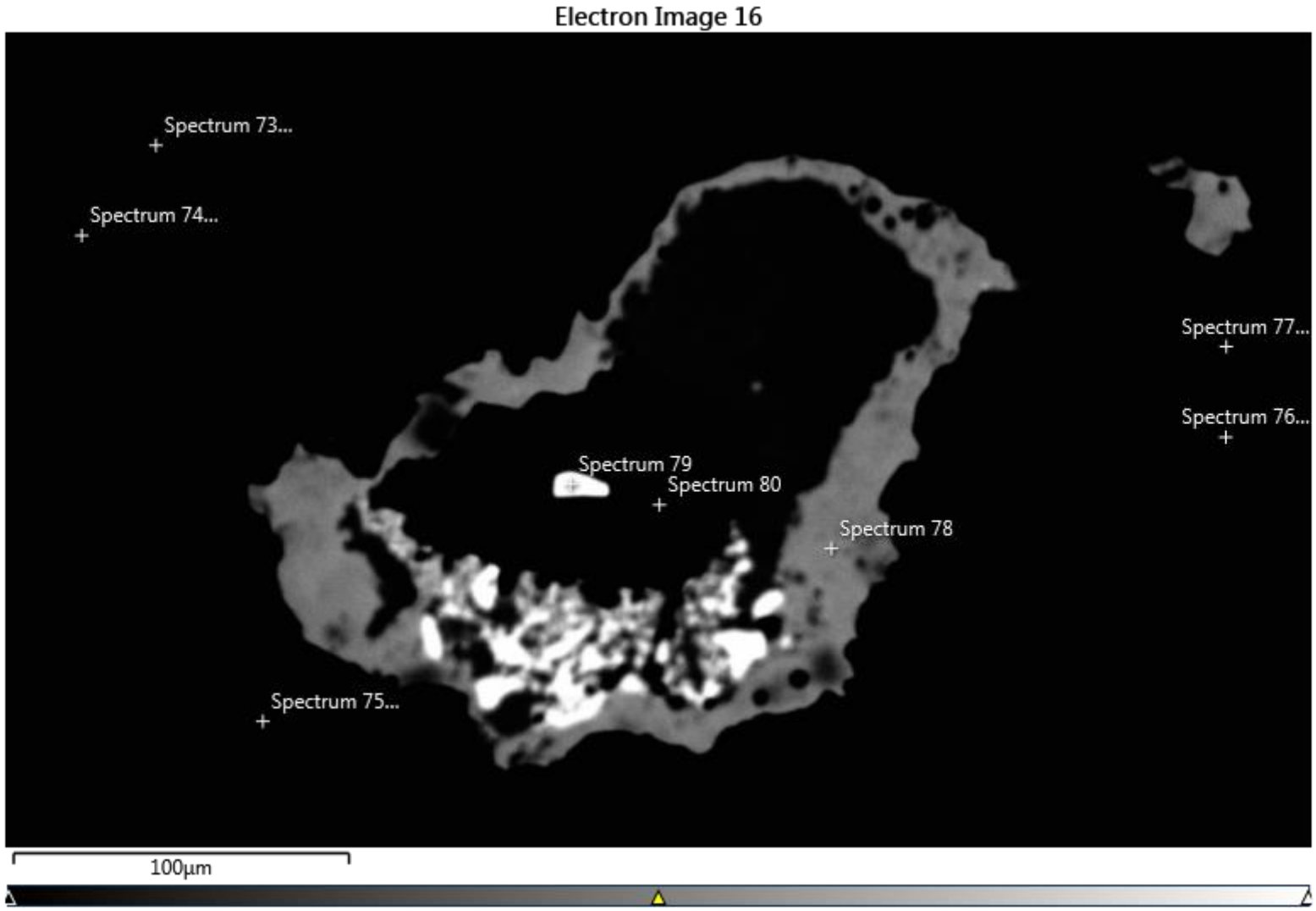

Same image as above with brightness reduced to illustrate the different domains.

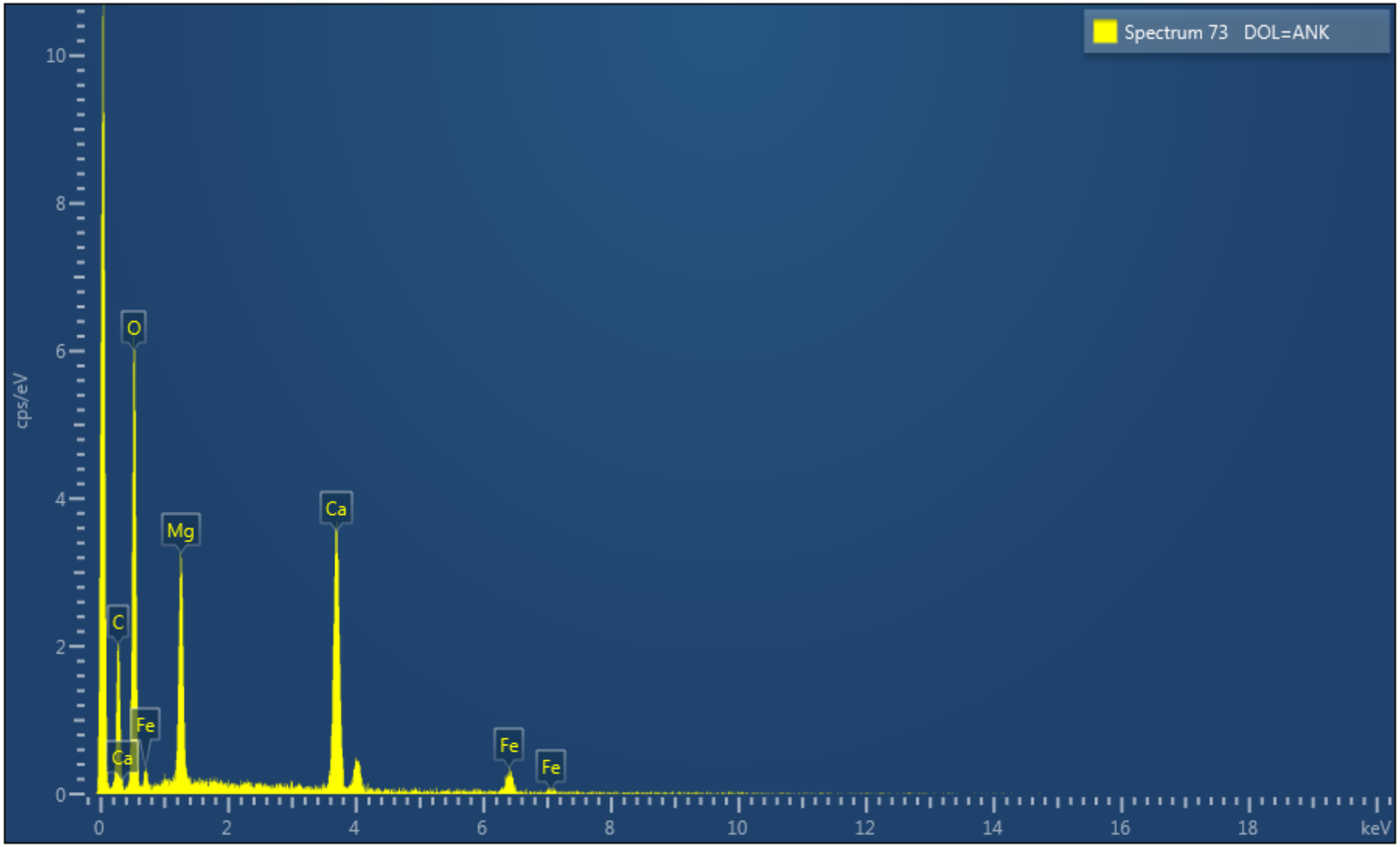
Spectrum 73 DOL=ANK
cps/eV
keV
O
C
Ca
Fe
Mg
Ca
Fe
Fe
0
2
4
6
8
10
12
14
16
18

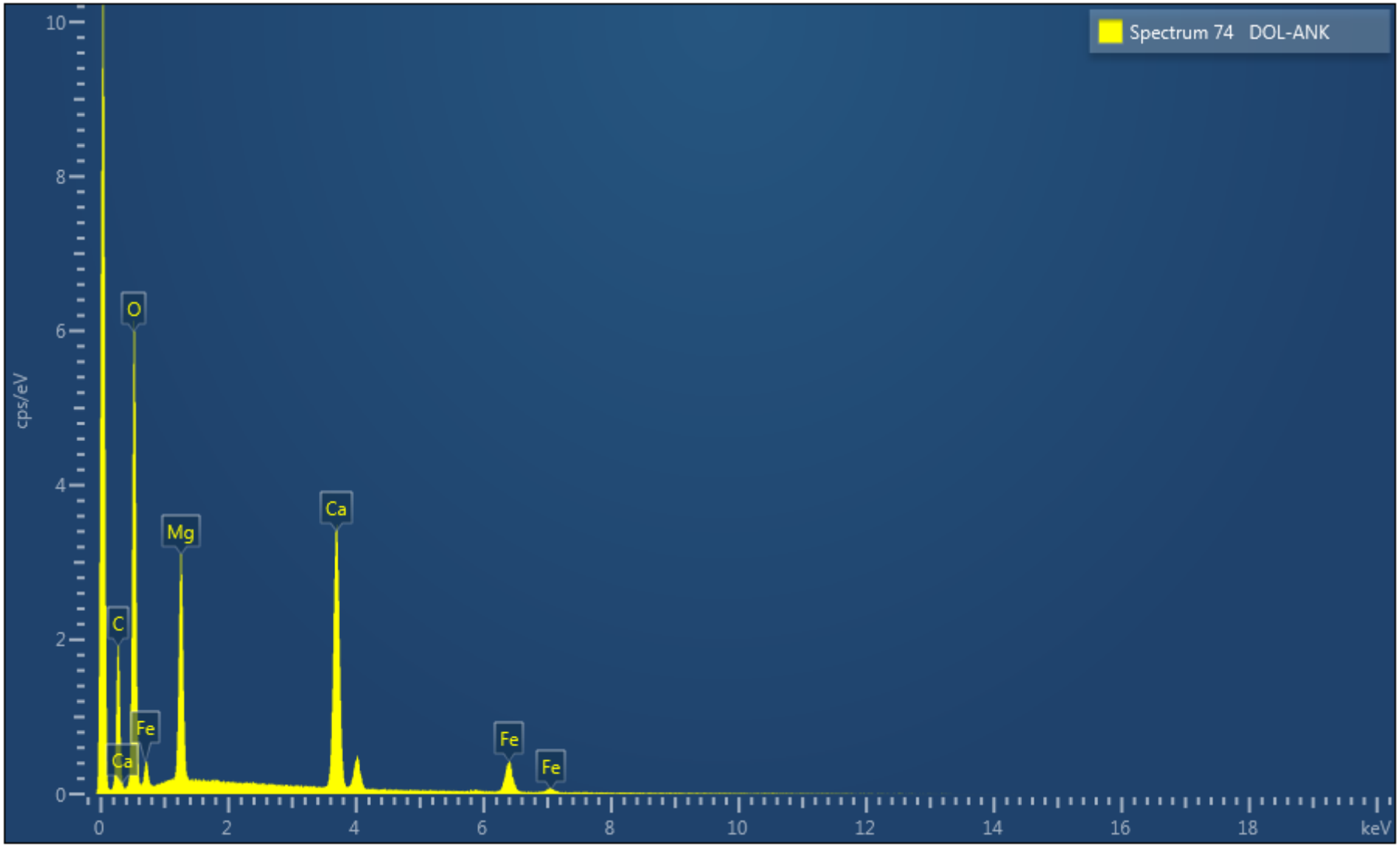
Spectrum 74 DOL-ANK
cps/eV
keV
O
C
Ca
Fe
Mg
Ca
Fe
Fe
0
2
4
6
8
10
12
14
16
18

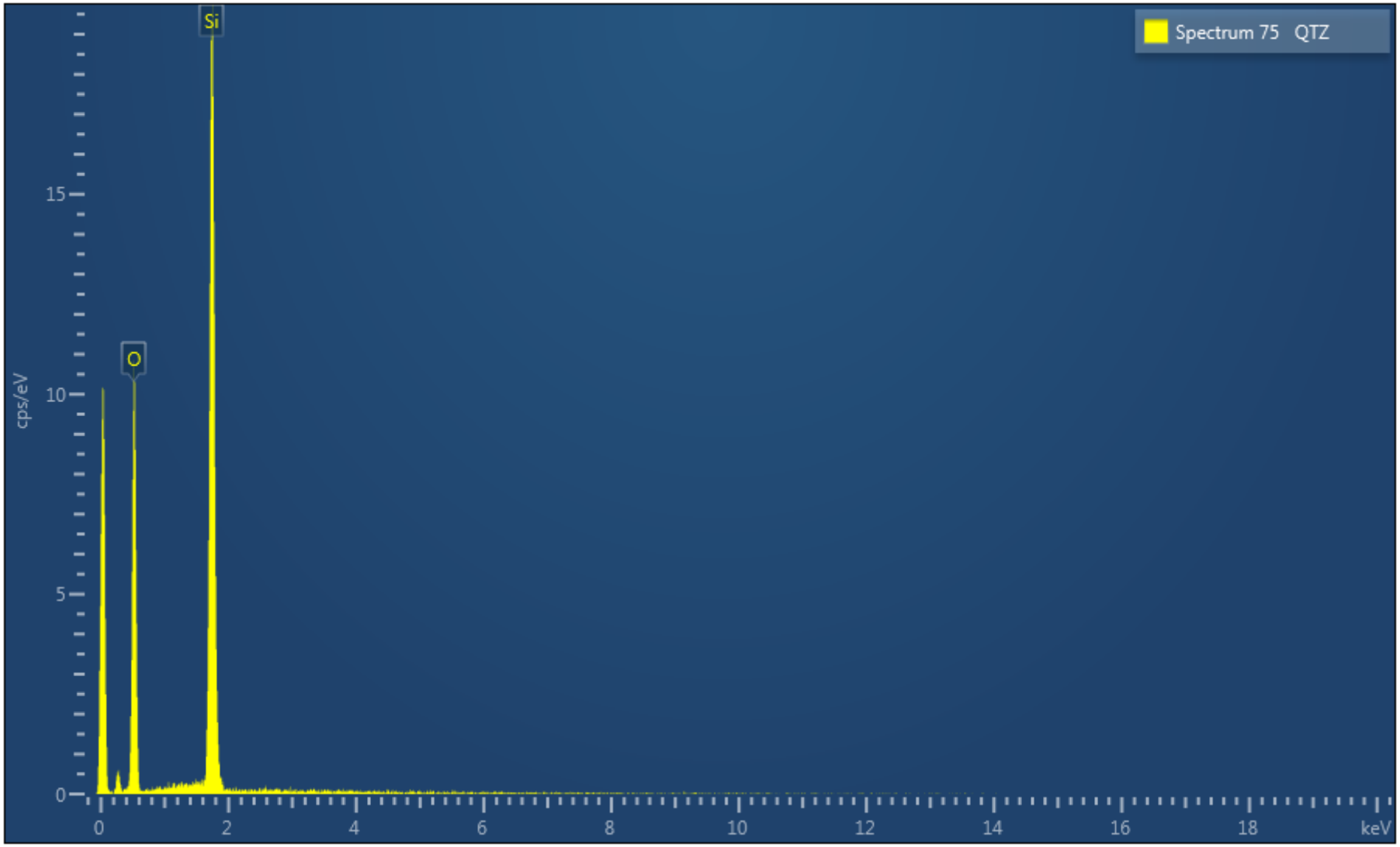
Spectrum 75 QTZ
Si
O
cps/eV
0
5
10
15
0
2
4
6
8
10
12
14
16
18
keV

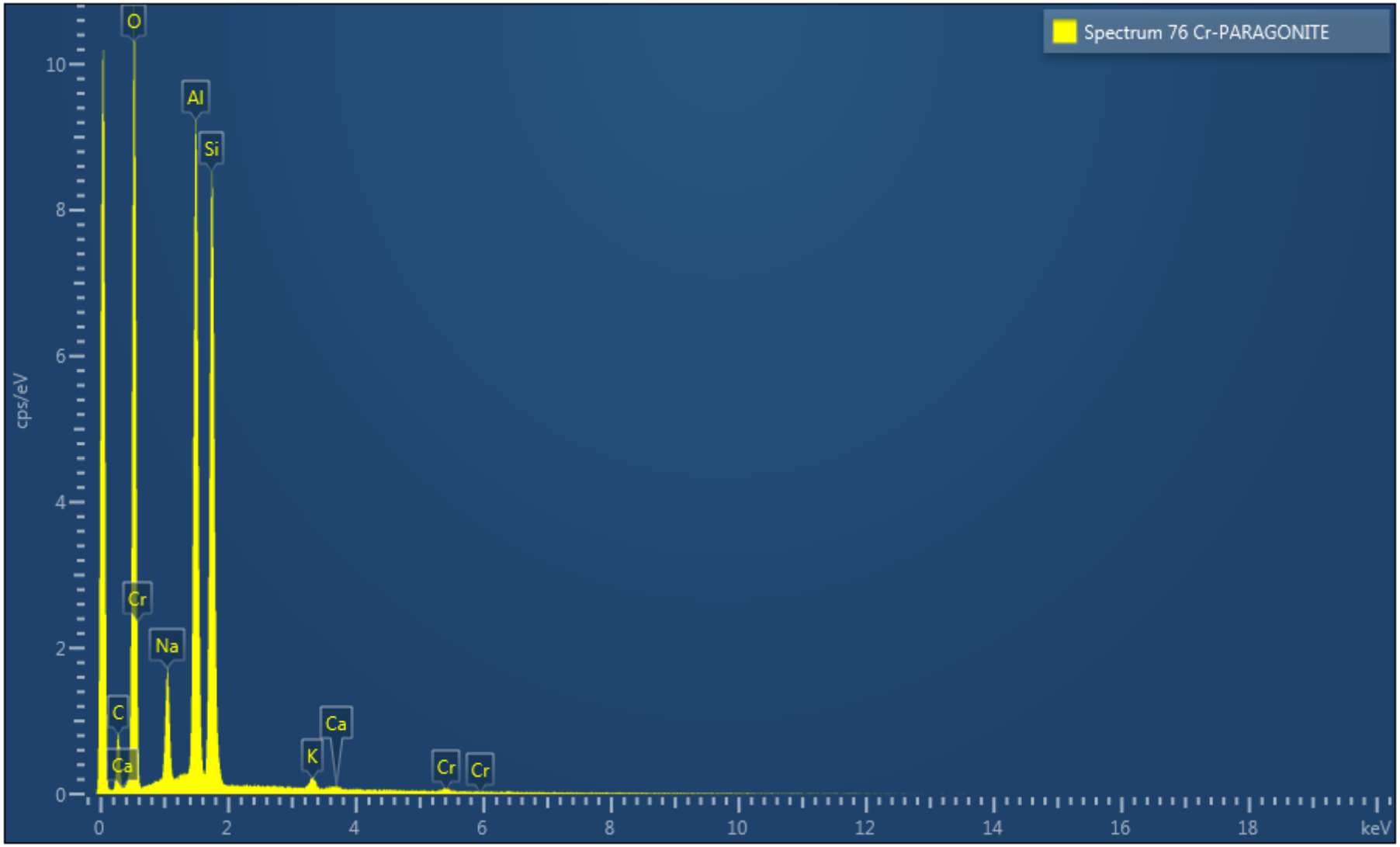
Spectrum 76 Cr-PARAGONITE
cps/eV
keV
O
Al
Si
Cr
Na
C
Ca
K
Ca
Cr
Cr
0
2
4
6
8
10
12
14
16
18

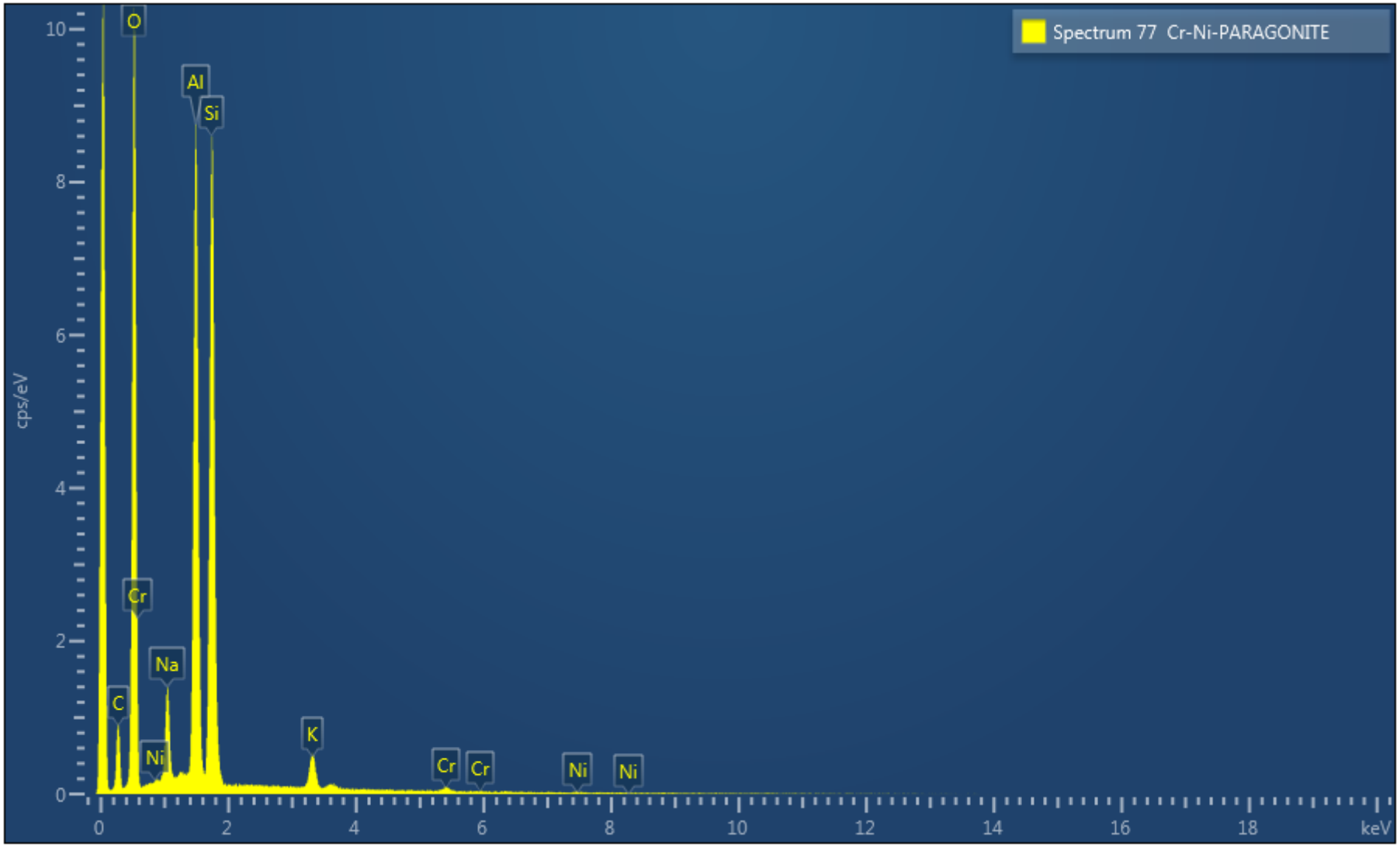
Spectrum 77 Cr-Ni-PARAGONITE
cps/eV
keV
O
Al
Si
Cr
Na
C
Ni
K
Cr
Cr
Ni
Ni

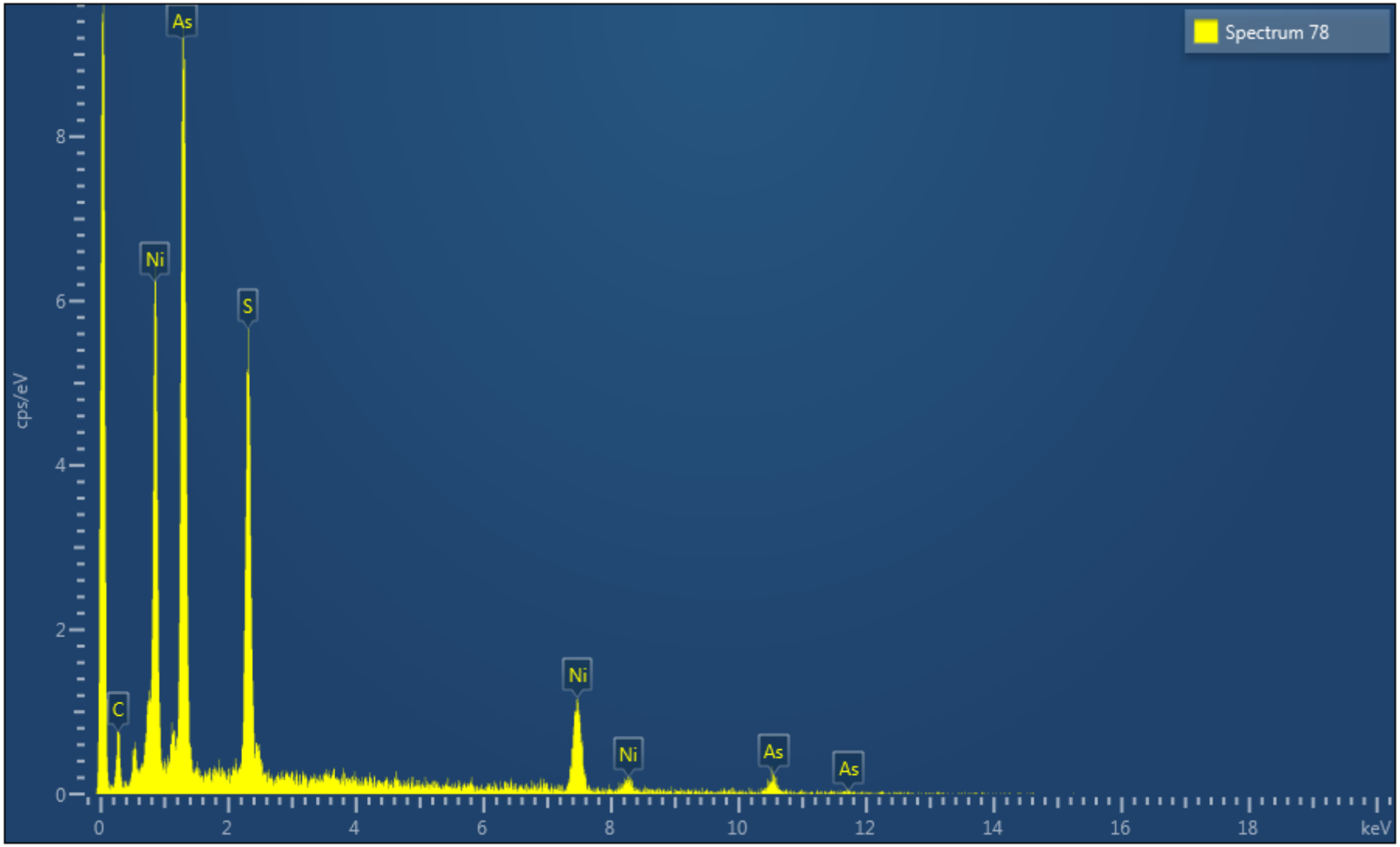
Spectrum 78
As
Ni
S
C
Ni
Ni
As
As
cps/eV
0
2
4
6
8
0
2
4
6
8
10
12
14
16
18
keV

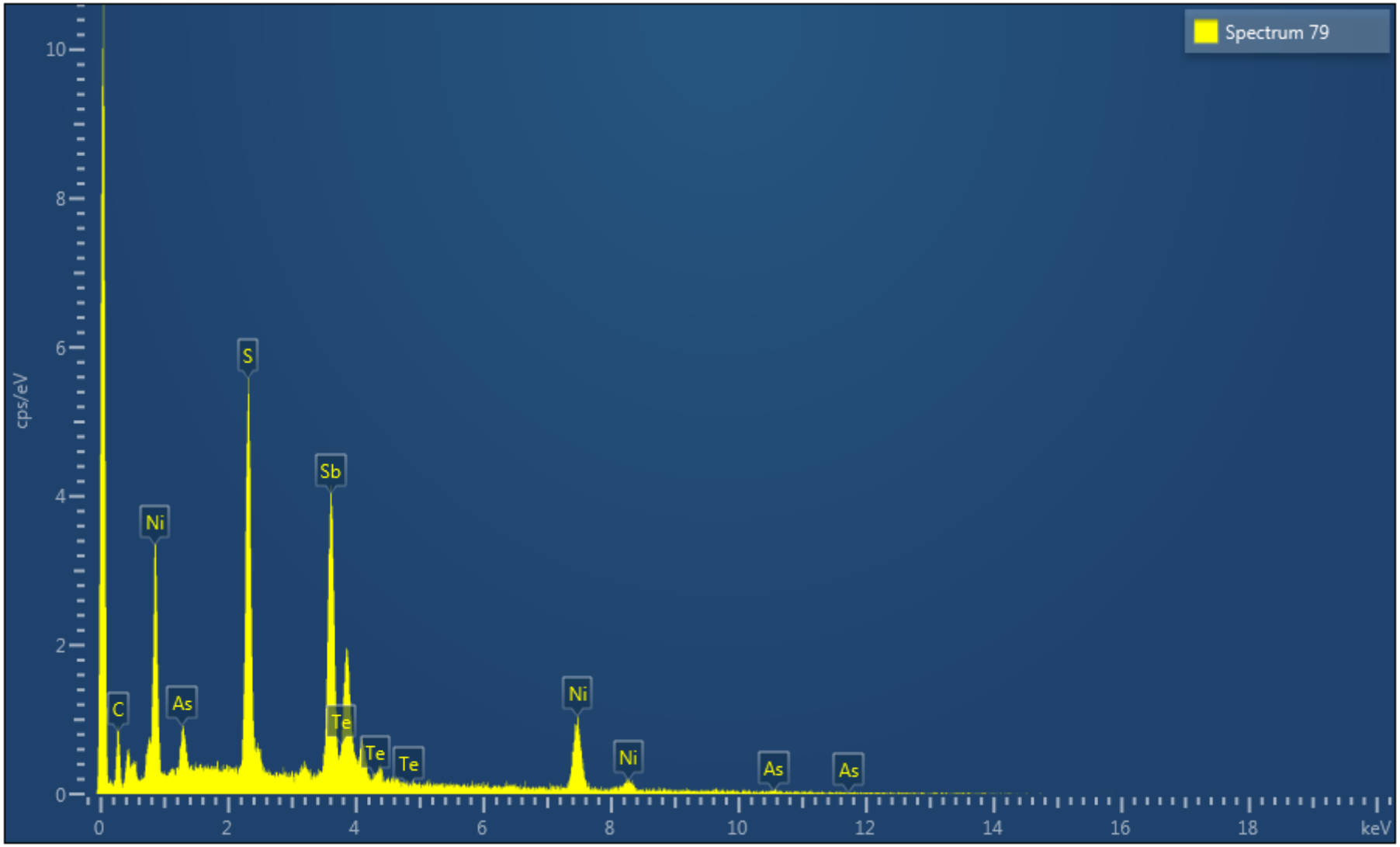
Spectrum 79
cps/eV
keV
C
Ni
As
S
Sb
Te
Te
Te
Ni
Ni
As
As

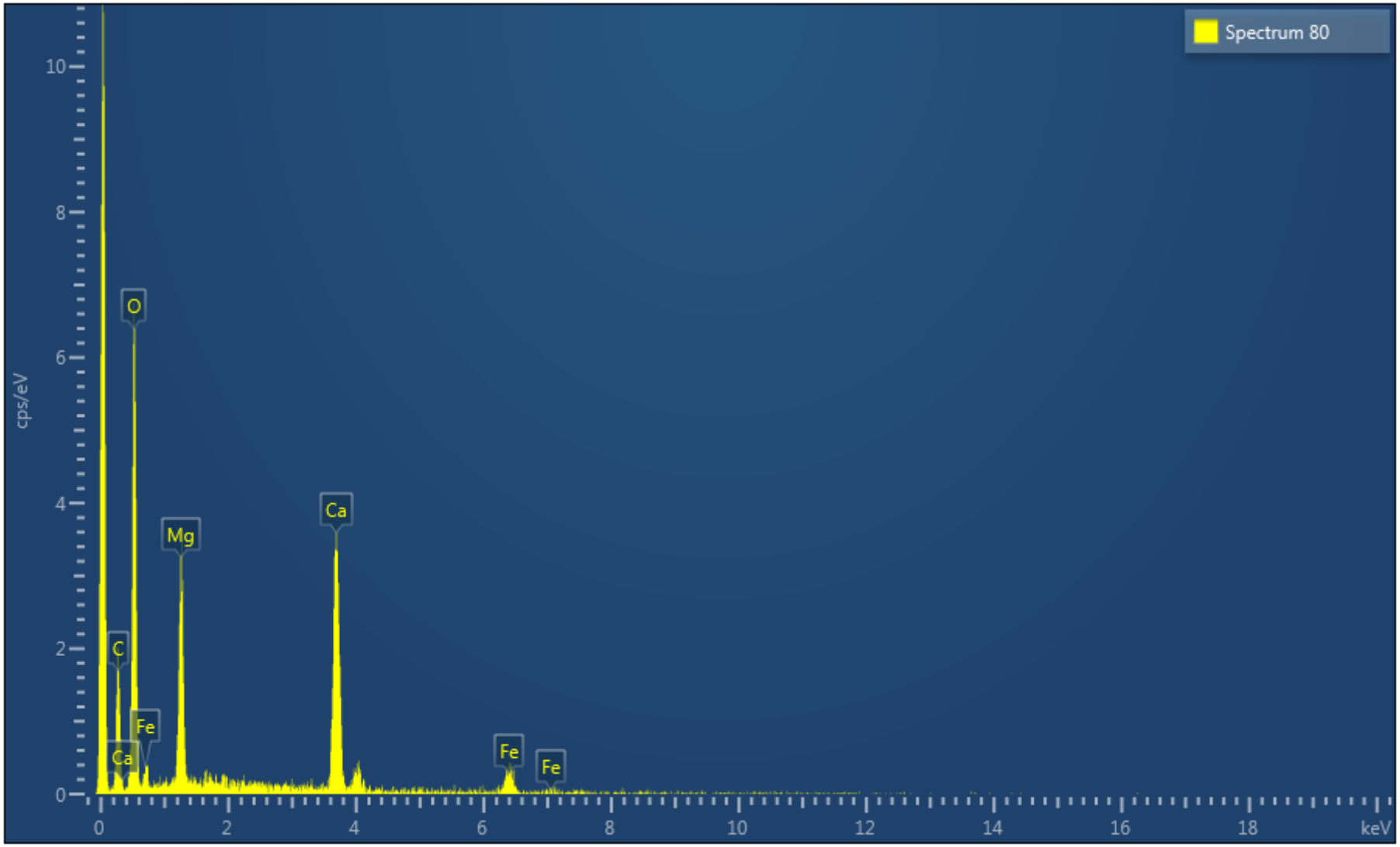
Spectrum 80
cps/eV
keV
O
C
Ca
Fe
Mg
Ca
Fe
Fe

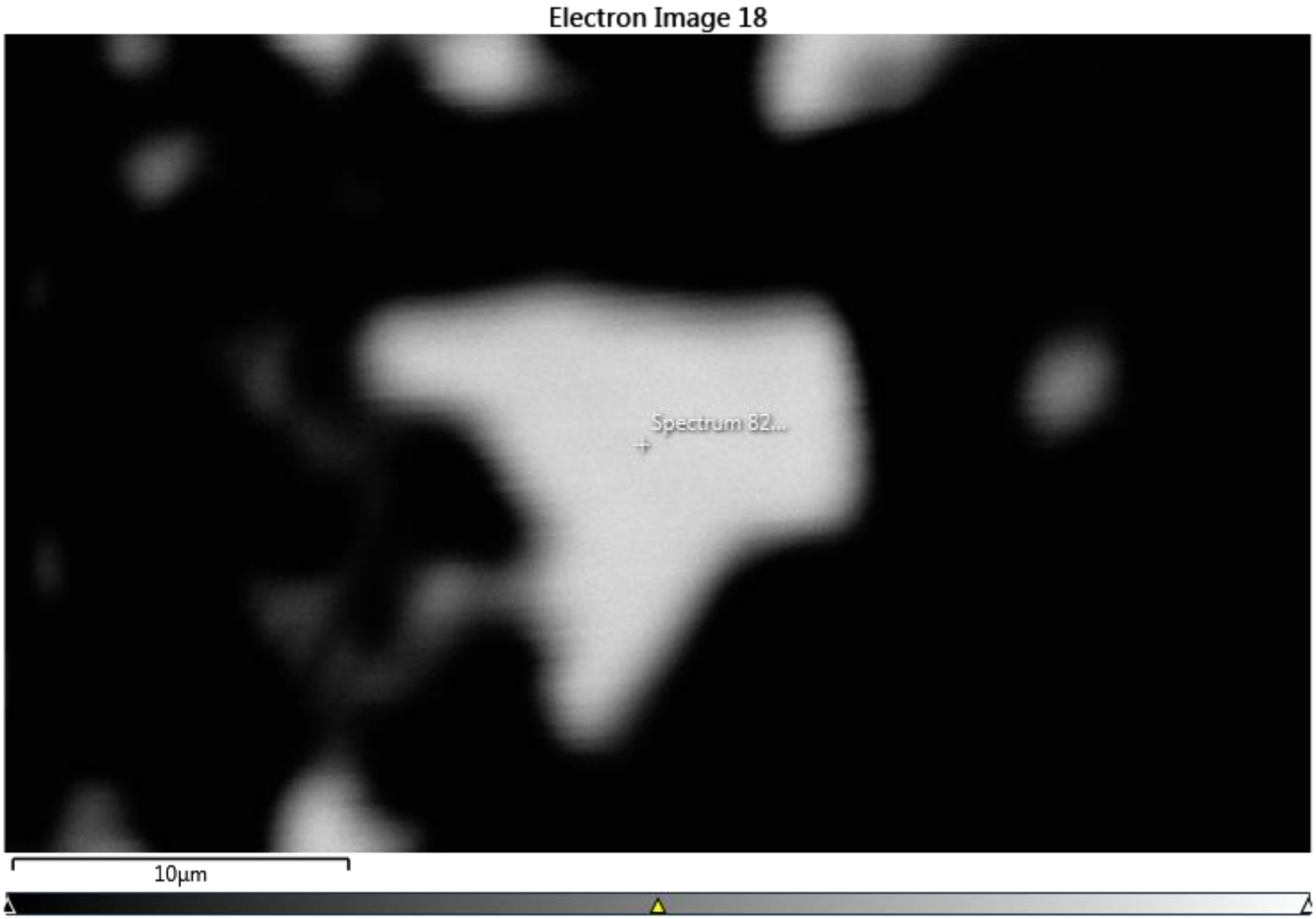

A higher magnification image of the the cluster of sulphides at the bottom of the image above. These grains are Sb-Ni-Te-As-S.

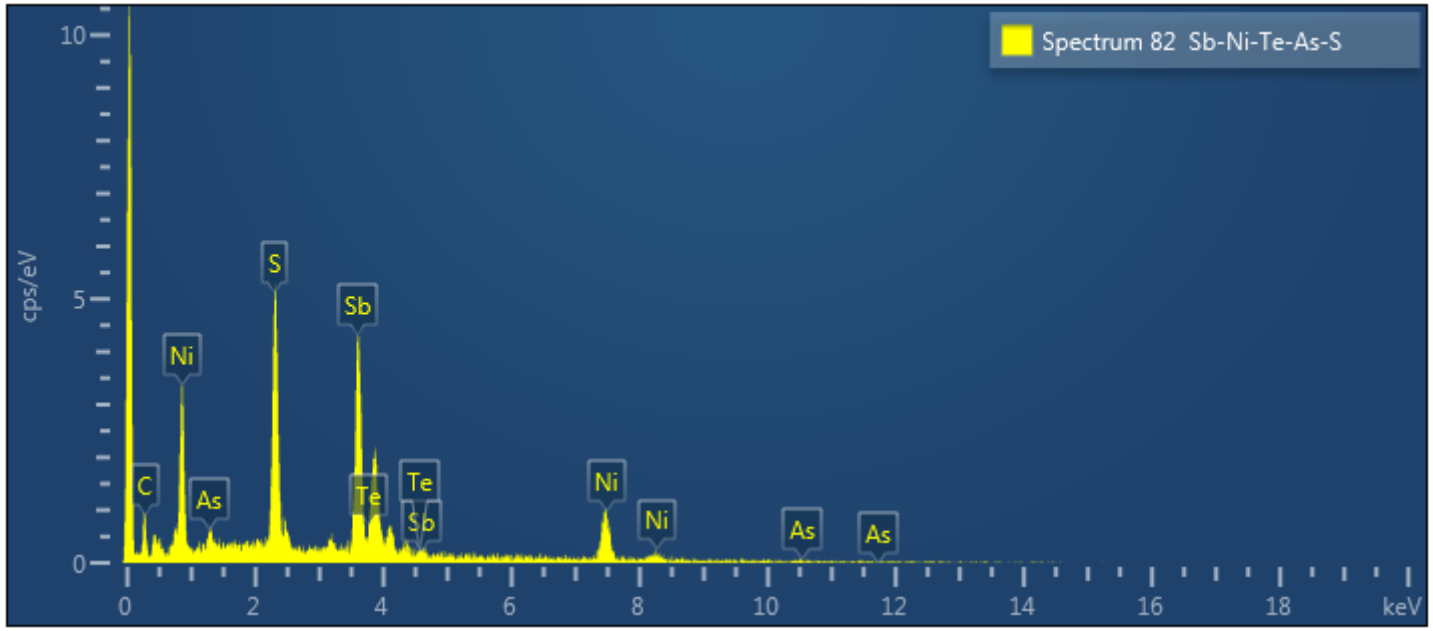

Spectrum 82 Sb-Ni-Te-As-S				
Element	**Line Type**	**Weight %**	**Weight % Sigma**	**Atomic %**
S	K series	17.96	0.57	40.01
Ni	K series	17.30	0.82	21.05
Sb	L series	57.77	1.15	33.88
As	L series	2.97	0.70	2.83
Te	L series	3.99	1.11	2.23
Total		100.00		100.00

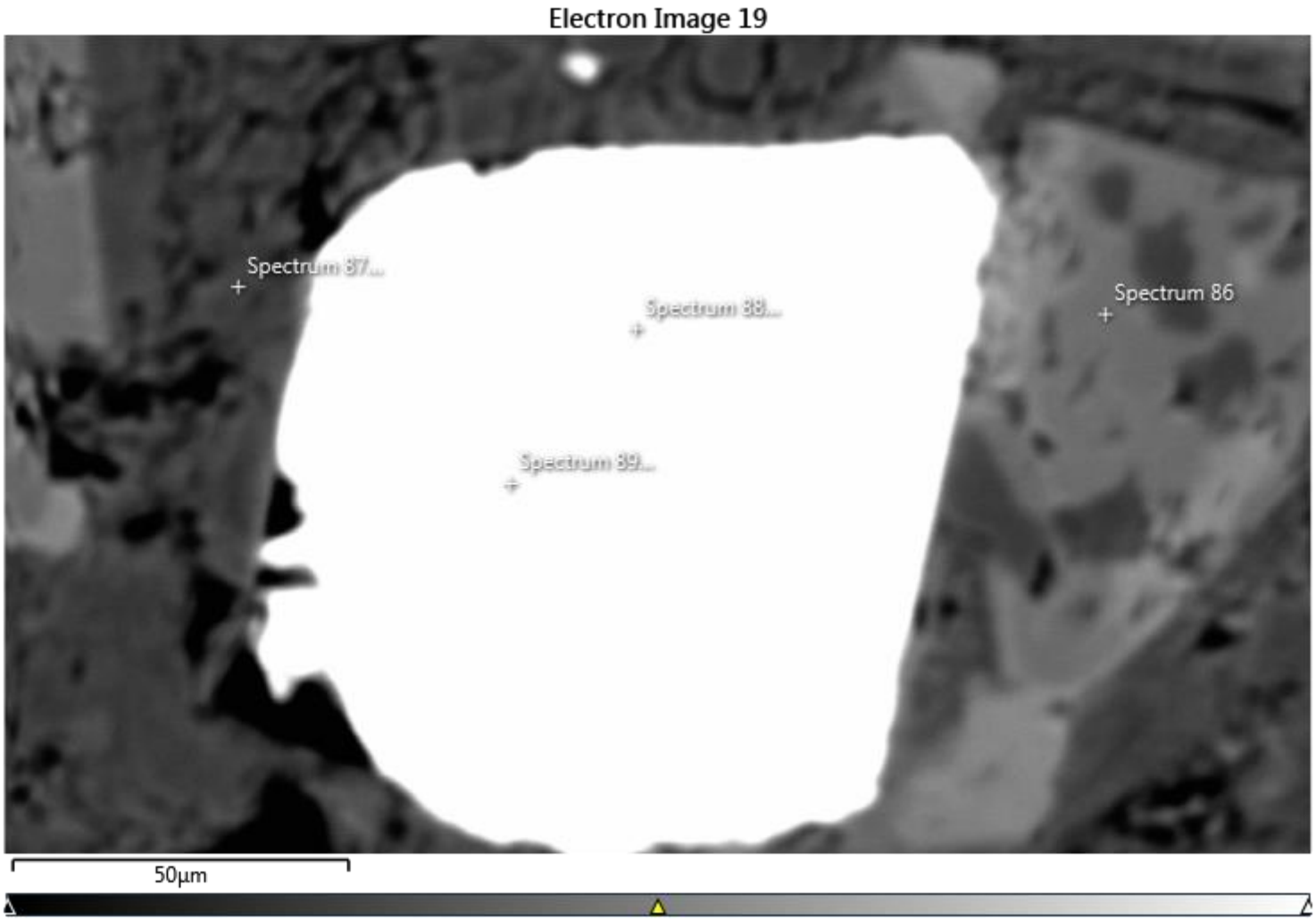

Backscatter image of a complexly zoned grain of As-Ni-Sb-S (spectrum 88) with an inclusion of Sb-Cu-Zn-Fe-S (spectrum 89) hosted within a groundmass of complexly zoned carbonate (spectrum 86) and Cr-paragonite (spectrum 87).

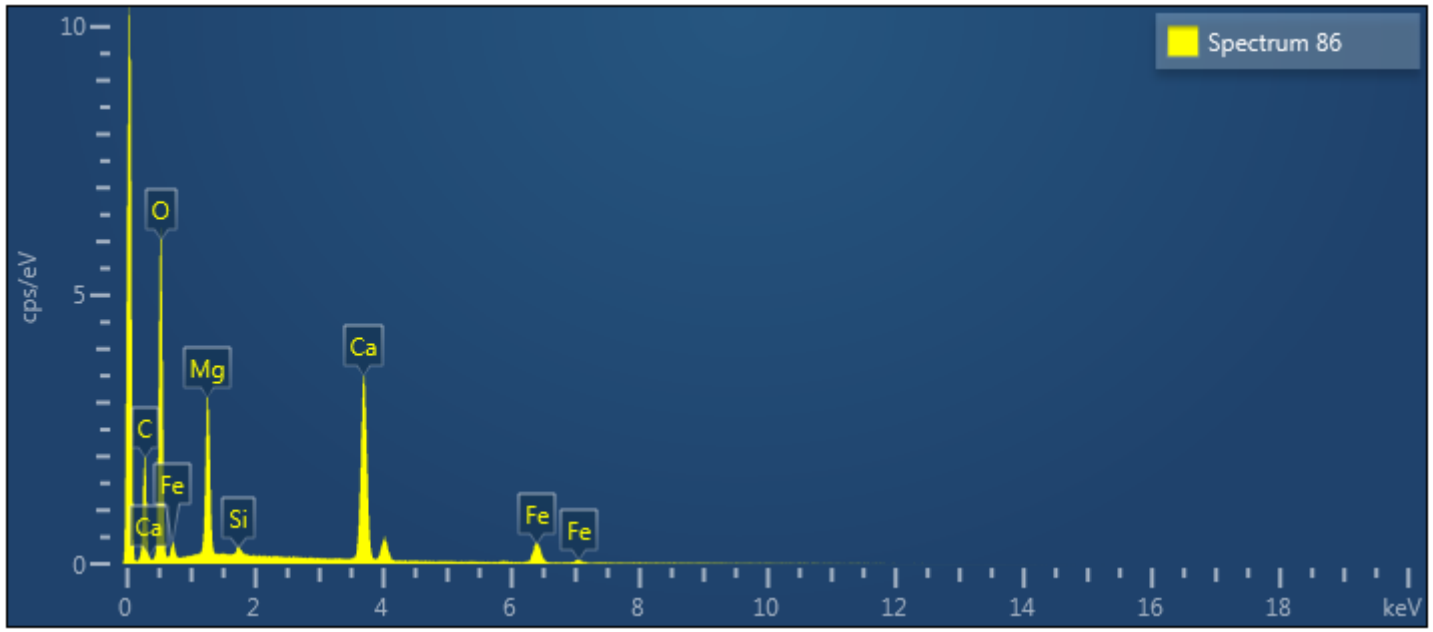
Spectrum 86
cps/eV
10
5
0
O
Mg
Ca
C
Fe
Ca
Si
Fe
Fe
0
2
4
6
8
10
12
14
16
18
keV

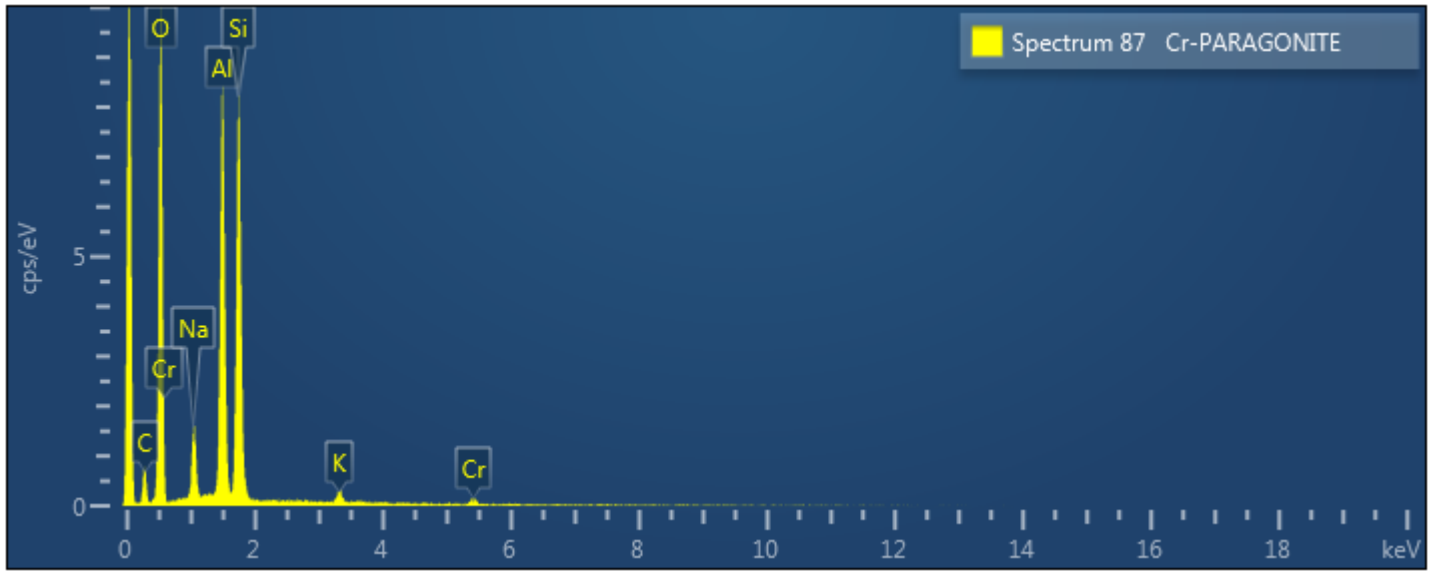

Spectrum 87 Cr-PARAGONITE							
Element	**Line Type**	**Weight %**	**Weight % Sigma**	**Atomic %**	**Oxide**	**Oxide %**	**Oxide % Sigma**
O	K series	48.10	0.33	61.35			
Na	K series	5.36	0.19	4.75	Na2O	7.22	0.26
Al	K series	20.74	0.25	15.68	Al2O3	39.18	0.48
Si	K series	23.81	0.28	17.30	SiO2	50.94	0.59
K	K series	0.99	0.09	0.52	K2O	1.19	0.11
Cr	K series	1.00	0.12	0.39	Cr2O3	1.47	0.18
Total		100.00		100.00		100.00	

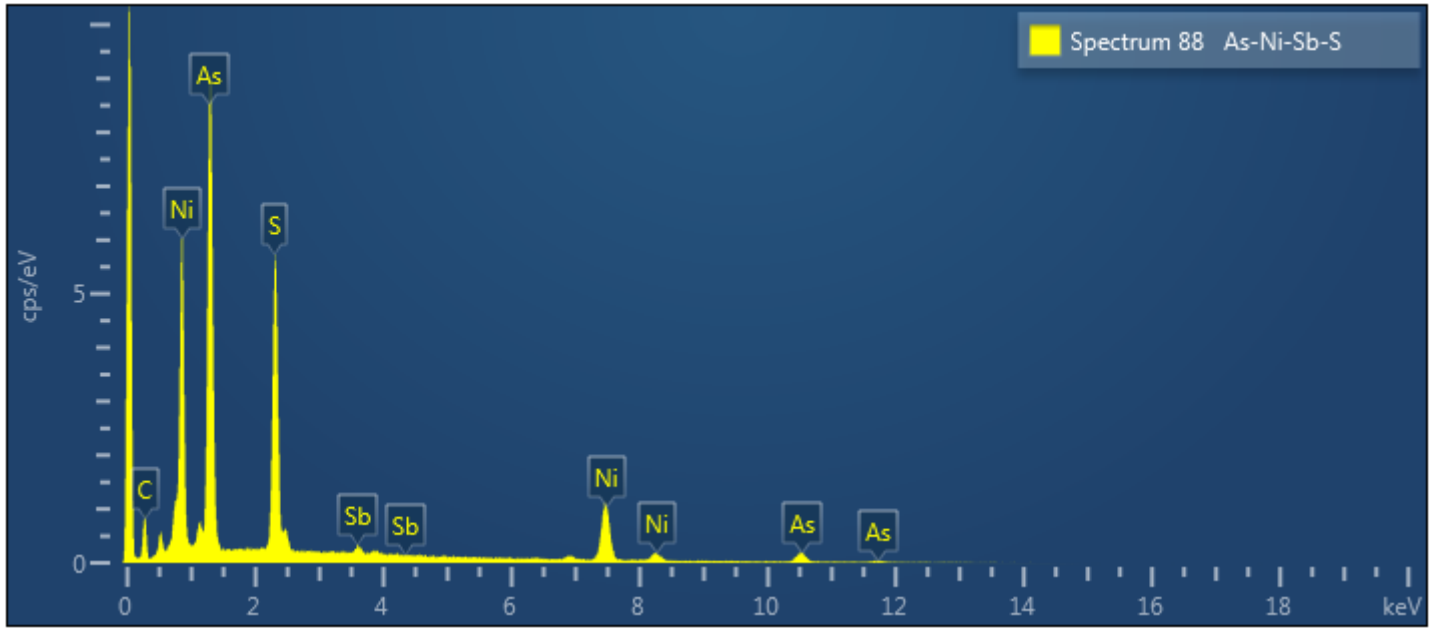

Spectrum 88 As-Ni-Sb-S				
Element	**Line Type**	**Weight %**	**Weight % Sigma**	**Atomic %**
S	K series	24.36	0.21	41.45
Ni	K series	20.14	0.26	18.71
As	L series	53.48	0.29	38.94
Sb	L series	2.02	0.18	0.91
Total		100.00		100.00

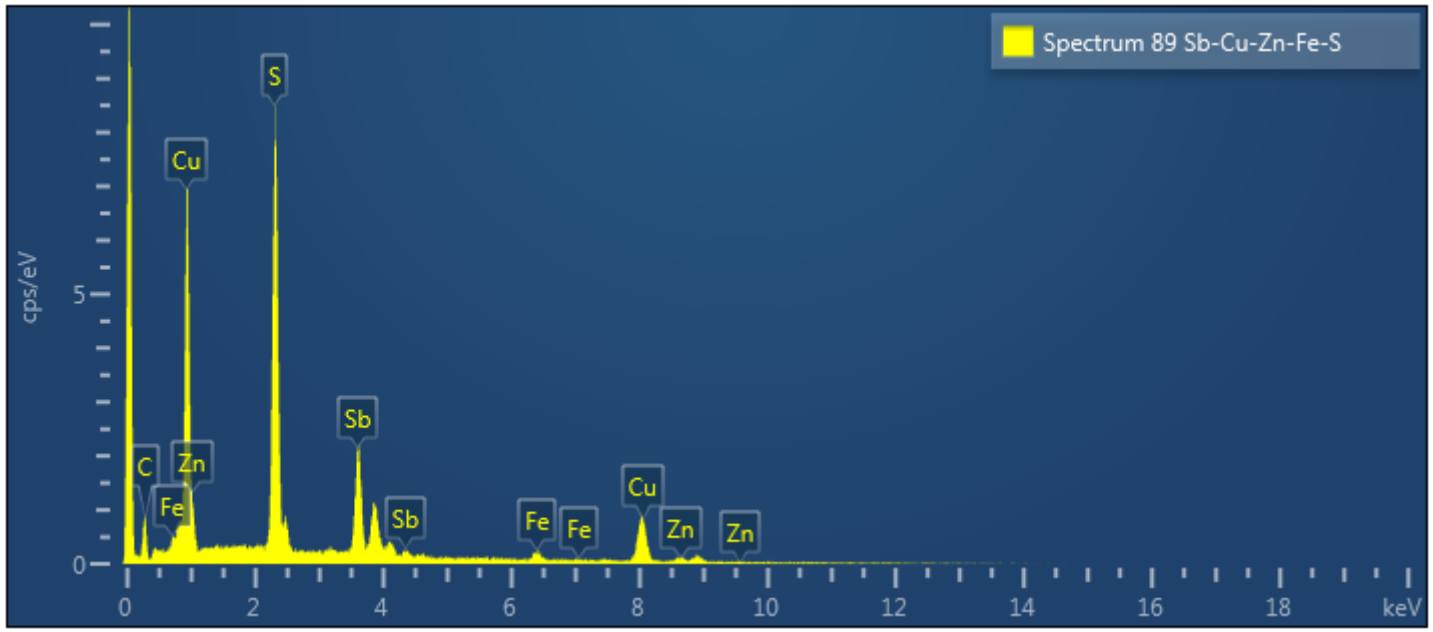

Spectrum 89 Sb-Cu-Zn-Fe-S				
Element	**Line Type**	**Weight %**	**Weight % Sigma**	**Atomic %**
S	K series	34.28	0.47	57.94
Cu	K series	25.42	0.58	21.68
Sb	L series	34.85	0.56	15.51
Zn	K series	2.96	0.44	2.45
Fe	K series	2.49	0.25	2.41
Total		100.00		100.00

Specimen Notes for 'ML-47'

Sample ML-47 is an intensely carbonated and sheared rock. The rock has undergone more than one generation of quartz-carbonate alteration evident in the above image and within the polished section. There is evidence of possible brecciation possibly due to deformation within a shear and then sealed by hydrothermal fluids. The groundmass is dominated by approximately 60% calcite, dolomite, dolomite-ankerite solid-solution carbonates intergrown with 30% polycrystalline quartz, 5% Cr-green mica (fuchsite), and disseminated Zn-bearing chromite grains. The rock is dominated by calcite and dolomite-ankerite solid-solution carbonate. The rock illustrates evidence of later cross-cutting coarser-grained veinlets of carbonate and finer-grained cryptocrystalline sugary quartz. The sulphide inventory is interesting and comprised of disseminated galena, coarse-grained pyrite cubes, Ni-sulphide (vaesite), and Ni-As-S minerals.

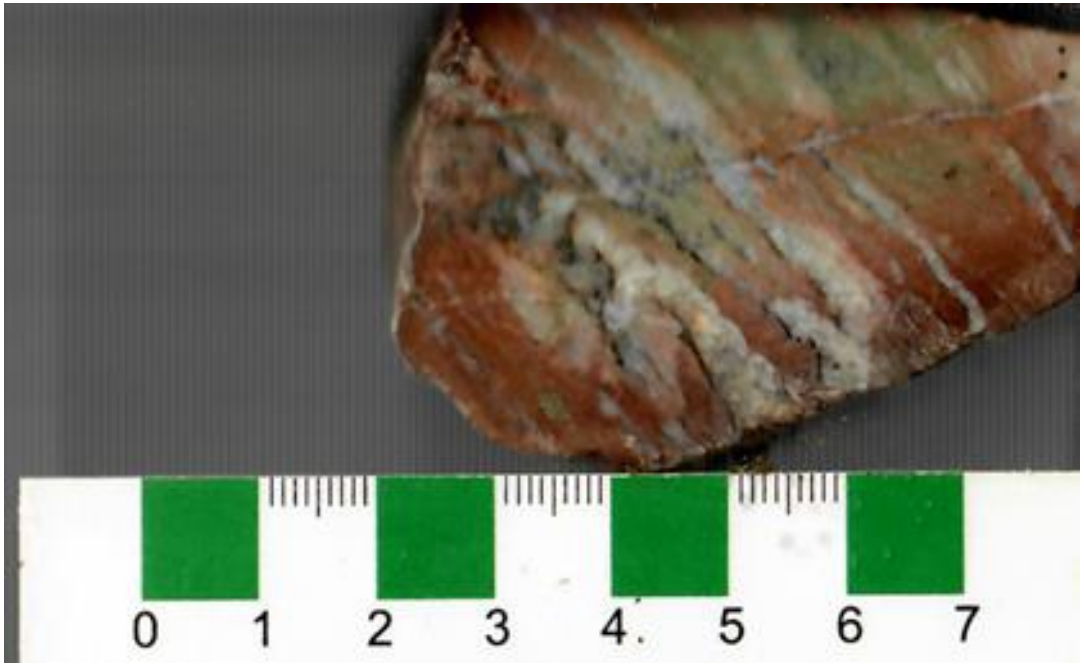

Handspecimen sample of ML-47 (with cm-scale card).

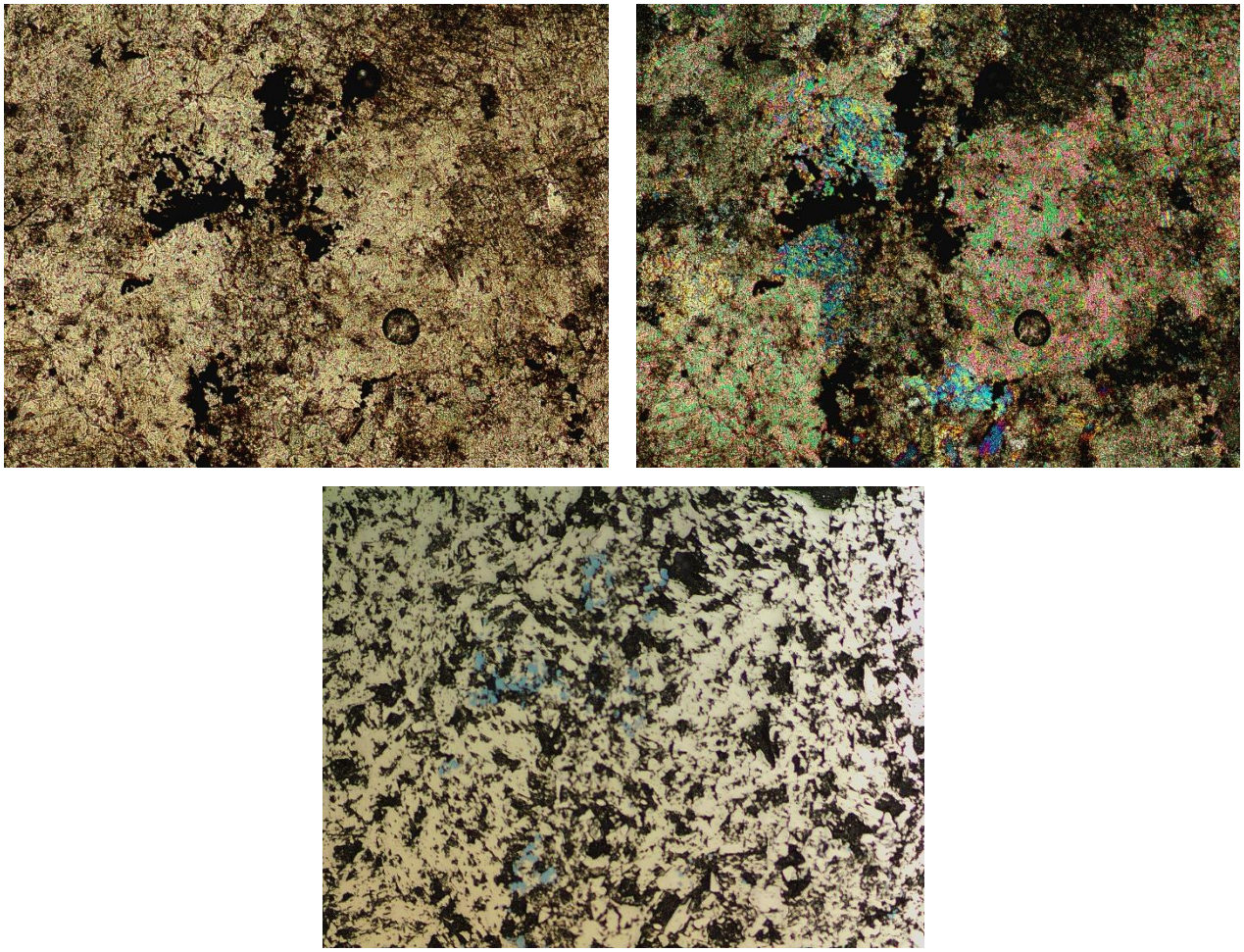

Plane light photomicrograph (left) and crossed polarized light image (right) illustrating the carbonate-dominated alteration. Bottom image is reflected light illustrating the blue-reflective sulphide mineralogy within the specimen consisting of Ni-S (vaesite) and Ni-As-S. Field of View = 2.2mm

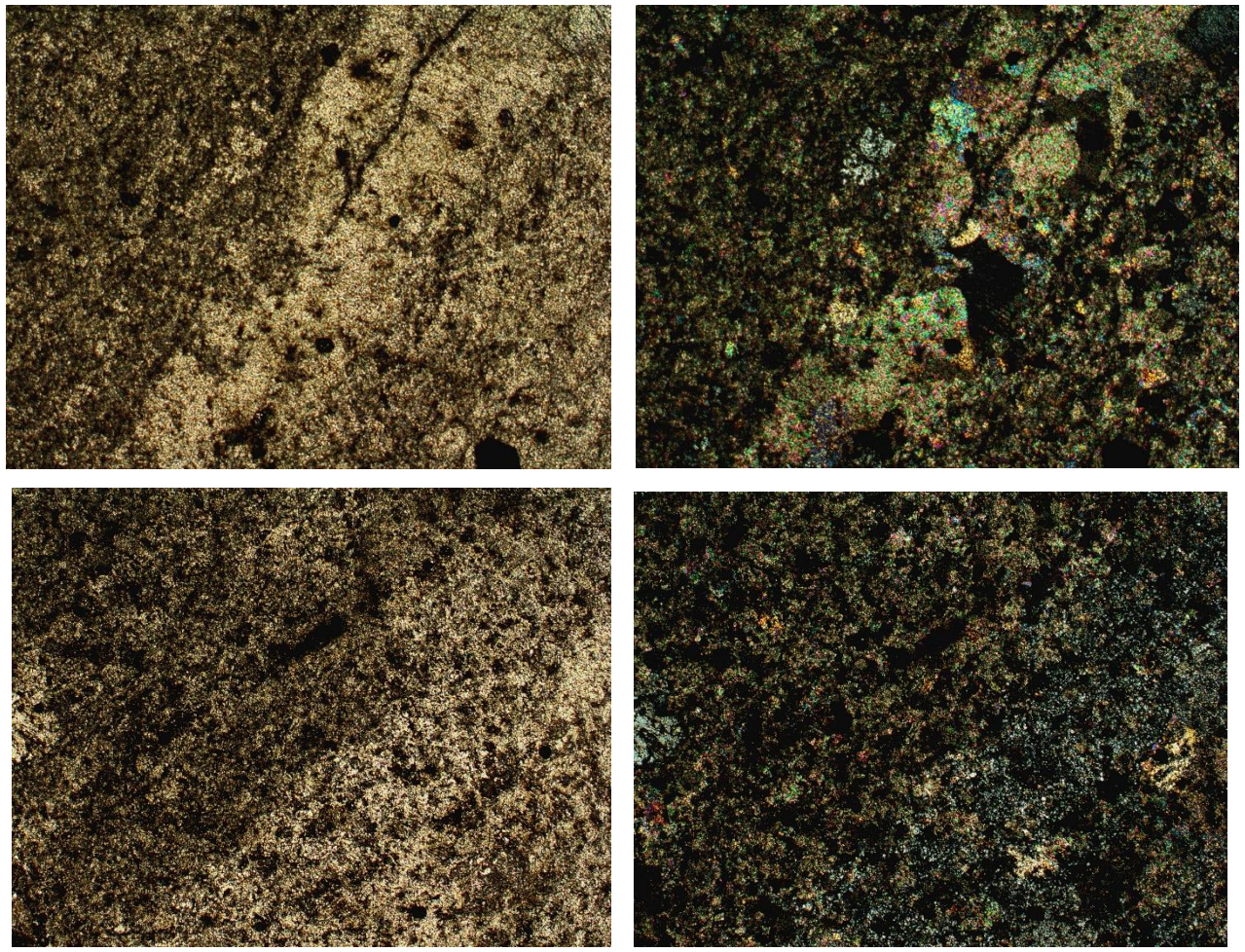

Plane light image (top left) and crossed-polarized image (top right) illustrating a dark brown-red groundmass dominated by carbonate cut by a late-stage diagonal highly birefringent carbonate veinlet. The bottom left image (plane light) and the bottom right image (crossed polarized light) illustrating a late-stage fine-grained cryptocrystalline sugary quartz veinlet cutting the sample at approximately 45 degrees. Field of View = 9mm

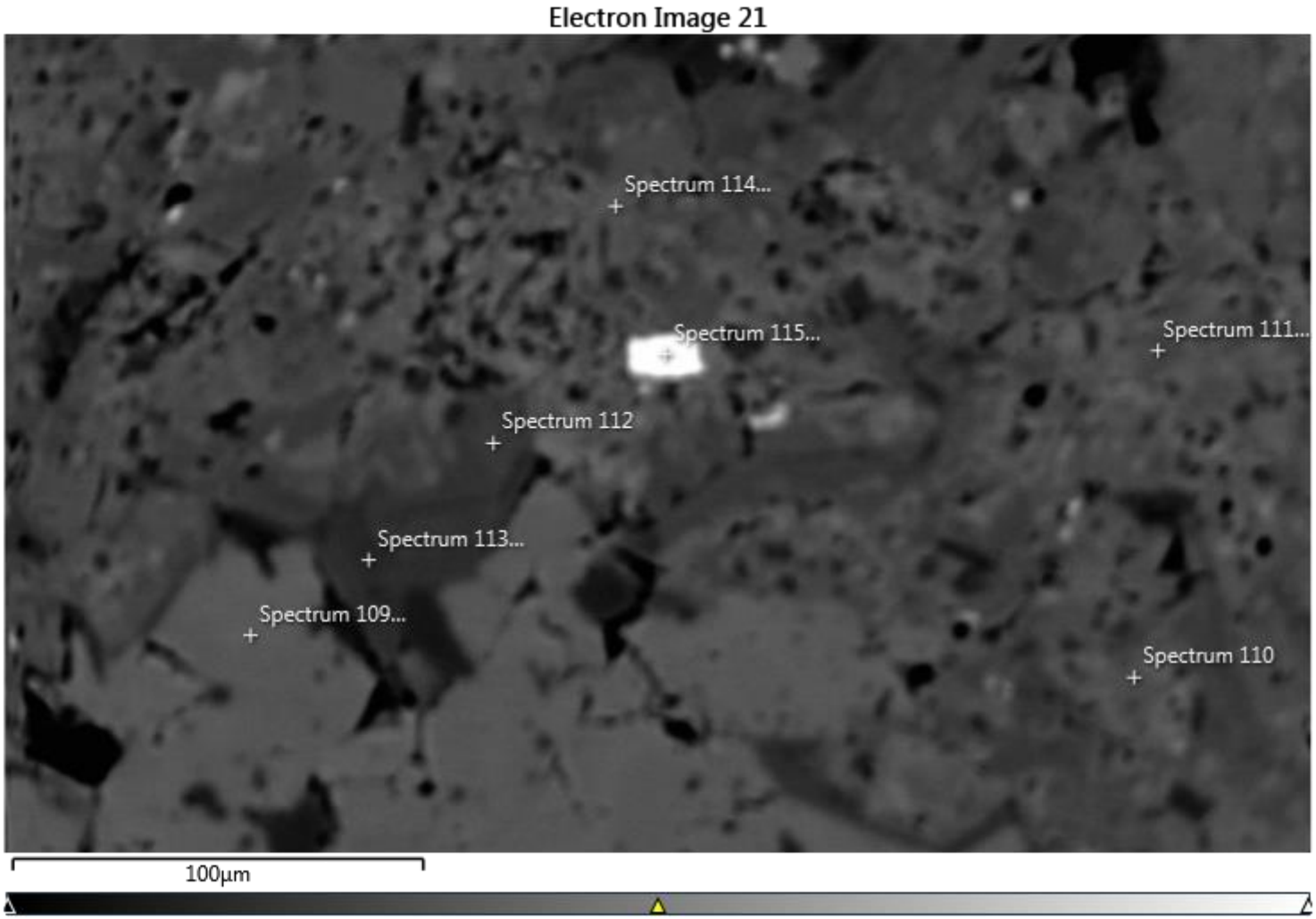

Backscatter image illustrating well-defined calcite crystals (spectrum 109) intergrown with dolomite and dolomite-ankerite solid solution carbonate (spectrum 110-113). A fine-grained Zn-chromite (spectrum 115) is intergrown with the carbonate species and contains 12.48 wt% ZnO.

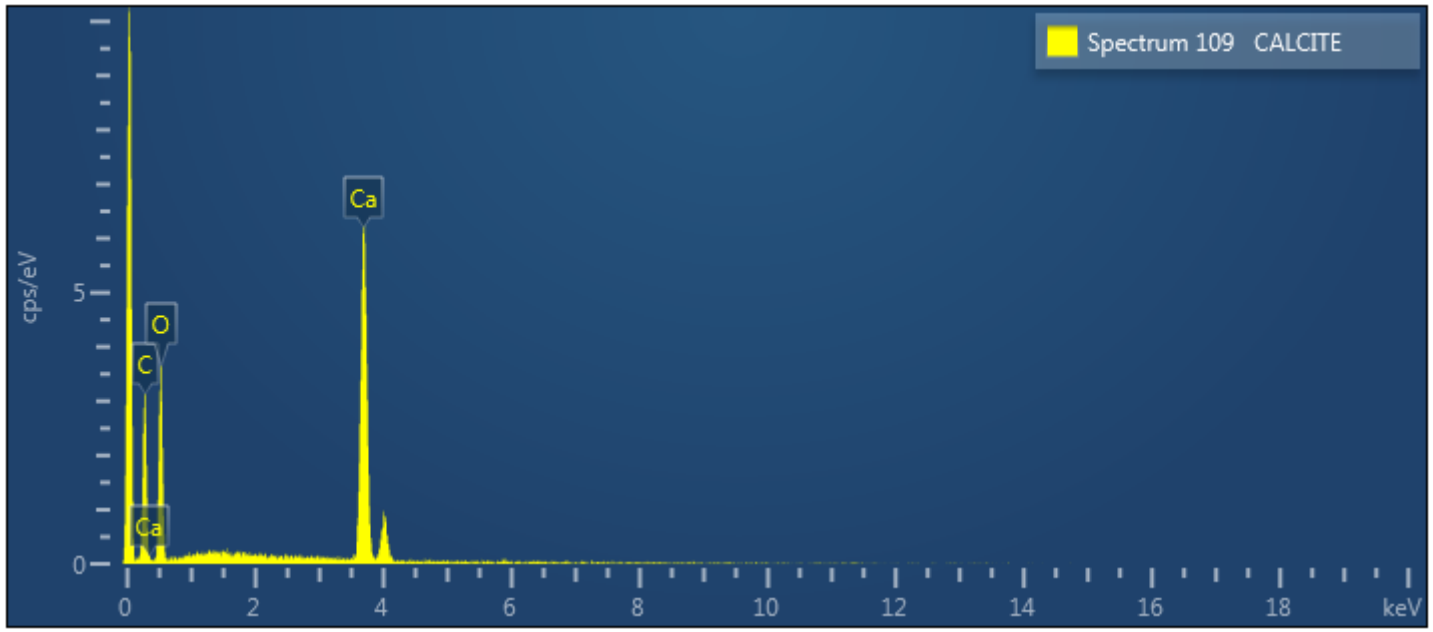
Spectrum 109 CALCITE
cps/eV
5
0
O
C
Ca
Ca
0
2
4
6
8
10
12
14
16
18
keV

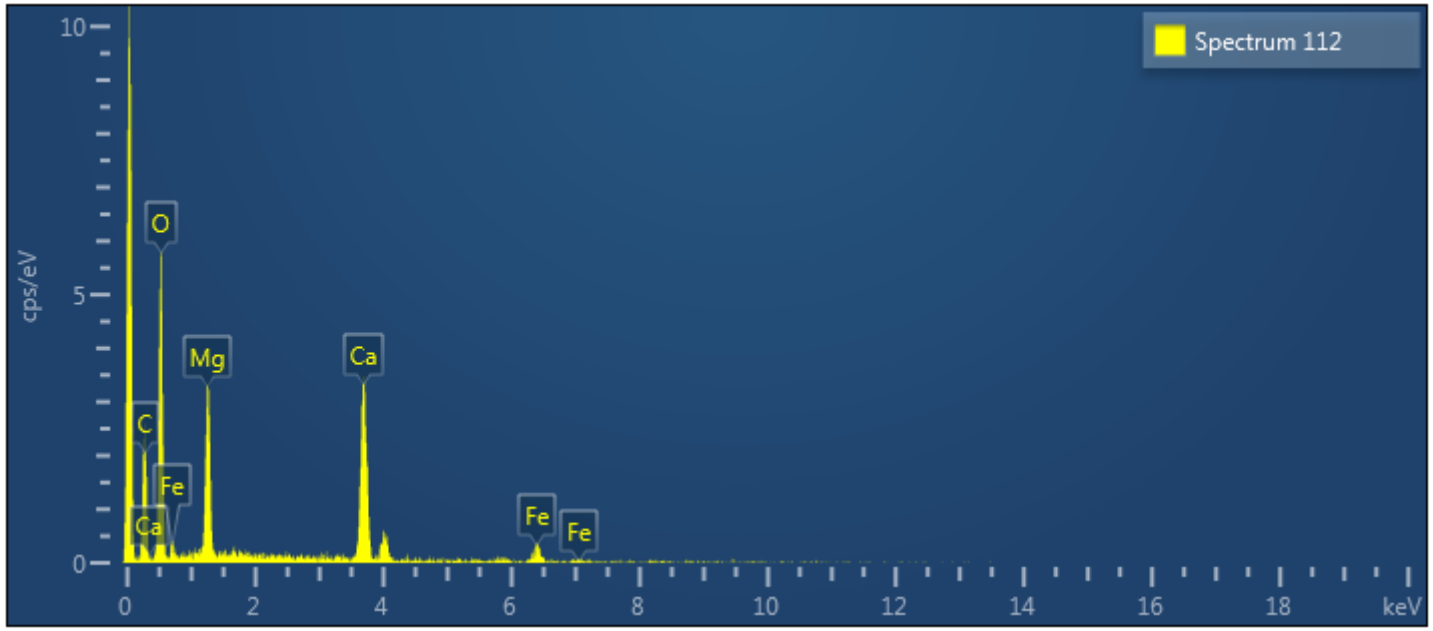
Spectrum 112
cps/eV
10
5
0
O
C
Ca
Fe
Mg
Ca
Fe
Fe
0
2
4
6
8
10
12
14
16
18
keV

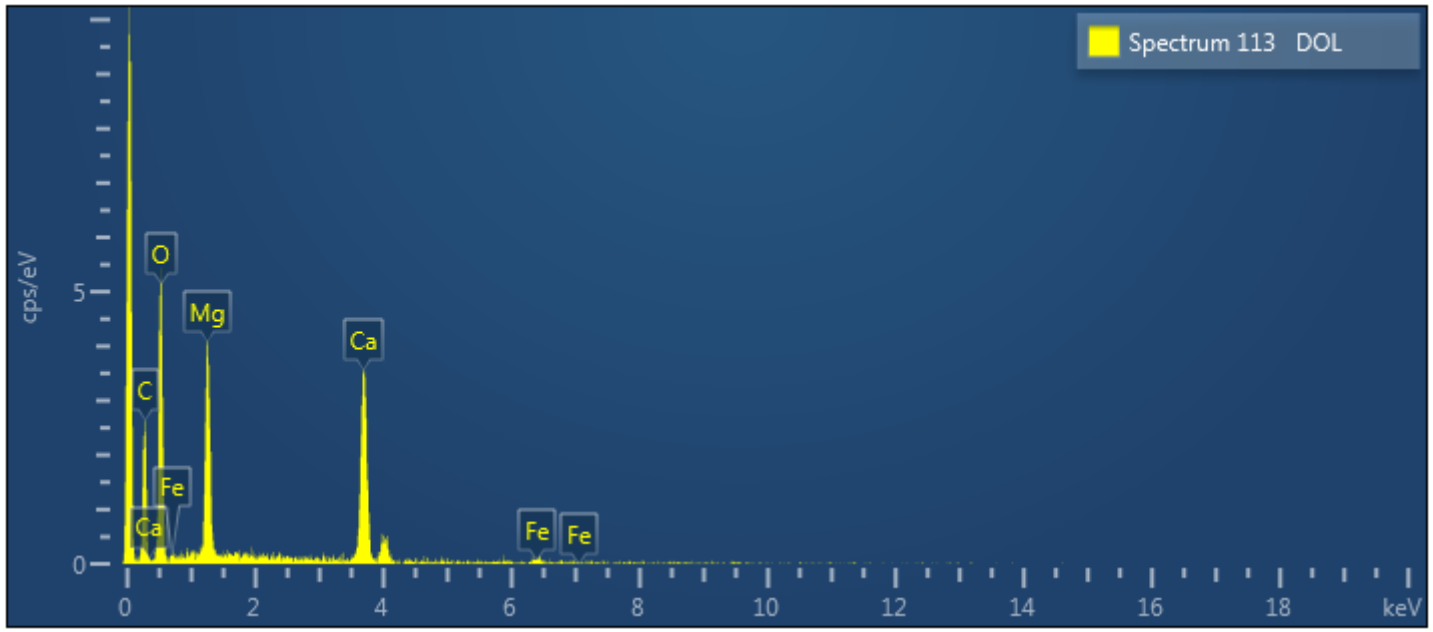
Spectrum 113 DOL
cps/eV
5
0
O
Mg
Ca
C
Fe
Ca
Fe
Fe
0
2
4
6
8
10
12
14
16
18
keV

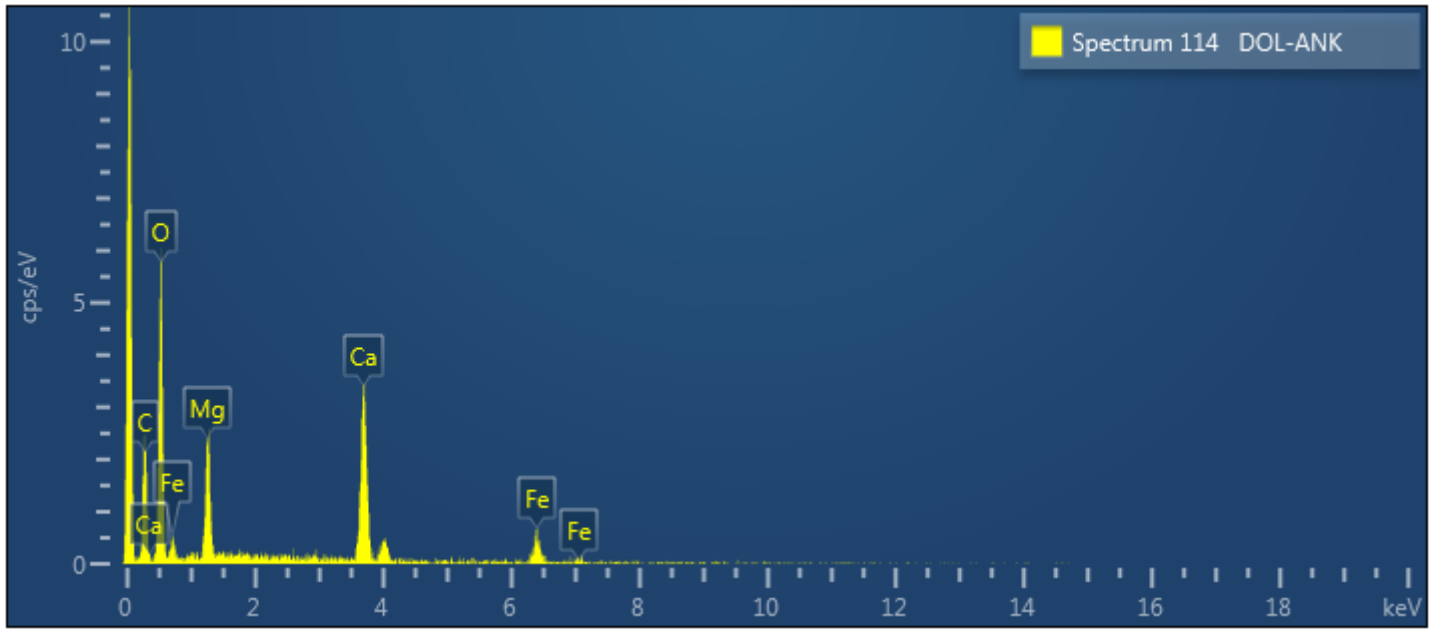
Spectrum 114 DOL-ANK
cps/eV
10
5
0
O
C
Ca
Fe
Mg
Ca
Fe
Fe
0
2
4
6
8
10
12
14
16
18
keV

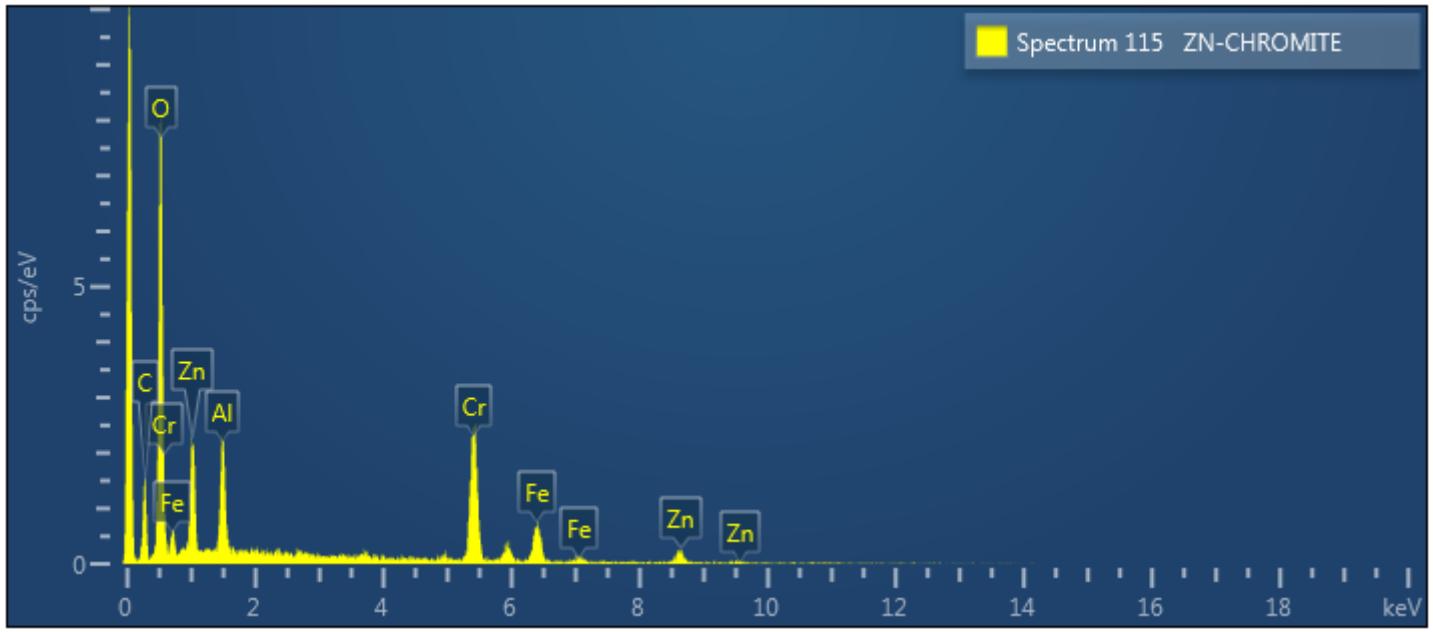

Spectrum 115 ZN-CHROMITE							
Element	**Line Type**	**Weight %**	**Weight % Sigma**	**Atomic %**	**Oxide**	**Oxide %**	**Oxide % Sigma**
O	K series	31.97	0.77	57.73			
Al	K series	11.90	0.47	12.74	Al2O3	22.48	0.88
Cr	K series	32.73	0.72	18.19	Cr2O3	47.84	1.06
Fe	K series	13.37	0.62	6.92	FeO	17.20	0.79
Zn	K series	10.03	0.82	4.43	ZnO	12.48	1.01
Total		100.00		100.00		100.00	

Specimen Notes for 'ML-49'

This rock appears to be a hydrothermal breccia where brecciated fragments comprised of Cr-paragonaite and dolomite-ankerite solid solution carbonate are sealed by coarse-grained polycrystalline quartz. The fragments are comprised of dolomite-ankerite solid solution carbonate, quartz, and Cr-paragonite mica. Importantly, the sulphide inventory is hosted within the breccia fragments and not the sealing quartz. The sulphide inventory consists of As-Ni-S, As-Ni-Sb-Co-S, As-Ni-Sb-S, Sb-Ni-As-S, As-Ni-Sb-Co-S, and Ni-S (vaesite).

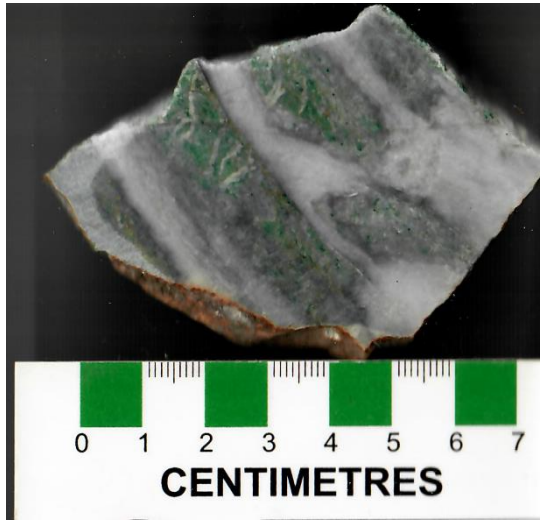

Handsample for ML-49.

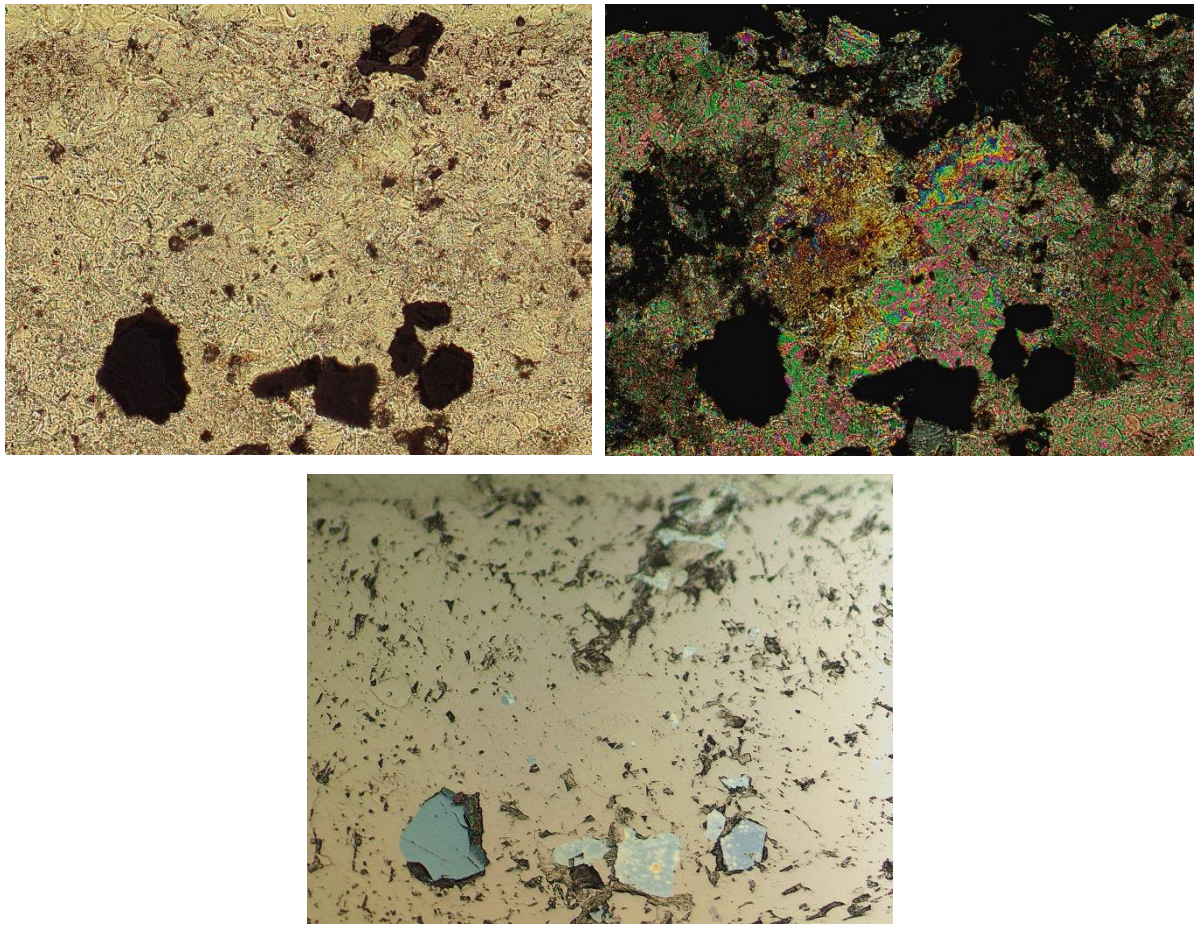

Plane light (top left) and crossed polarized light image (top right) illustrating the dominant carbonate and highly birefringent Cr-paragonite with opaque minerals. The reflected light image (bottom) shows arsenian pyrite (far left grain), two grains of Ni-S (vaesite) in the middle, and As-Ni-Co-Sb-S (far right grains). Field of view = 1.2mm. See backscatter image below.

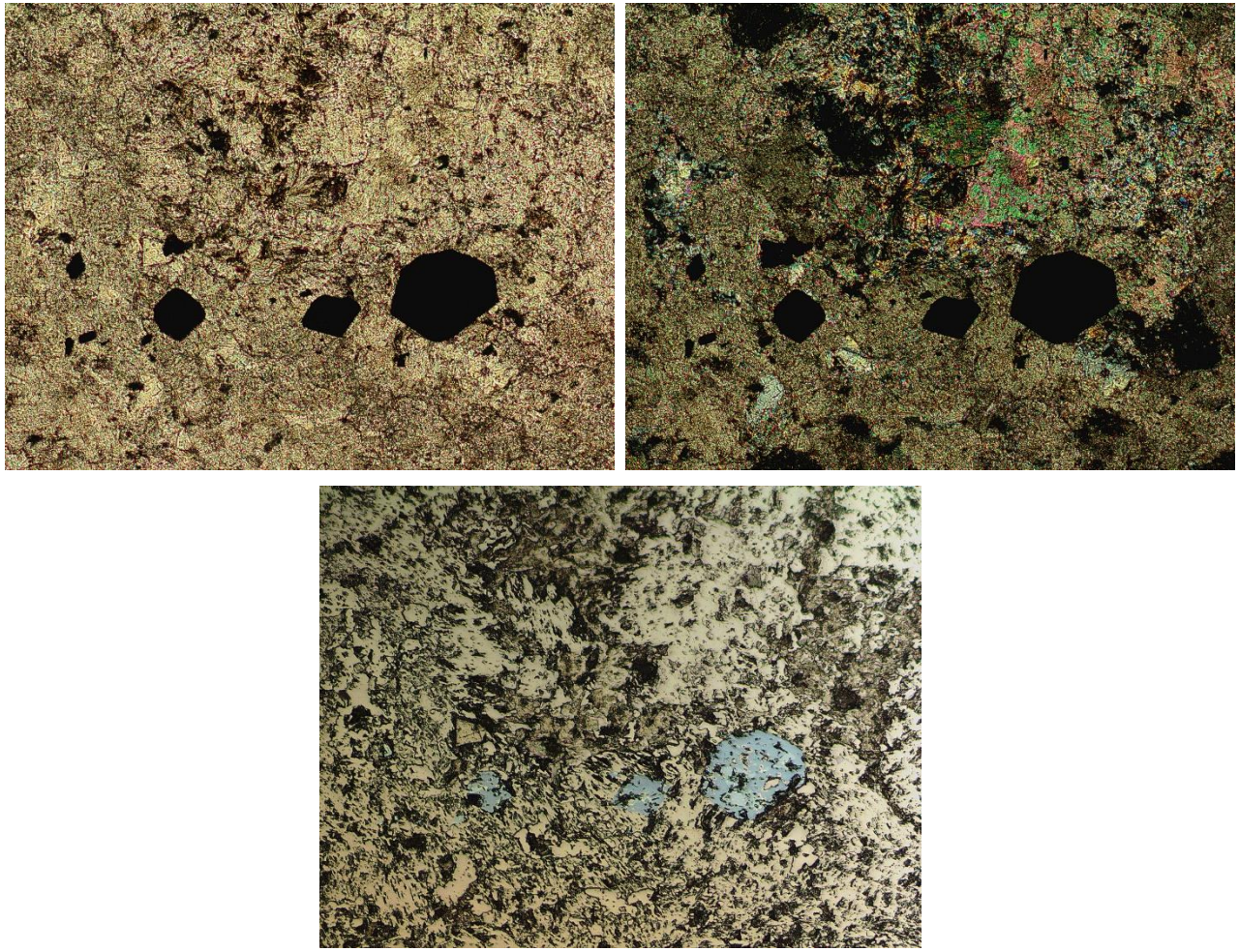

Plane light (top left) and crossed polarized light image (top right) illustrating the dominant carbonate and highly birefringent Cr-paragonite with opaque minerals. The reflected light image (bottom) shows As-Ni-Sb-Co-S (far left grain), a middle grain of Ni-S (vaesite), and a Ni-S (vaesite) with included As-Ni-Sb-S. Field of view = 2.2mm. See backscatter image below.

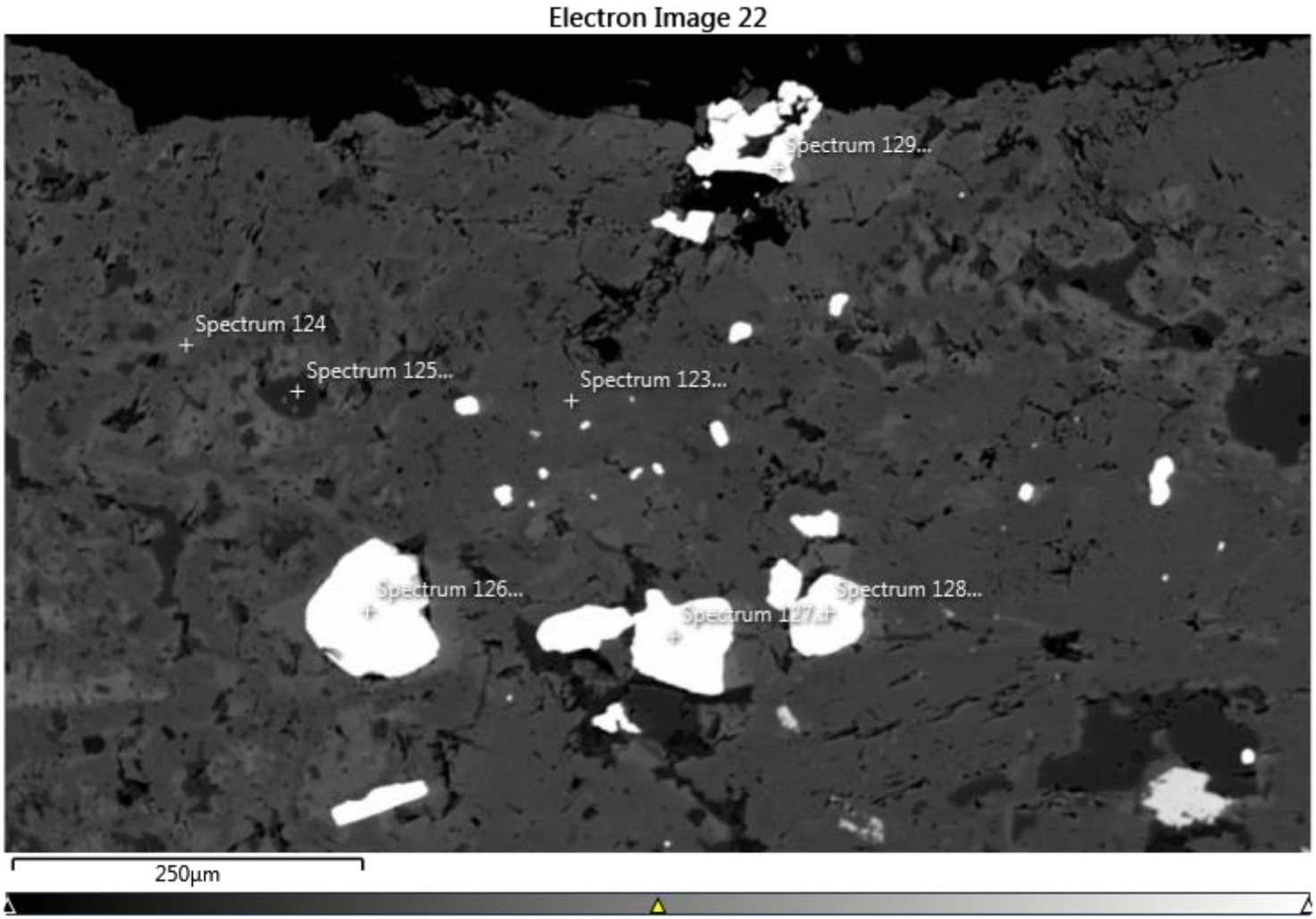

Backscatter image illustrating the compositional variation of the carbonate groundmass (spectrum 123, 124), intergrown with quartz (spectrum 125), and Cr-paragonite with disseminated grains of arsenian pyrite (spectrum 126), two grains of Ni-S (vaesite – spectrum 127), and As-Ni-Co-Sb-S (spectrum 128).

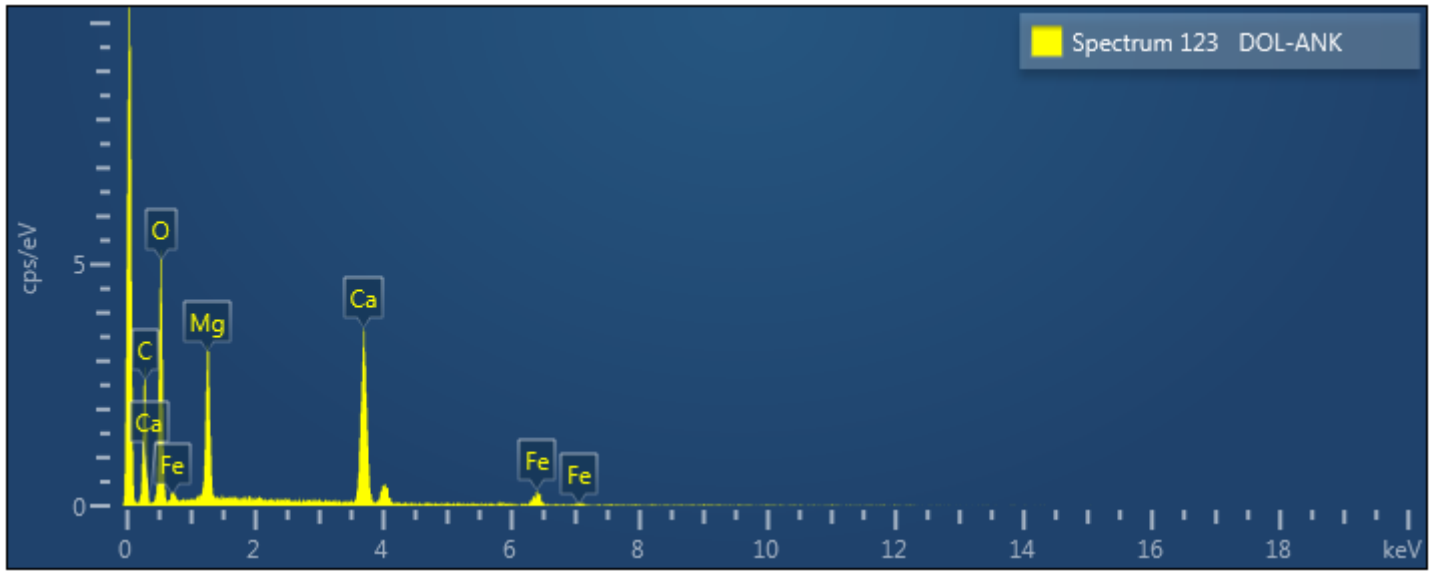
Spectrum 123 DOL-ANK
cps/eV
5
0
O
C
Ca
Fe
Mg
Ca
Fe
Fe
0
2
4
6
8
10
12
14
16
18
keV

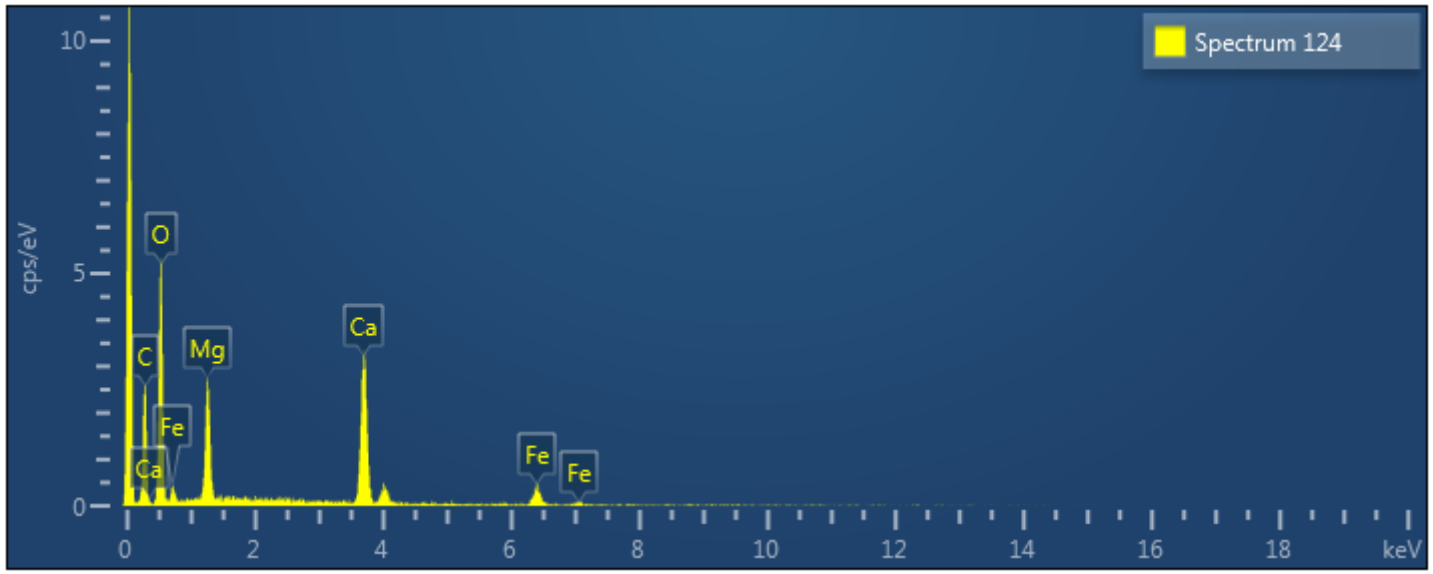
Spectrum 124
cps/eV
10
5
0
O
C
Mg
Ca
Fe
Ca
Fe
Fe
0
2
4
6
8
10
12
14
16
18
keV

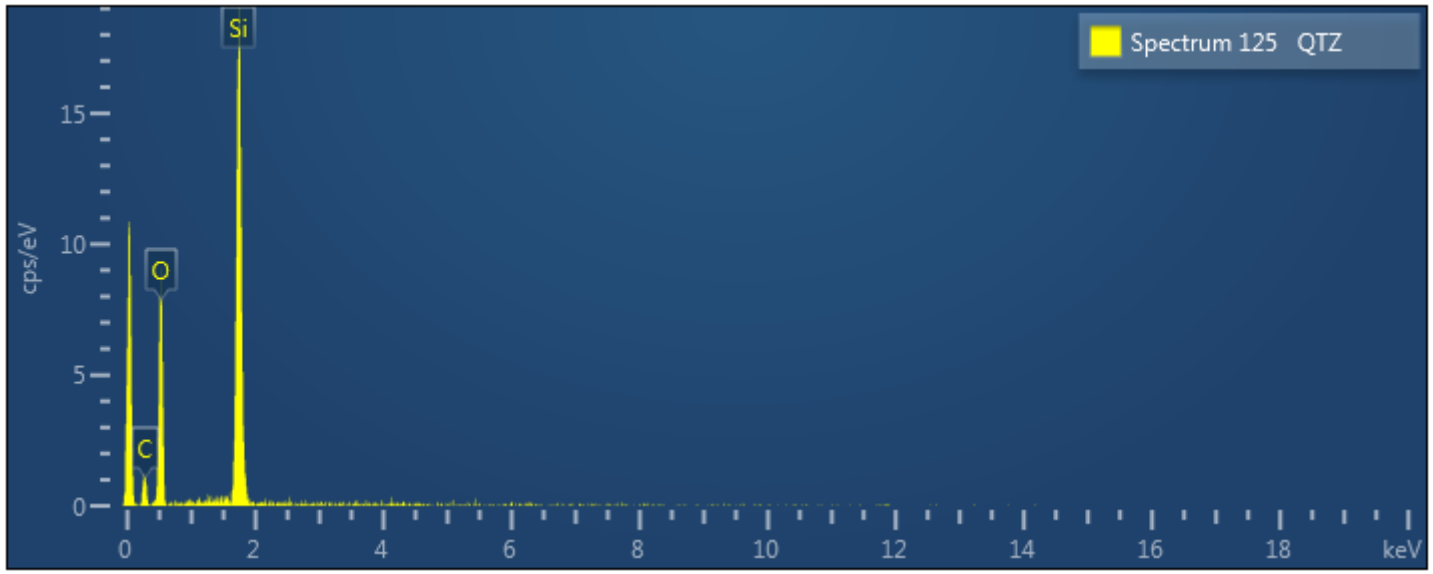

Spectrum 125 QTZ							
Element	**Line Type**	**Weight %**	**Weight % Sigma**	**Atomic %**	**Oxide**	**Oxide %**	**Oxide % Sigma**
O	K series	53.26	1.02	66.67			
Si	K series	46.74	1.02	33.33	SiO2	100.00	2.18
Total		100.00		100.00		100.00	

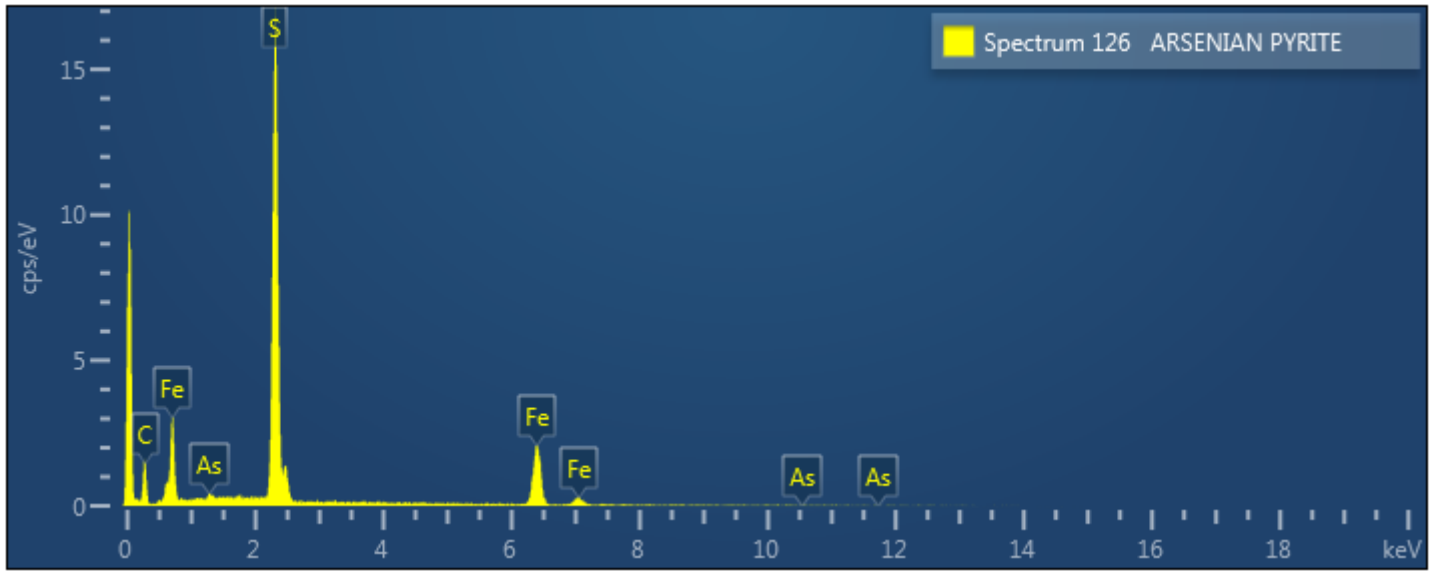

Spectrum 126 ARSENIAN PYRITE				
Element	**Line Type**	**Weight %**	**Weight % Sigma**	**Atomic %**
S	K series	64.25	0.56	75.99
Fe	K series	34.22	0.54	23.23
As	L series	1.54	0.34	0.78
Total		100.00		100.00

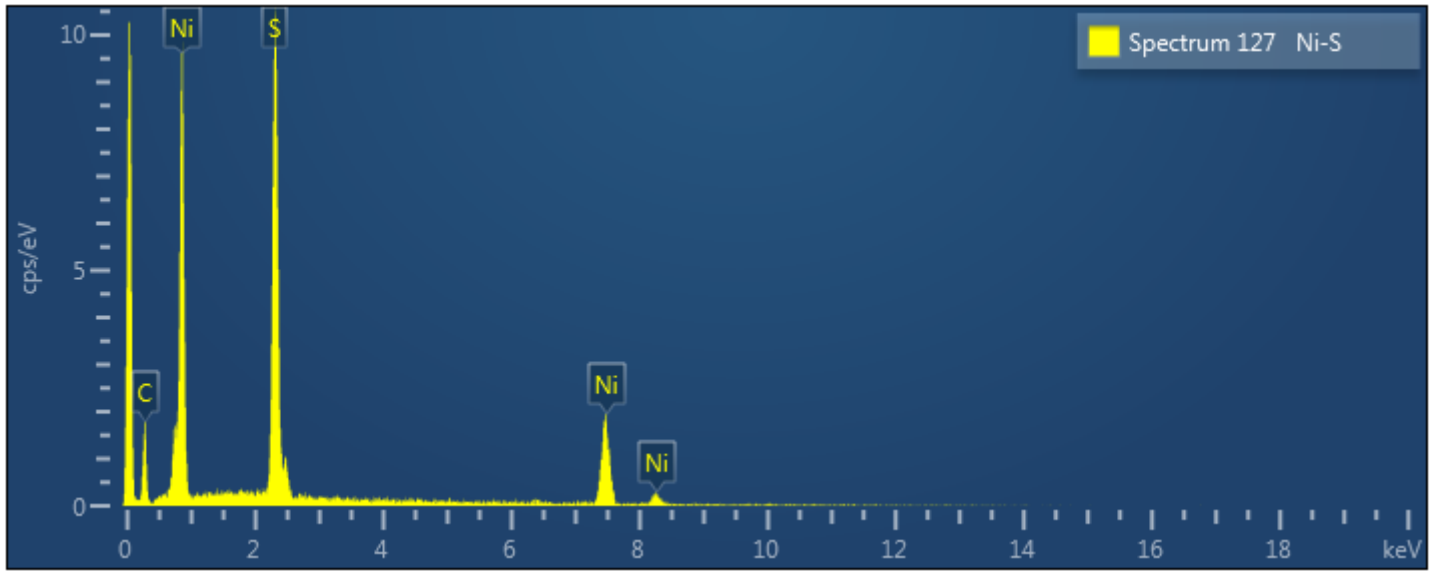

Spectrum 127 Ni-S				
Element	**Line Type**	**Weight %**	**Weight % Sigma**	**Atomic %**
S	K series	50.93	0.81	65.53
Ni	K series	49.07	0.81	34.47
Total		100.00		100.00

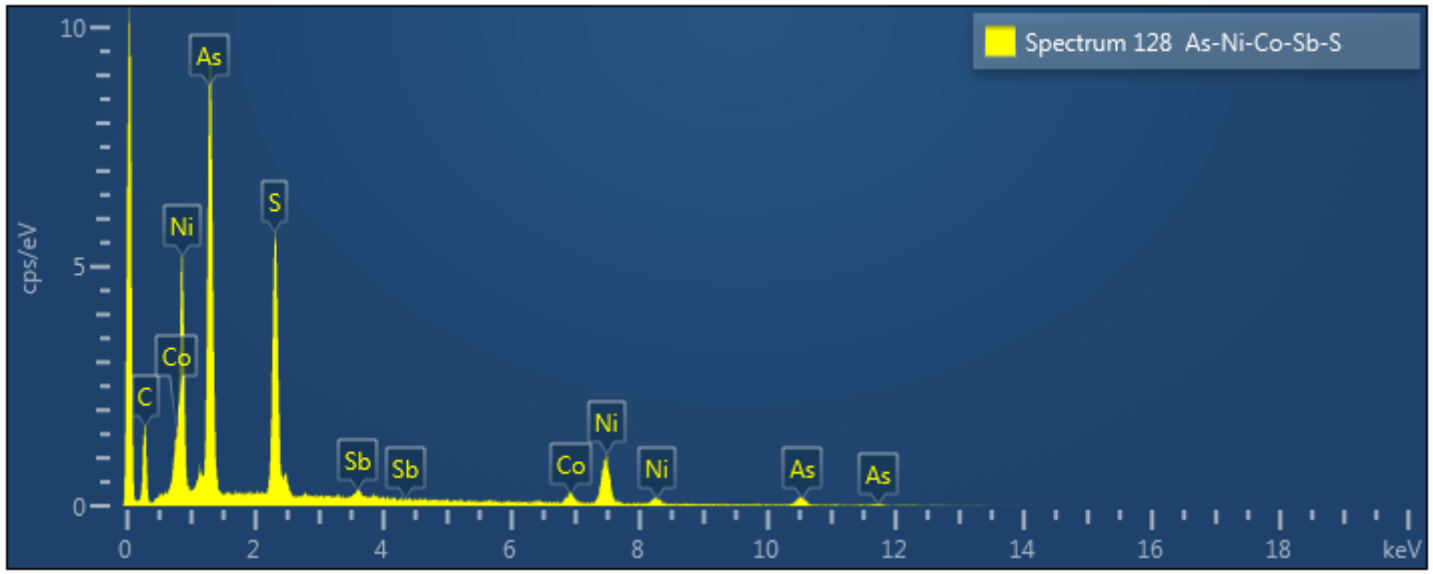

Spectrum 128 As-Ni-Co-Sb-S				
Element	**Line Type**	**Weight %**	**Weight % Sigma**	**Atomic %**
S	K series	23.69	0.32	40.49
Ni	K series	17.85	0.40	16.66
As	L series	53.29	0.47	38.98
Co	K series	3.22	0.24	2.99
Sb	L series	1.94	0.28	0.87
Total		100.00		100.00

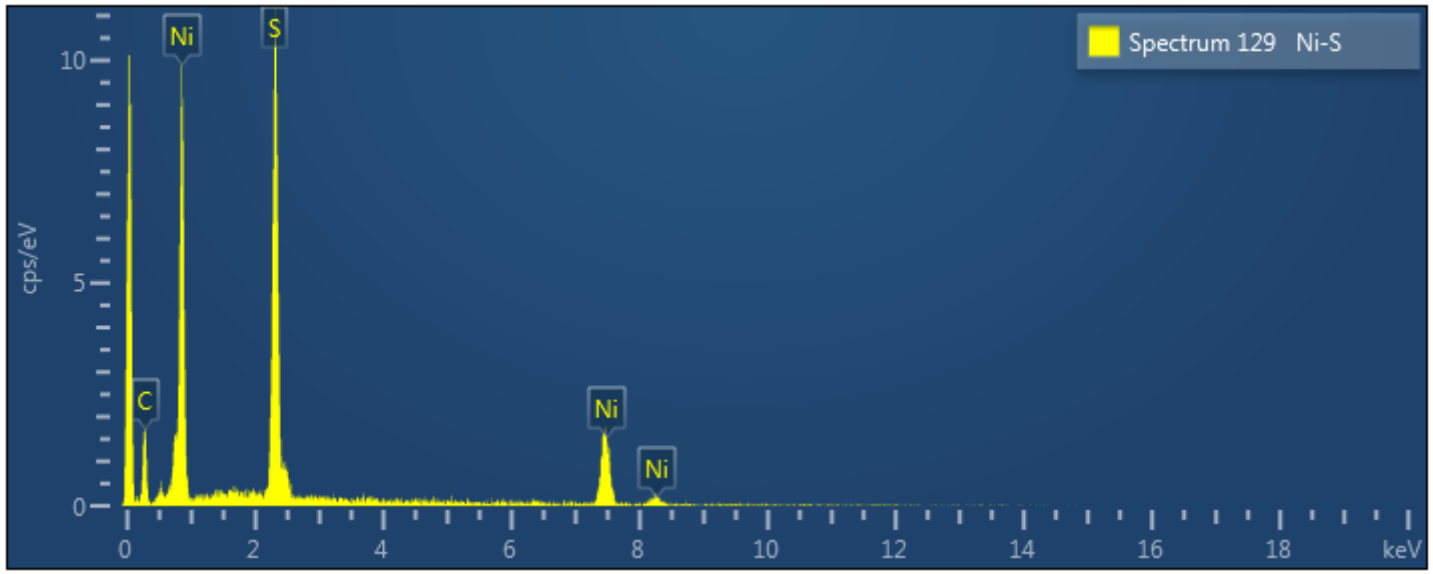

Spectrum 129 Ni-S				
Element	**Line Type**	**Weight %**	**Weight % Sigma**	**Atomic %**
S	K series	52.83	1.17	67.22
Ni	K series	47.17	1.17	32.78
Total		100.00		100.00

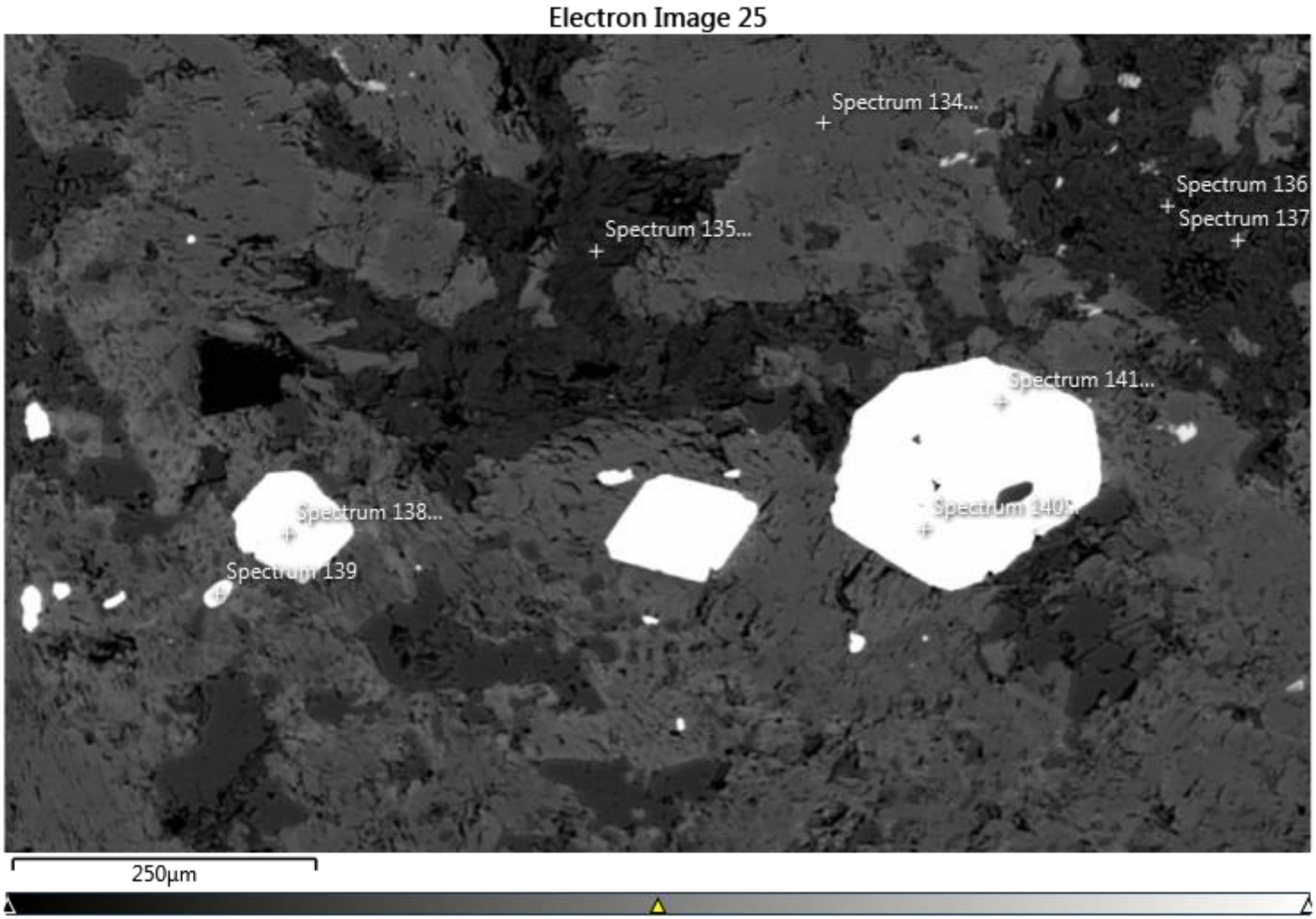

Backscatter image illustrating the compositional variation of the carbonate groundmass (spectrum 134), intergrown with quartz, and Cr-paragonite (spectrum 135, 136) with disseminated grains of As-Ni-Sb-Co-S (spectrum 138), a middle grain of Ni-S (vaesite), and a Ni-S (vaesite) with included As-Ni-Sb-S (spectrum 140, 141).

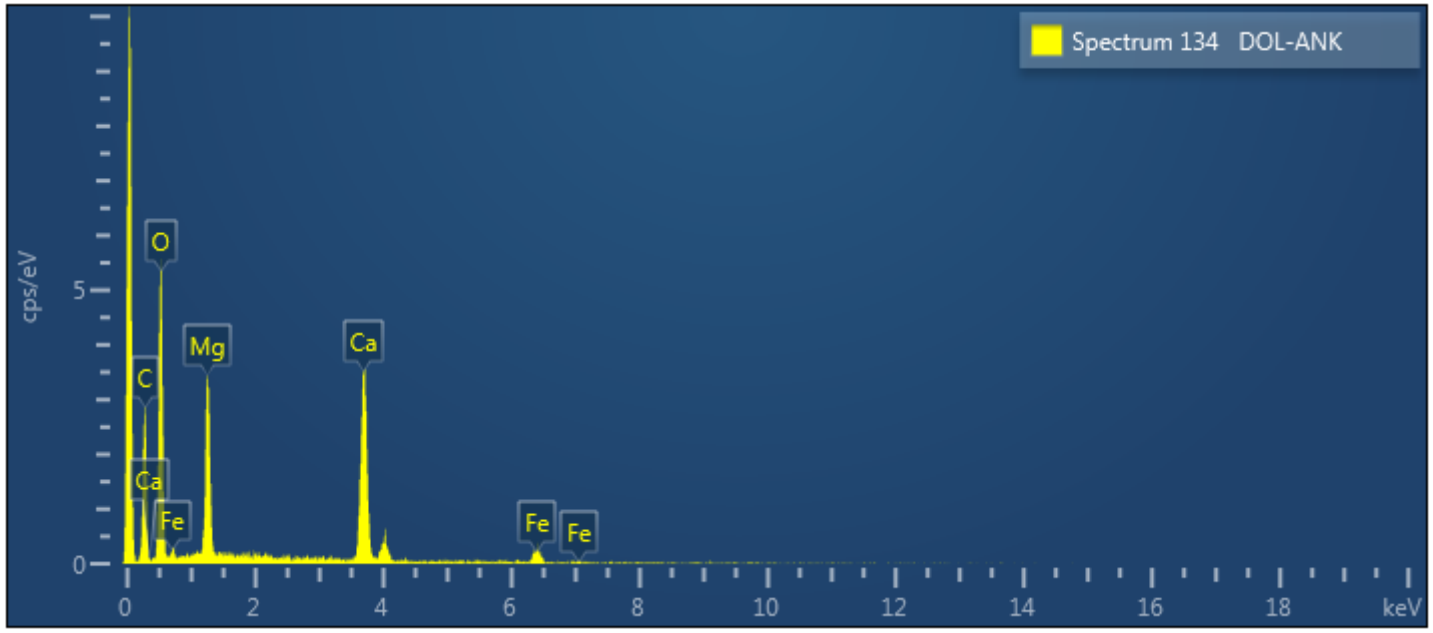
Spectrum 134 DOL-ANK
cps/eV
5
0
O
C
Ca
Fe
Mg
Ca
Fe
Fe
0
2
4
6
8
10
12
14
16
18
keV

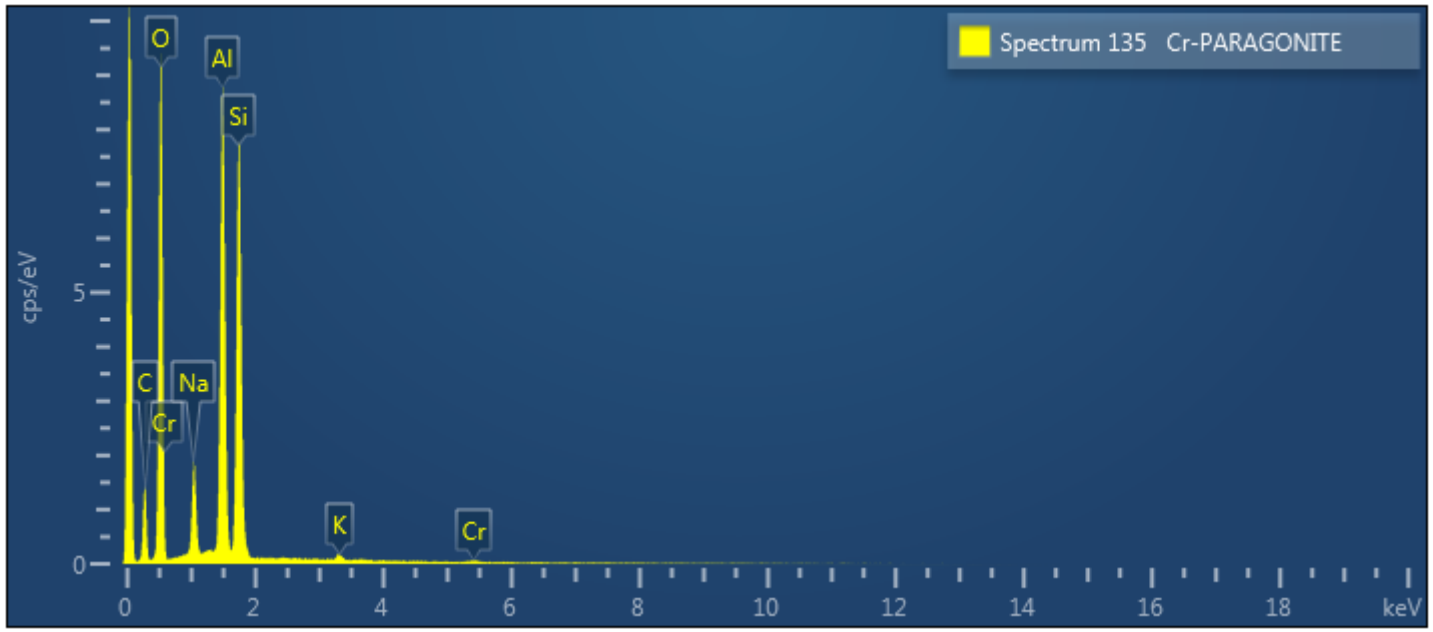

Spectrum 135 Cr-PARAGONITE							
Element	**Line Type**	**Weight %**	**Weight % Sigma**	**Atomic %**	**Oxide**	**Oxide %**	**Oxide % Sigma**
O	K series	48.22	0.18	61.16			
Na	K series	6.01	0.10	5.30	Na2O	8.10	0.14
Al	K series	21.82	0.14	16.41	Al2O3	41.22	0.26
Si	K series	23.29	0.15	16.82	SiO2	49.82	0.31
K	K series	0.43	0.04	0.22	K2O	0.52	0.05
Cr	K series	0.23	0.05	0.09	Cr2O3	0.34	0.08
Total		100.00		100.00		100.00	

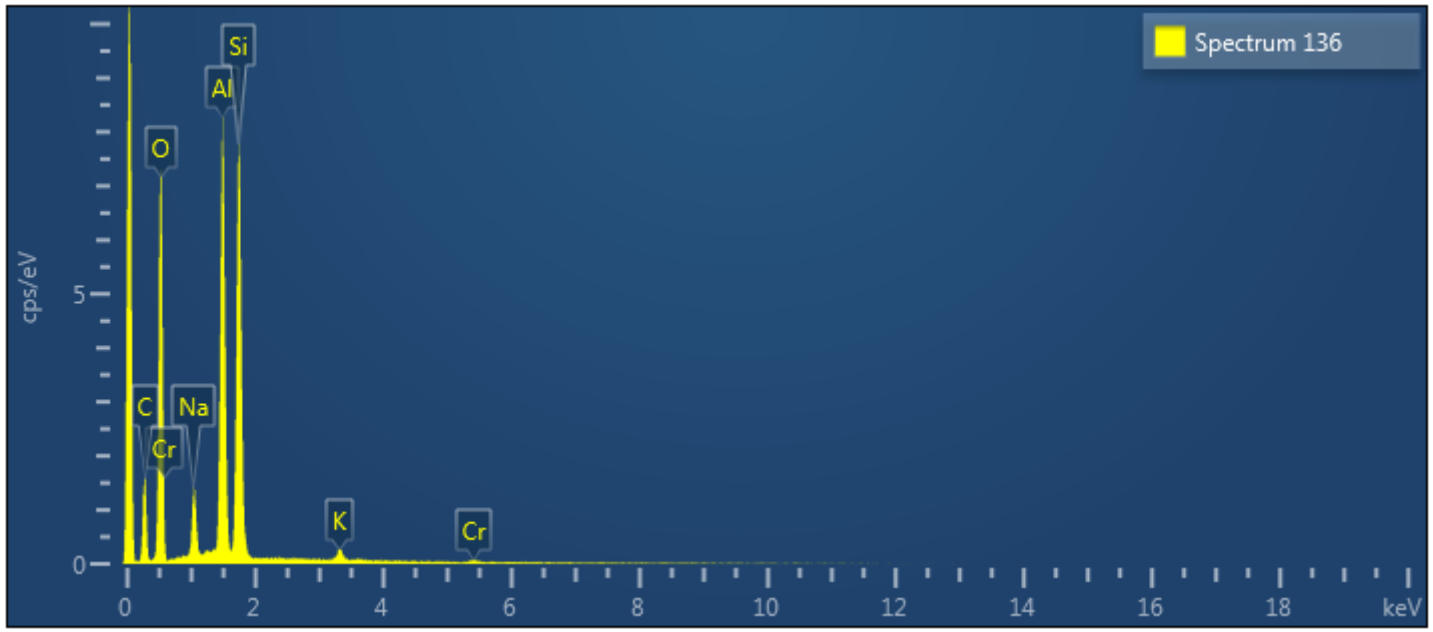

Spectrum 136							
Element	**Line Type**	**Weight %**	**Weight % Sigma**	**Atomic %**	**Oxide**	**Oxide %**	**Oxide % Sigma**
O	K series	48.47	0.24	61.60			
Na	K series	4.89	0.14	4.33	Na2O	6.59	0.18
Al	K series	21.05	0.19	15.86	Al2O3	39.77	0.35
Si	K series	24.29	0.21	17.59	SiO2	51.96	0.44
K	K series	0.91	0.07	0.47	K2O	1.10	0.08
Cr	K series	0.39	0.08	0.15	Cr2O3	0.58	0.12
Total		100.00		100.00		100.00	

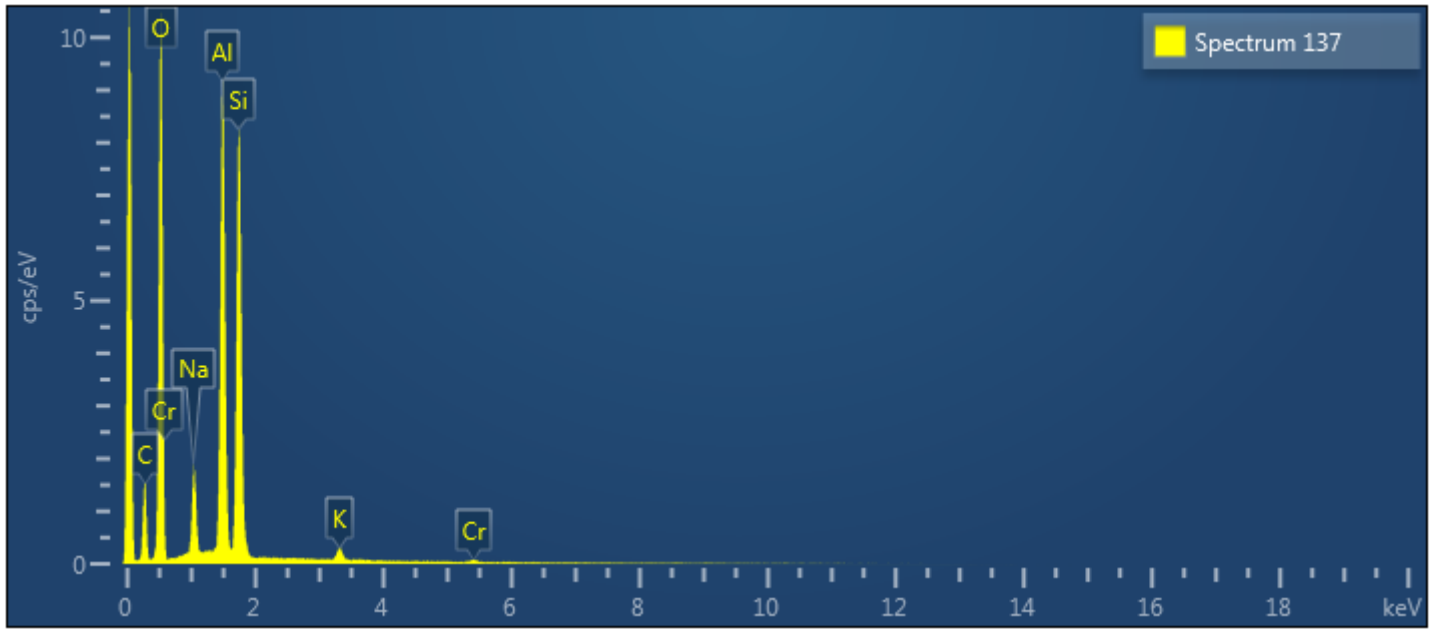

Spectrum 137							
Element	**Line Type**	**Weight %**	**Weight % Sigma**	**Atomic %**	**Oxide**	**Oxide %**	**Oxide % Sigma**
O	K series	48.14	0.17	61.20			
Na	K series	5.66	0.10	5.01	Na2O	7.63	0.14
Al	K series	21.47	0.13	16.18	Al2O3	40.56	0.25
Si	K series	23.45	0.14	16.99	SiO2	50.17	0.31
K	K series	0.91	0.05	0.47	K2O	1.10	0.06
Cr	K series	0.37	0.05	0.14	Cr2O3	0.54	0.08
Total		100.00		100.00		100.00	

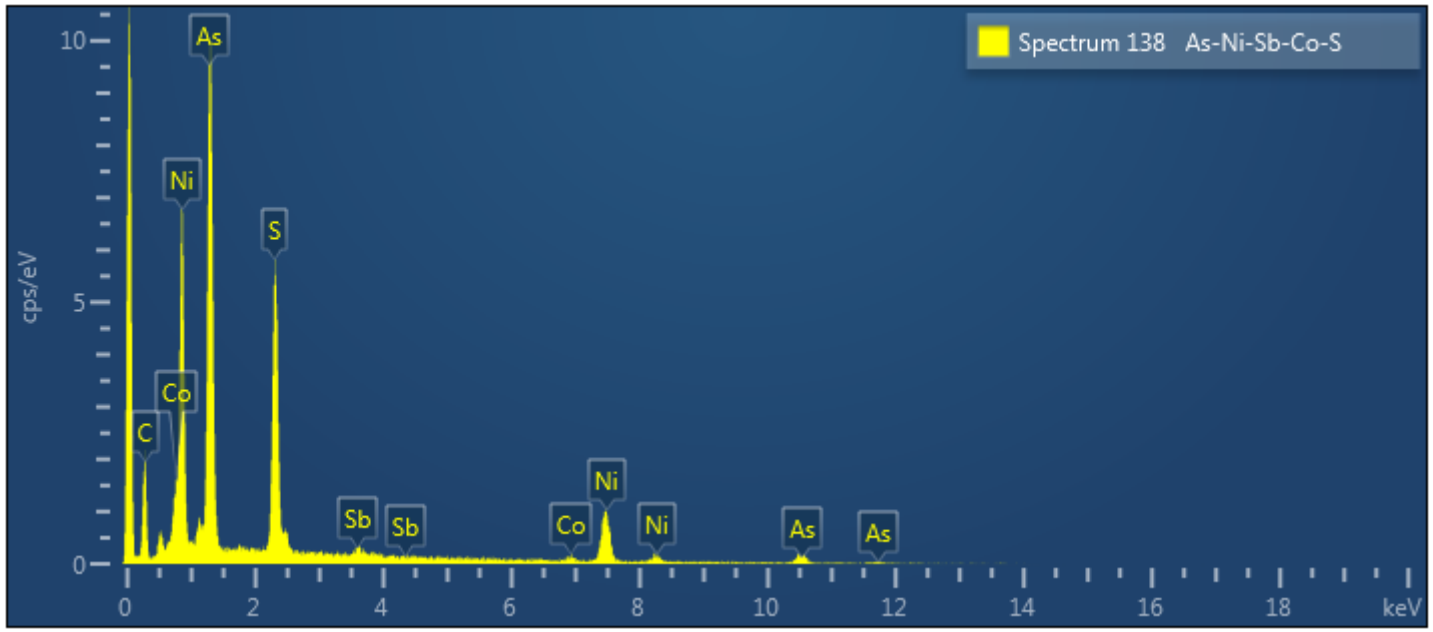

Spectrum 138 As-Ni-Sb-Co-S				
Element	**Line Type**	**Weight %**	**Weight % Sigma**	**Atomic %**
S	K series	23.62	0.39	40.52
Ni	K series	17.78	0.48	16.66
As	L series	55.60	0.56	40.82
Sb	L series	1.68	0.33	0.76
Co	K series	1.33	0.24	1.24
Total		100.00		100.00

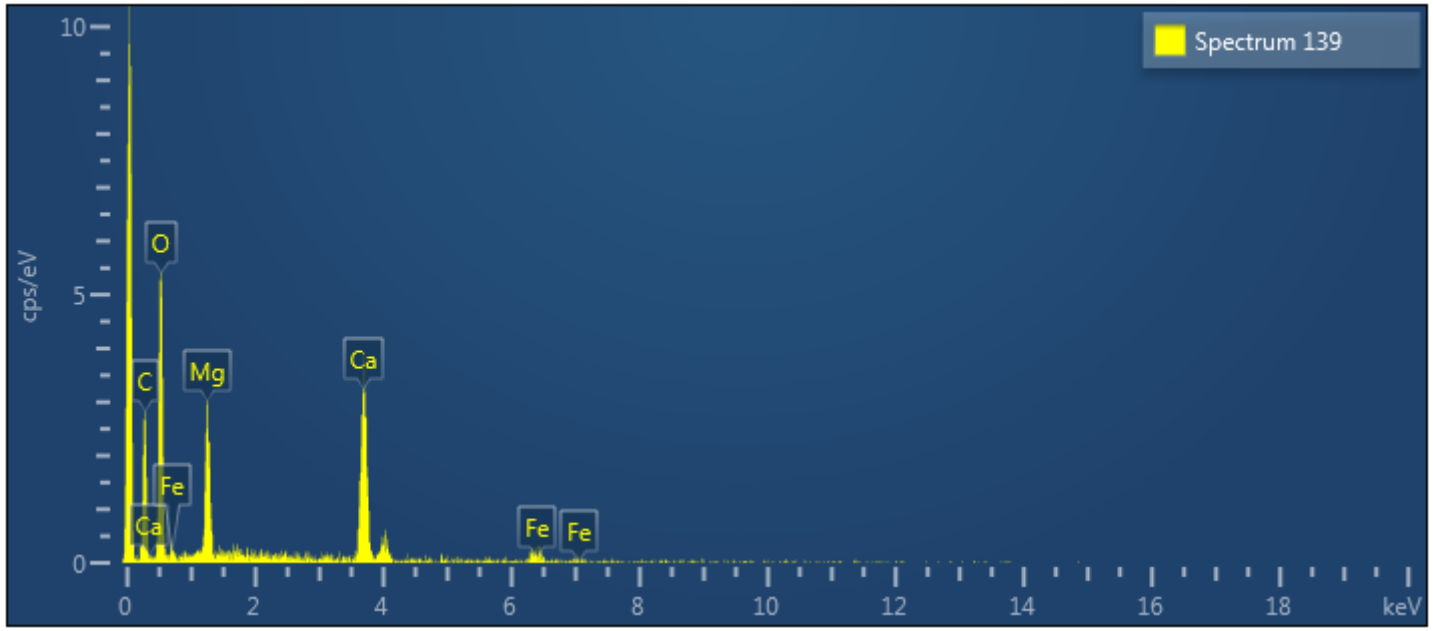

Spectrum 139							
Element	**Line Type**	**Weight %**	**Weight % Sigma**	**Atomic %**	**Oxide**	**Oxide %**	**Oxide % Sigma**
O	K series	32.19	1.47	50.00			
Mg	K series	22.57	1.30	23.07	MgO	37.42	2.16
Ca	K series	38.83	1.46	24.08	CaO	54.33	2.05
Fe	K series	6.41	1.41	2.85	FeO	8.25	1.82
Total		100.00		100.00		100.00	

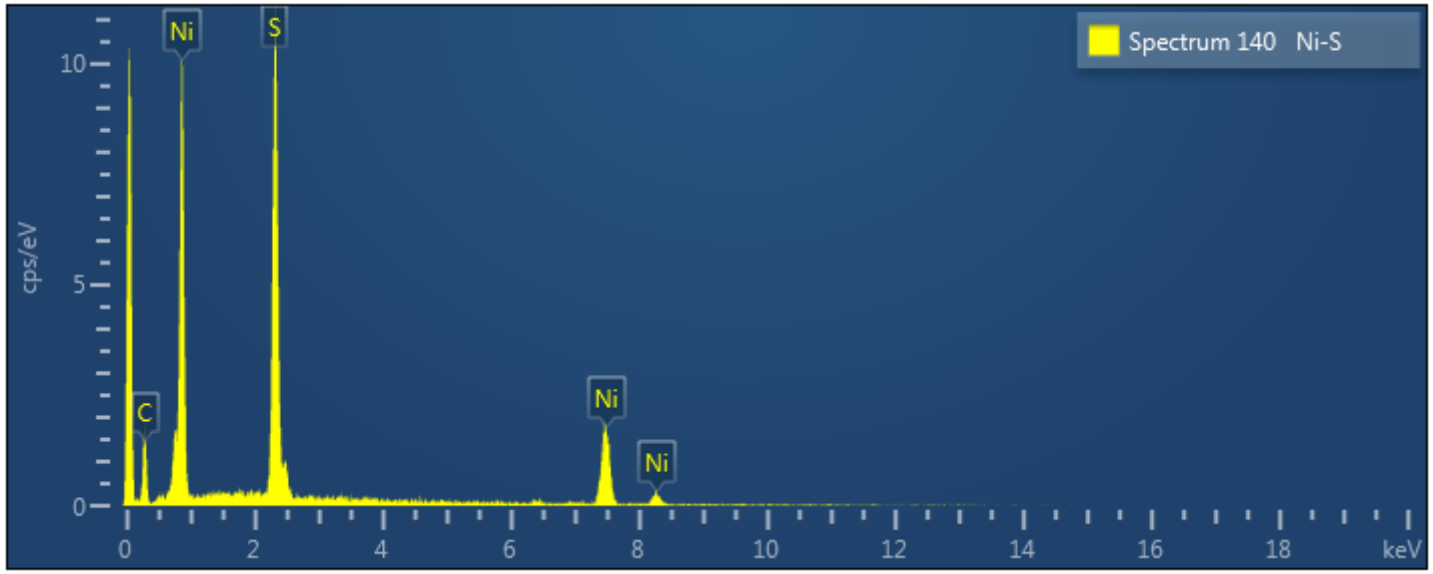

Spectrum 140 Ni-S				
Element	**Line Type**	**Weight %**	**Weight % Sigma**	**Atomic %**
S	K series	50.86	0.82	65.46
Ni	K series	49.14	0.82	34.54
Total		100.00		100.00

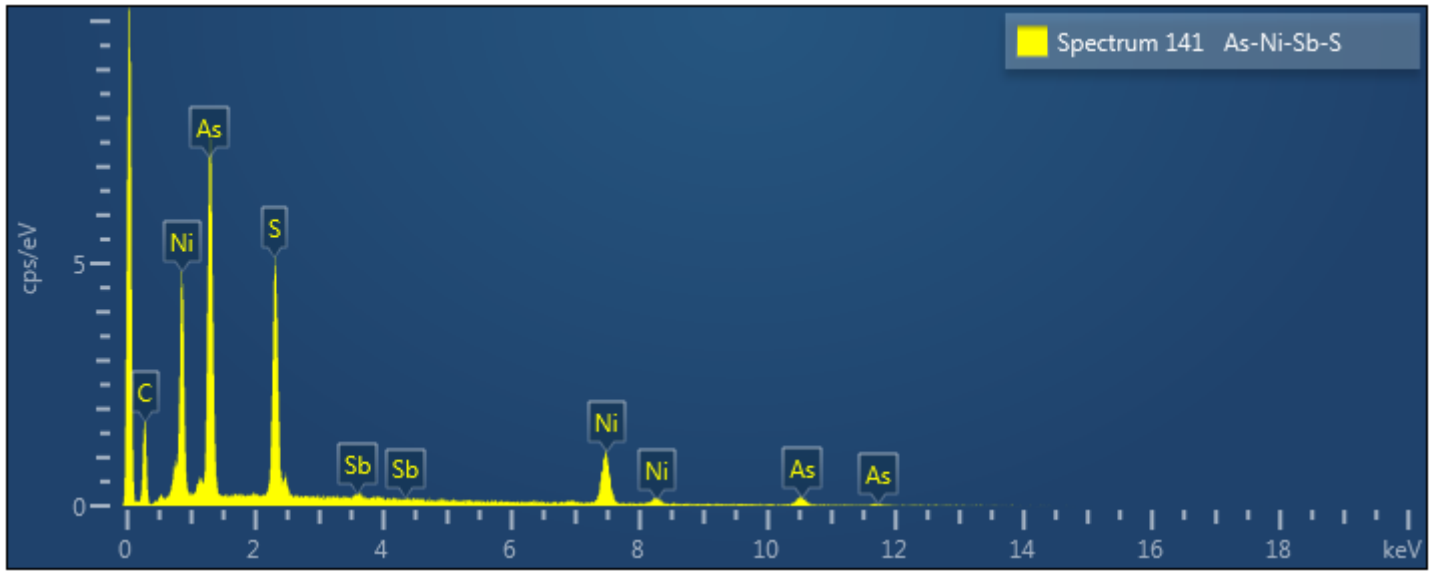

Spectrum 141 As-Ni-Sb-S				
Element	**Line Type**	**Weight %**	**Weight % Sigma**	**Atomic %**
S	K series	24.19	0.36	40.98
Ni	K series	22.17	0.46	20.52
As	L series	52.28	0.50	37.90
Sb	L series	1.35	0.30	0.60
Total		100.00		100.00

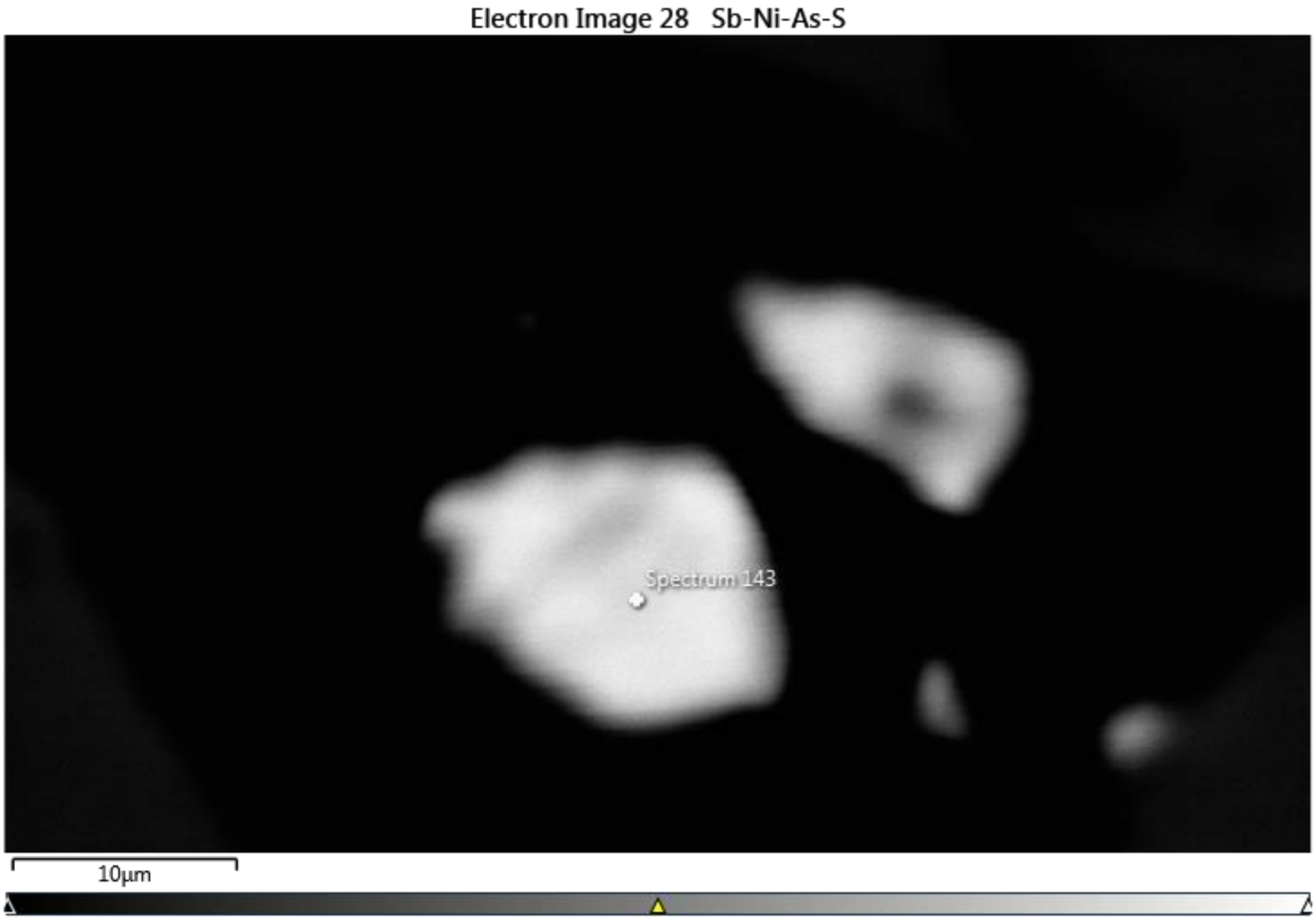

Higher magnification backscatter image of the above field of view showing two grains of Sb-Ni-As-S (spectrum 143).

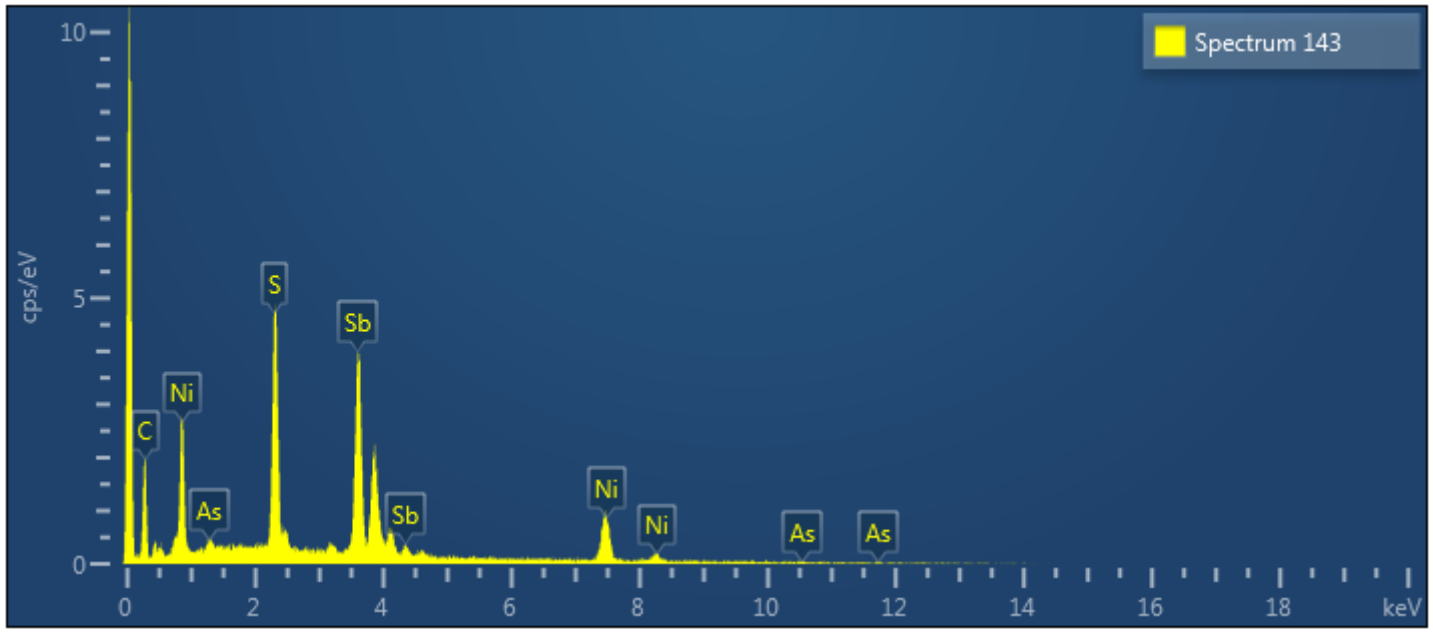

Spectrum 143				
Element	**Line Type**	**Weight %**	**Weight % Sigma**	**Atomic %**
S	K series	19.11	0.36	41.43
Ni	K series	19.00	0.54	22.49
Sb	L series	59.80	0.62	34.14
As	L series	2.10	0.45	1.94
Total		100.00		100.00

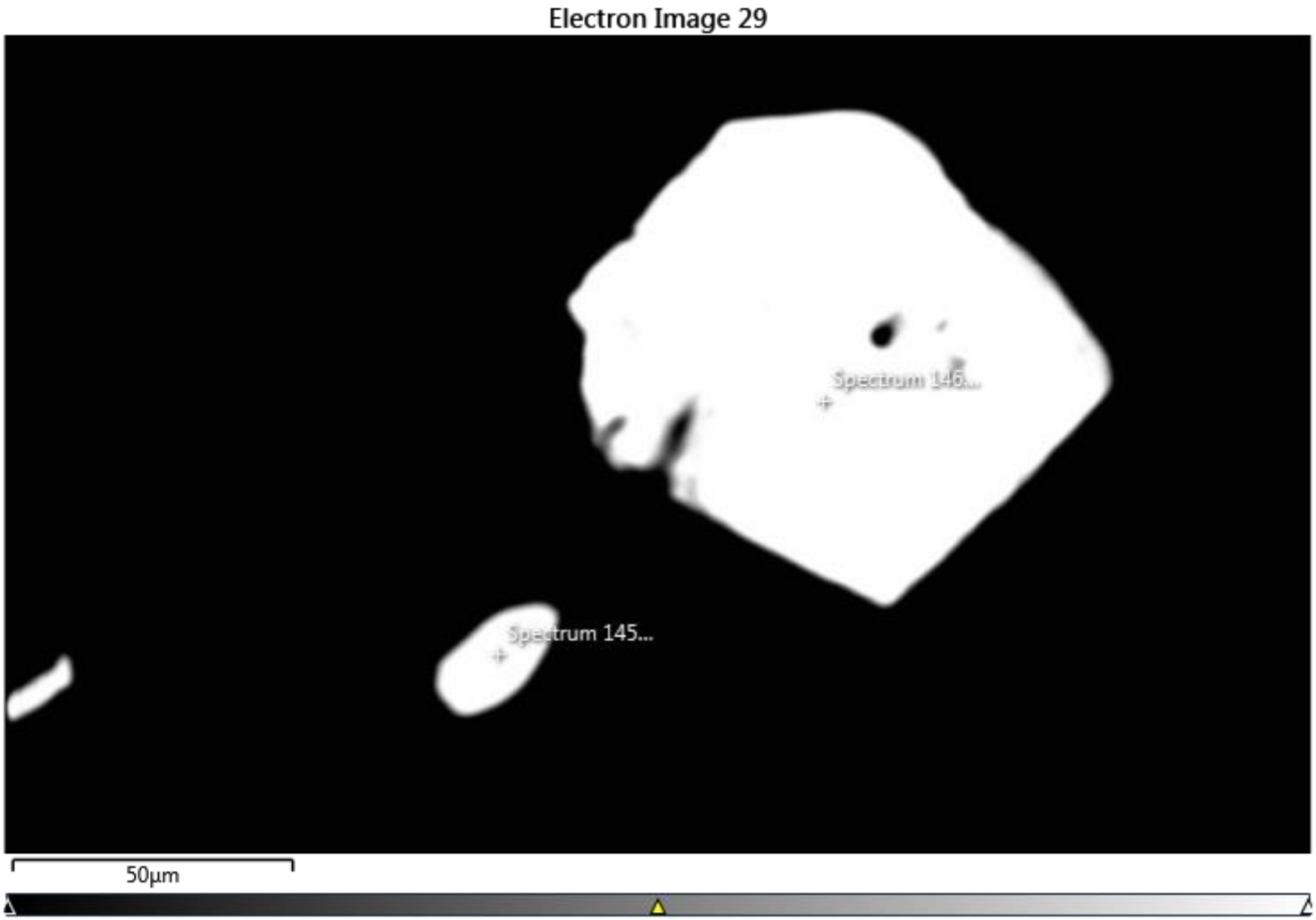

Backscatter image of a grain of Ni-S (vaesite – spectrum 145) and a coarser grain of Ni-As-Sb-Co-S (spectrum 146).

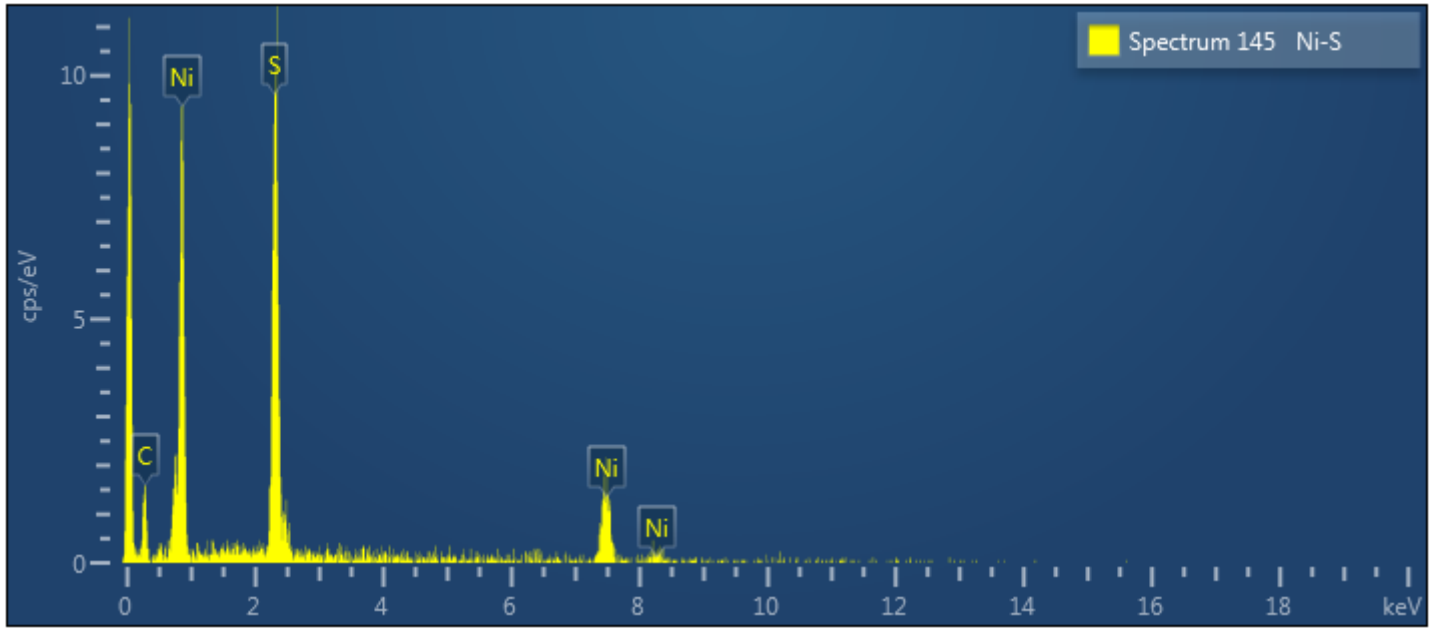

Spectrum 145 Ni-S				
Element	**Line Type**	**Weight %**	**Weight % Sigma**	**Atomic %**
S	K series	51.98	2.20	66.46
Ni	K series	48.02	2.20	33.54
Total		100.00		100.00

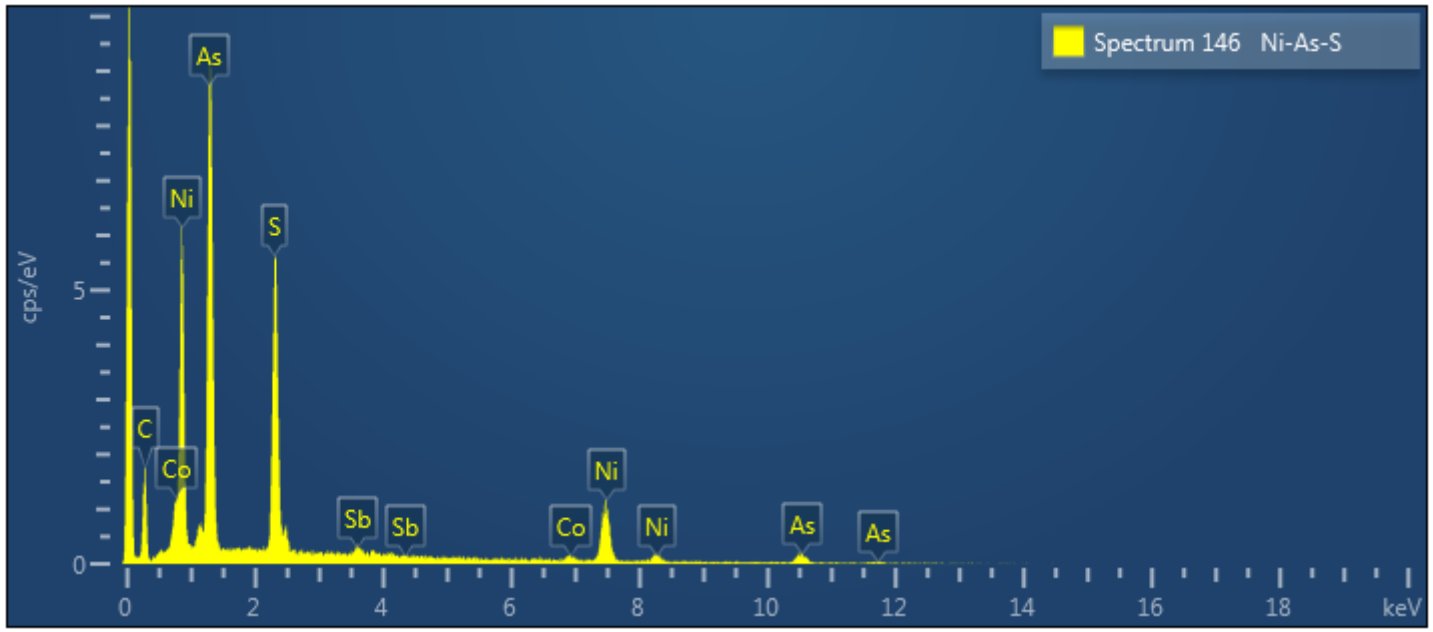

Spectrum 146 Ni-As-S				
Element	**Line Type**	**Weight %**	**Weight % Sigma**	**Atomic %**
S	K series	23.64	0.35	40.45
Ni	K series	19.45	0.44	18.18
As	L series	53.57	0.50	39.23
Sb	L series	1.99	0.30	0.90
Co	K series	1.34	0.22	1.25
Total		100.00		100.00

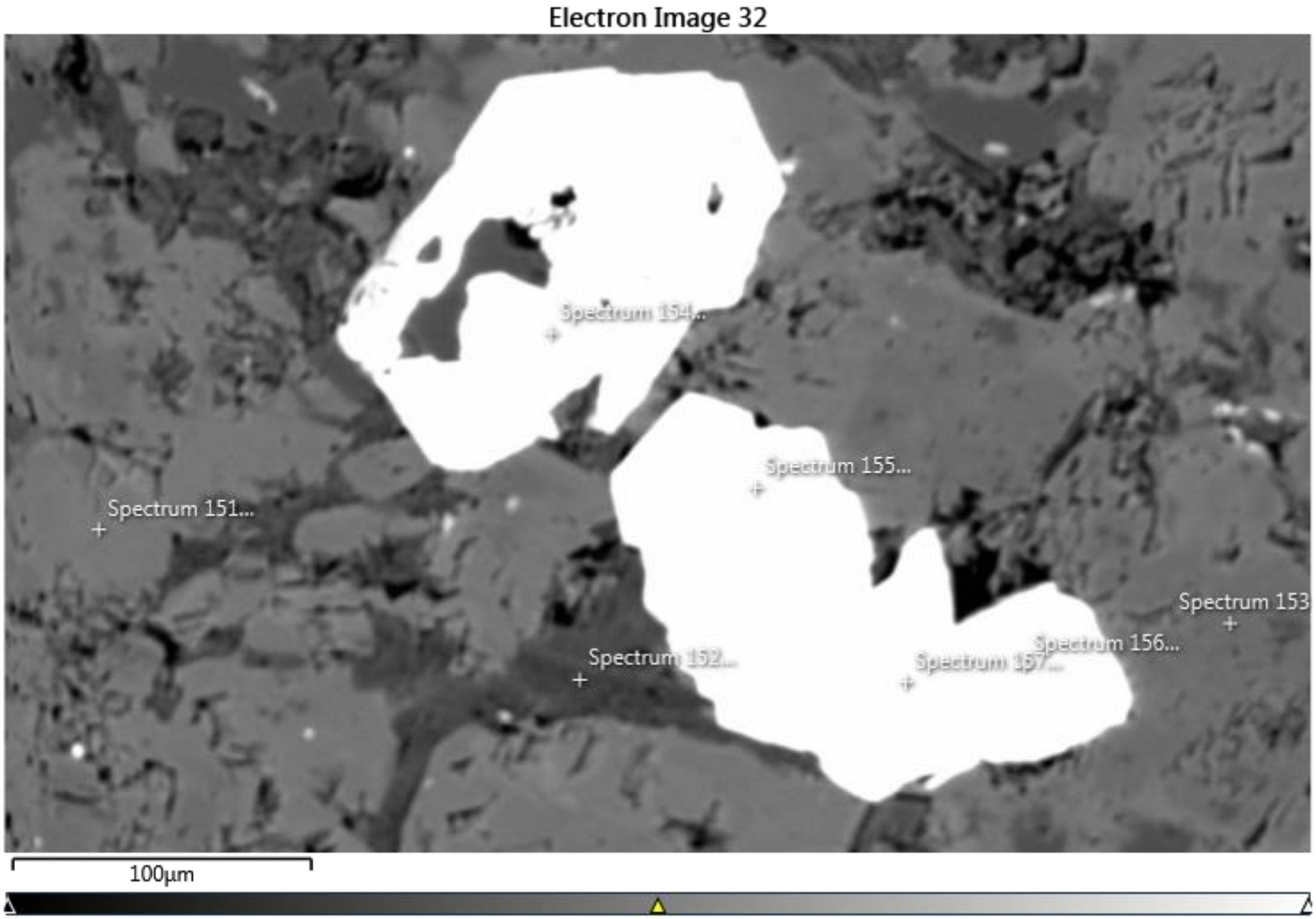

Backscatter image illustrating a groundmass dominated by compositionally zoned carbonate (spectrum 151, 153), Cr-paragonite (spectrum 152), quartz, with coarse grains of chalcopyrite (spectrum 154), arsenian pyrite (spectrum 155), As-Ni-Sb-S (spectrum 156), and As-Ni-Co-S (spectrum 157).

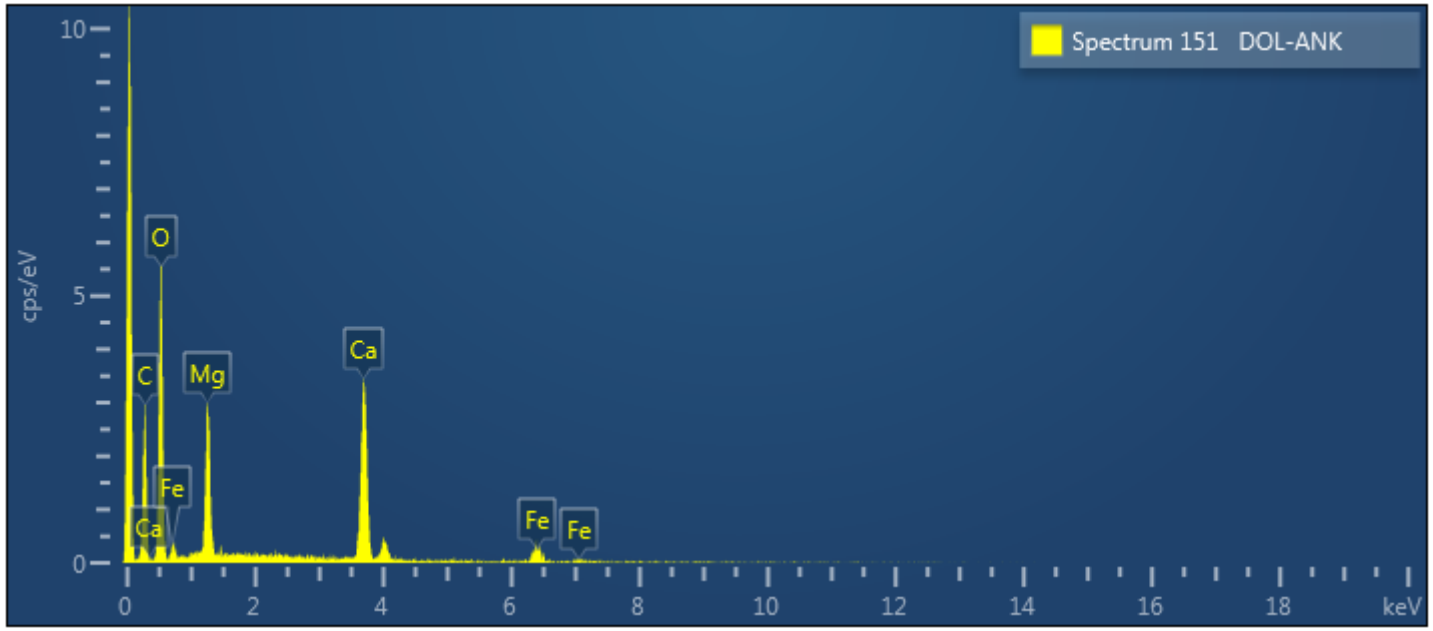

Spectrum 151 DOL-ANK							
Element	**Line Type**	**Weight %**	**Weight % Sigma**	**Atomic %**	**Oxide**	**Oxide %**	**Oxide % Sigma**
O	K series	31.98	0.82	50.00			
Mg	K series	22.70	0.73	23.35	MgO	37.64	1.21
Ca	K series	36.07	0.79	22.51	CaO	50.46	1.10
Fe	K series	9.25	0.79	4.14	FeO	11.90	1.01
Total		100.00		100.00		100.00	

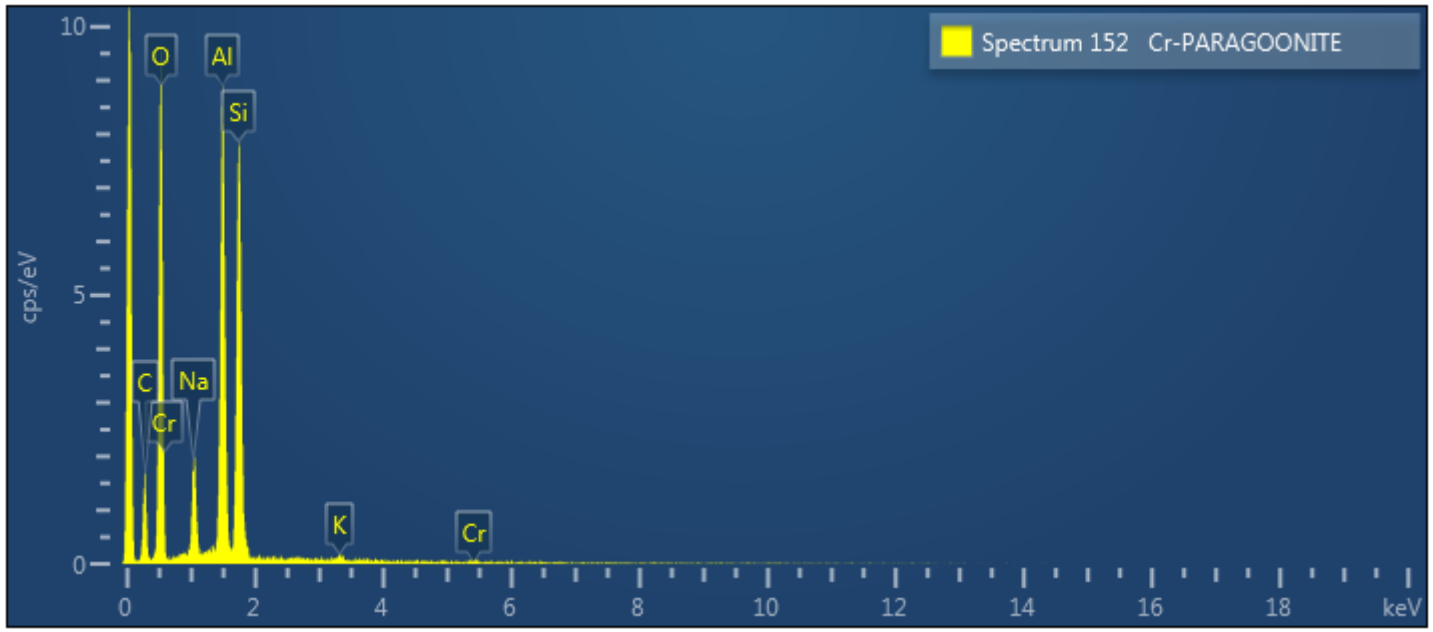

Spectrum 152 Cr-PARAGOONITE							
Element	**Line Type**	**Weight %**	**Weight % Sigma**	**Atomic %**	**Oxide**	**Oxide %**	**Oxide % Sigma**
O	K series	48.06	0.40	60.98			
Na	K series	6.57	0.24	5.80	Na2O	8.85	0.32
Al	K series	21.24	0.30	15.98	Al2O3	40.14	0.57
Si	K series	23.36	0.33	16.89	SiO2	49.98	0.71
K	K series	0.36	0.09	0.19	K2O	0.44	0.11
Cr	K series	0.41	0.12	0.16	Cr2O3	0.60	0.18
Total		100.00		100.00		100.00	

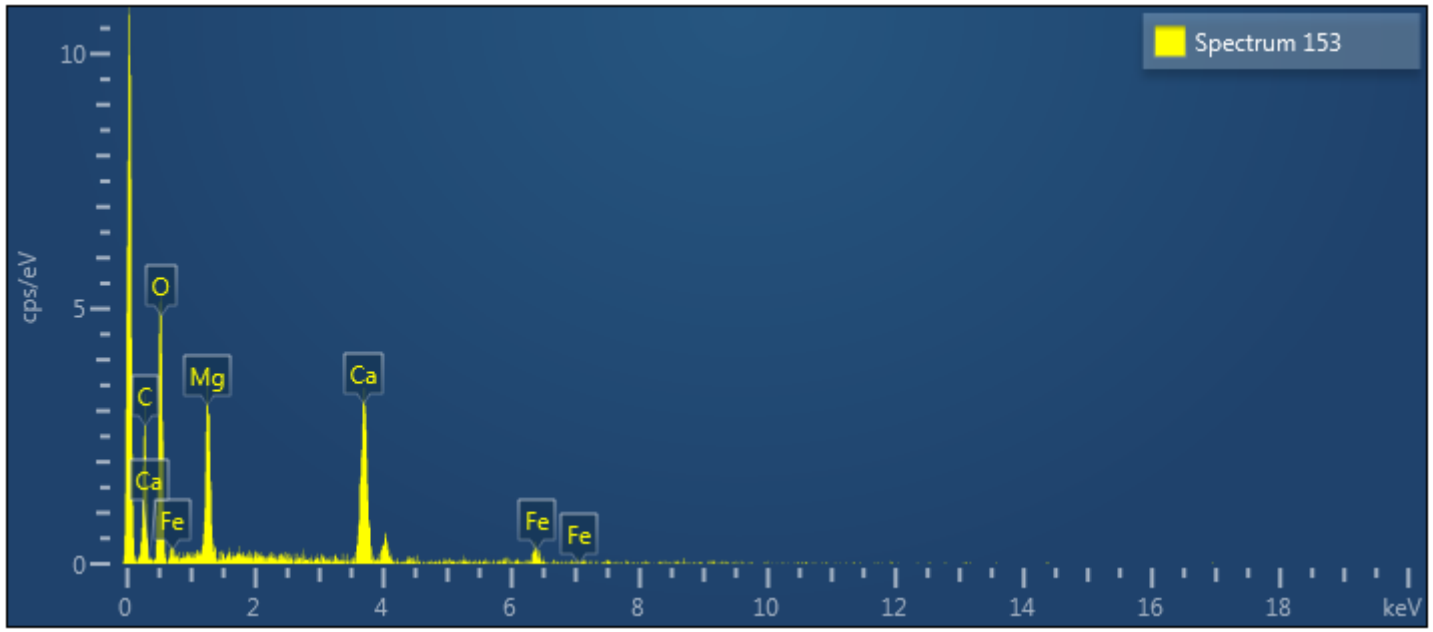

Spectrum 153							
Element	**Line Type**	**Weight %**	**Weight % Sigma**	**Atomic %**	**Oxide**	**Oxide %**	**Oxide % Sigma**
O	K series	32.52	1.42	50.00			
Mg	K series	25.09	1.31	25.39	MgO	41.61	2.17
Ca	K series	34.31	1.36	21.06	CaO	48.01	1.91
Fe	K series	8.07	1.22	3.55	FeO	10.38	1.57
Total		100.00		100.00		100.00	

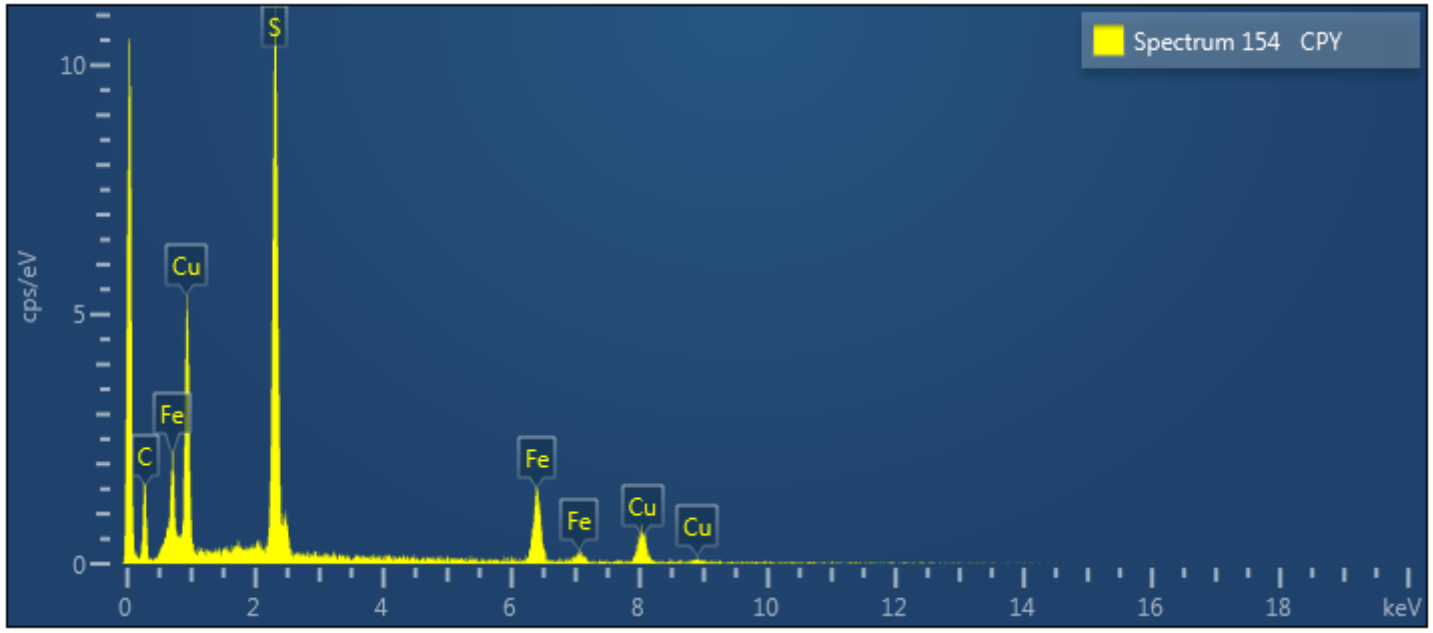

Spectrum 154 CPY				
Element	**Line Type**	**Weight %**	**Weight % Sigma**	**Atomic %**
S	K series	50.88	0.96	65.72
Fe	K series	25.24	0.86	18.72
Cu	K series	23.88	1.07	15.57
Total		100.00		100.00

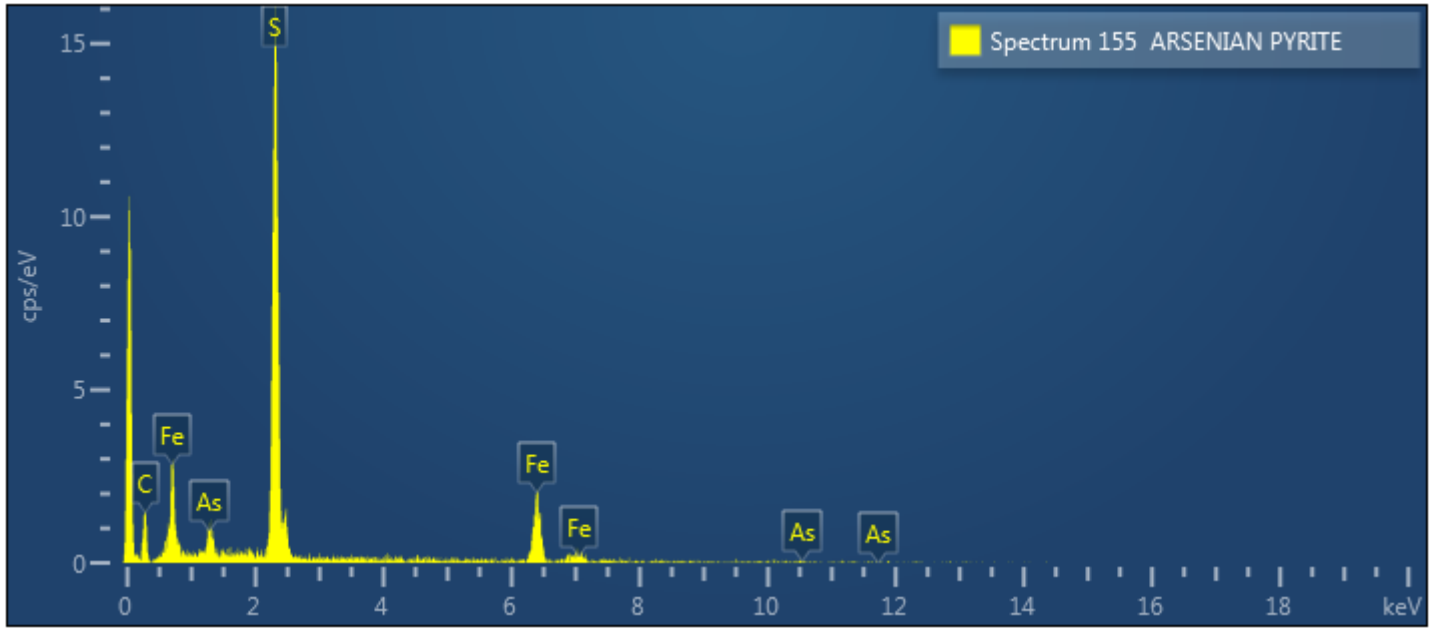

Spectrum 155 ARSENIAN PYRITE				
Element	**Line Type**	**Weight %**	**Weight % Sigma**	**Atomic %**
S	K series	62.16	1.28	74.94
Fe	K series	31.45	1.20	21.77
As	L series	6.38	0.98	3.29
Total		100.00		100.00

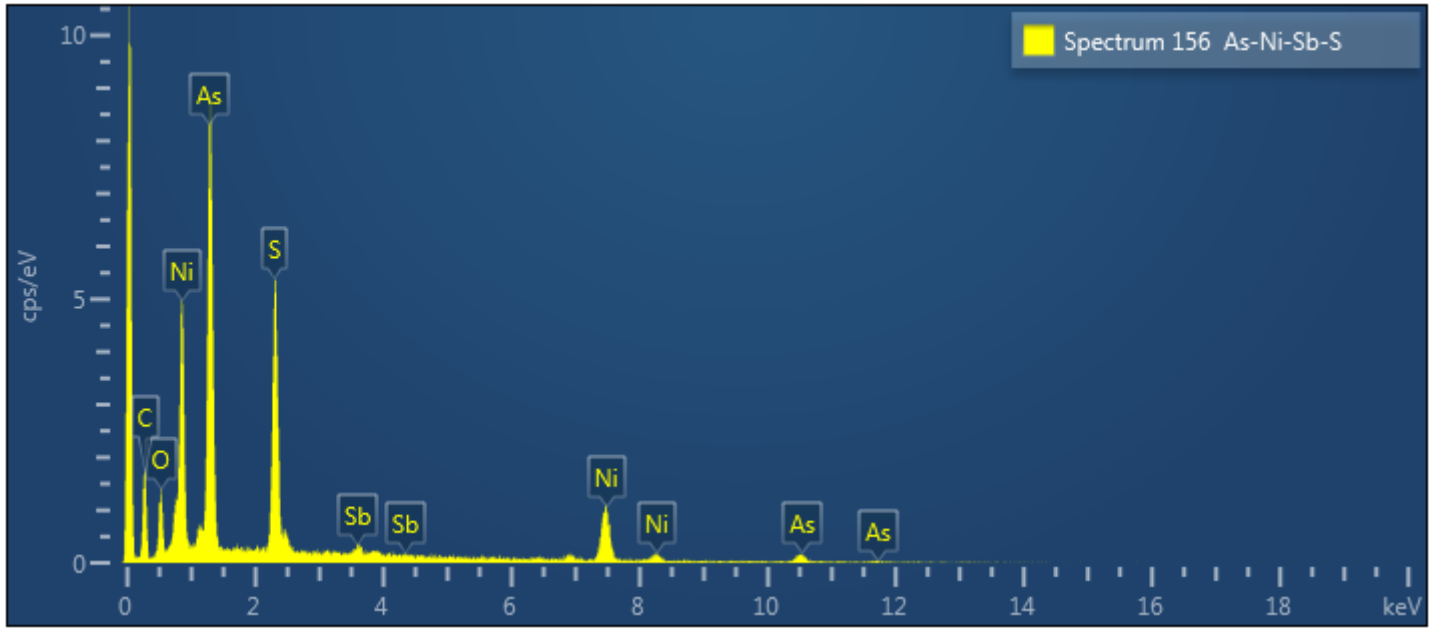

Spectrum 156 As-Ni-Sb-S				
Element	**Line Type**	**Weight %**	**Weight % Sigma**	**Atomic %**
O	K series	14.50	0.71	37.03
S	K series	19.40	0.38	24.72
Ni	K series	17.50	0.50	12.17
As	L series	46.61	0.65	25.41
Sb	L series	1.99	0.32	0.67
Total		100.00		100.00

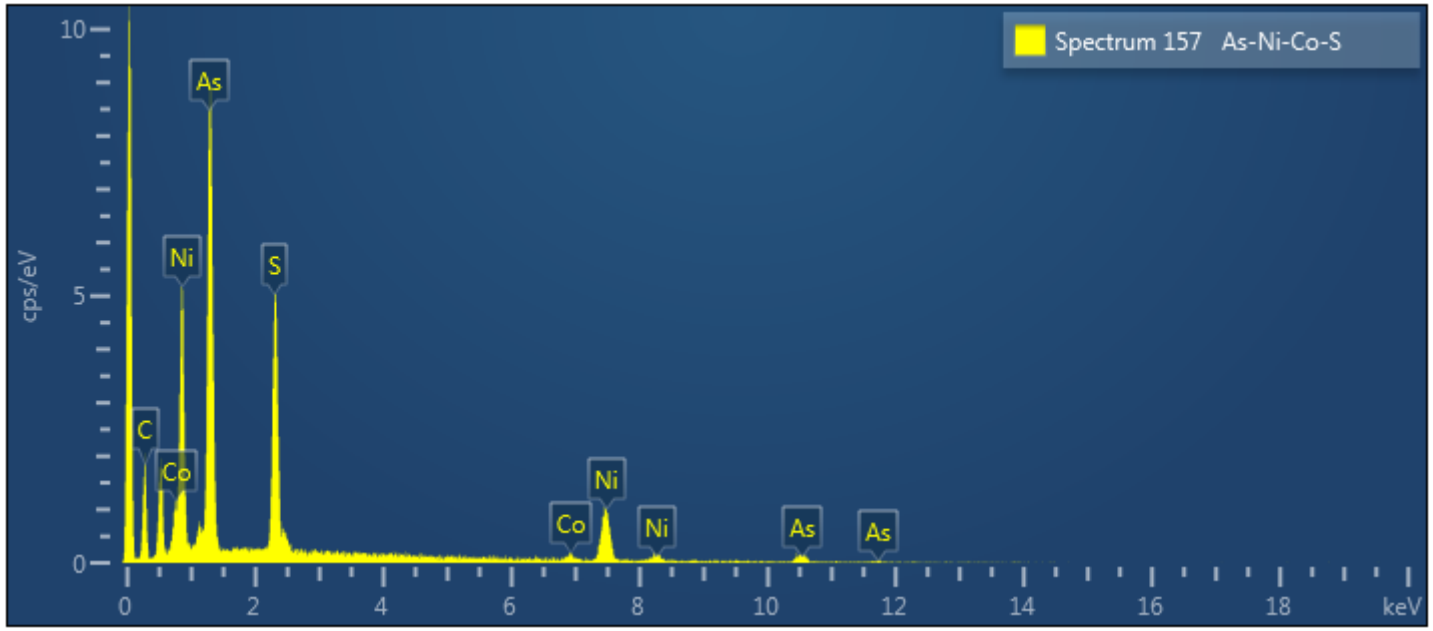

Spectrum 157 As-Ni-Co-S				
Element	**Line Type**	**Weight %**	**Weight % Sigma**	**Atomic %**
S	K series	23.00	0.43	39.32
Ni	K series	19.85	0.56	18.54
As	L series	55.53	0.61	40.64
Co	K series	1.61	0.29	1.50
Total		100.00		100.00

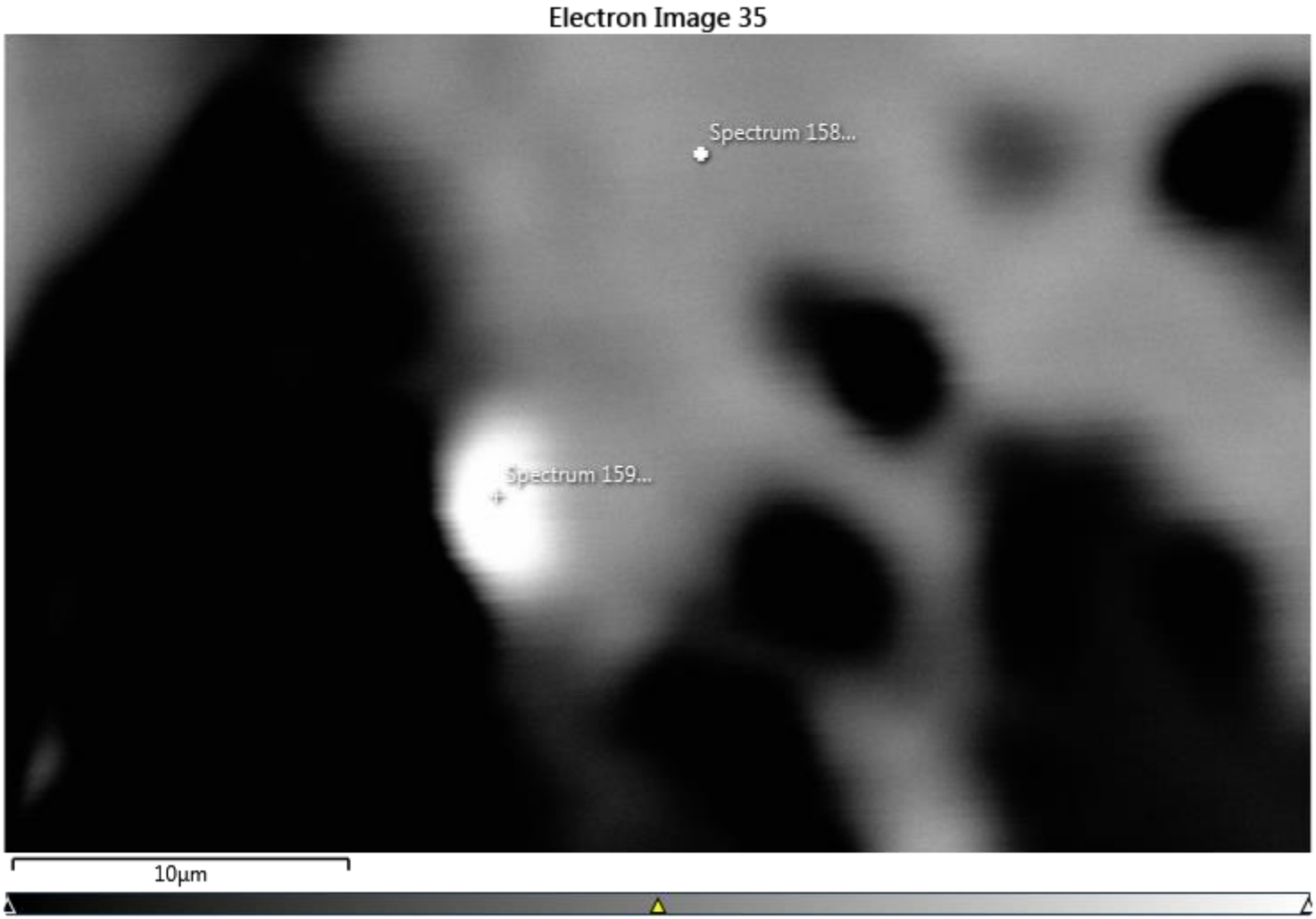

A higher magnification image of As-Ni-Sb-Co-S (spectrum 158) and Sb-Ni-As-Te-S (spectrum 159).

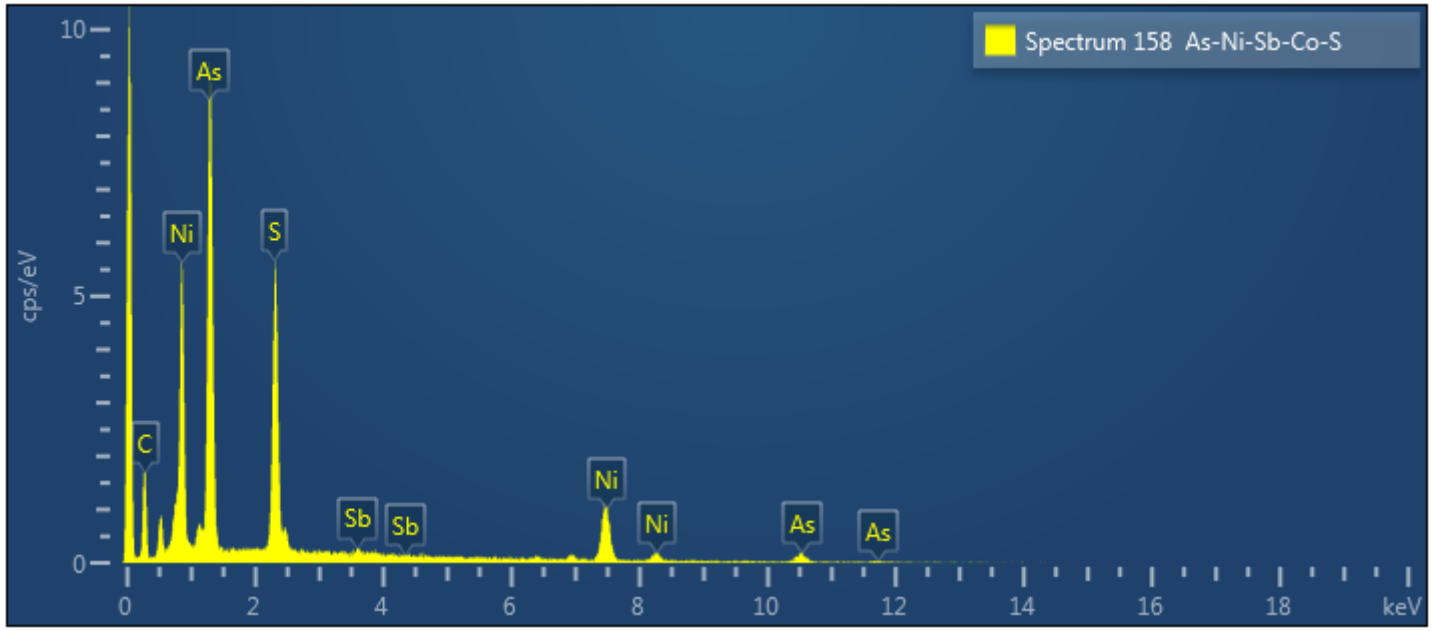

Spectrum 158 As-Ni-Sb-Co-S				
Element	**Line Type**	**Weight %**	**Weight % Sigma**	**Atomic %**
S	K series	23.57	0.35	40.32
Ni	K series	20.30	0.44	18.96
As	L series	54.75	0.49	40.09
Sb	L series	1.38	0.29	0.62
Total		100.00		100.00

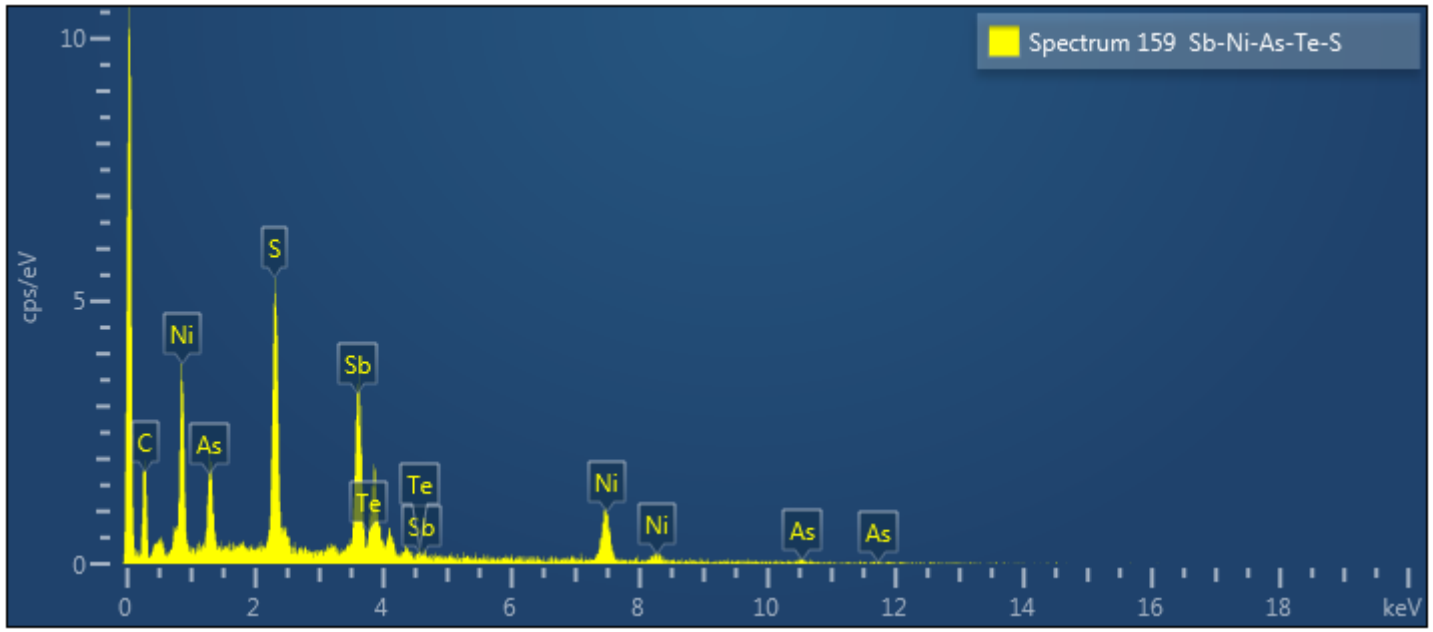

Spectrum 159 Sb-Ni-As-Te-S				
Element	**Line Type**	**Weight %**	**Weight % Sigma**	**Atomic %**
S	K series	18.67	0.59	39.46
Ni	K series	17.44	0.81	20.13
As	L series	14.24	0.86	12.88
Sb	L series	45.49	1.07	25.32
Te	L series	4.17	1.03	2.22
Total		100.00		100.00

Dr. Jim Renaud P.Geo, PhD.
Renaud Geological Consulting Ltd.
21272 Denfield Rd, London, Ontario, N6H-5L2
519-473-3766 rgcltd@execulink.com

CERIFICATE of AUTHOR

I, Jim Renaud, **Professional Geologist**, do certify that:

1. I am the **President** and the holder of a **Certificate of Authorization** for: Renaud Geological Consulting Ltd., 21272 Denfield Rd, London, Ontario, Canada N6H-5L2

2. That I have the degree of Bachelor of Science (Chemistry and Geology), 1999, from Western University; the degree of Honors Standing in Geology, 2000, from Western University; Masters of Science (Economic Geology), 2003, from Western University; and Doctor of Philosophy in Geology, 2014, from Western University

3. I am an active member of: Association of Professional Geoscientists of Ontario, APGO
   Prospectors and Developers Association of Canada, PDAC

4. I have been a **licensed Prospector in Ontario** since 2000.

5. I have worked continuously as a Geologist for 19 years.

6. Unless stated otherwise, **I am responsible** for the preparation of all sections of the Assessment Report titled:
   Petrographic and Electron Microprobe Examination of Listwanite Samples from the Laroma Prospect, Midlothian Lake Property, Larder Lake Mining Division, Midlothian Township, Ontario

7. I am not aware of any material fact or material change with respect to the subject matter of the Assessment Report that is not contained in the Assessment Report and its omission to disclose makes the Assessment Report misleading.

Dated this 30th day of January 2022